Isolation of Phenolic Compounds from Arecae Pericarpium Guided by Inhibition of LPS-Induced Nitric Oxide Production in RAW 264.7 Cells

RAW 264.7 세포내 지질다당류로 유도된 산화질소의 생성 억제에 따른 대복피 유래 페놀성 화합물의 분리

August 2015

Amelia Indriana

Natural Product Science Major
College of Pharmacy
Master Course in Graduate School
Seoul National University

Abstract

Isolation of Phenolic Compounds from Arecae Pericarpium Guided by Inhibition of LPS-Induced Nitric Oxide Production in RAW 264.7 Cells

Amelia Indriana

Natural Products Science Major

College of Pharmacy

Master Course in the Graduate School

Seoul National University

Arecae Pericarpium is the nut husk of *Areca catechu* L. (Arecaceae). In Traditional Chinese Medicine, it is used in Huo Xiang Zheng Qi formula to cure abdominal distension, vomiting, and diarrhea and Gami-Jeonggisan formula in Traditional Korean Medicine to treat vascular diseases. Arecae Pericarpium has been studied for its antioxidative activity, antifungal activity, and phytochemical compounds isolation. However, its antiinflammatory activity has not been reported yet. This study aimed to isolate compounds from Arecae Pericarpium guided by the inhibition of nitric oxide production on RAW 264.7 macrophage cells.

Dried Arecae Pericarpium was macerated in methanol. The macerate was evaporated, dissolved in 10% methanol and partitioned with hexane, methylene chloride, ethyl acetae and *n*-butanol. Methylene chloride and ethyl acetate fraction,

which inhibited nitric oxide production to lower levels compared to other fractions, were further separated. Methylene chloride fraction was subjected to repeated silica gel column chromatography to obtain seven fractions (MC1A to MC1G fraction). MC1A, MC1B and MC1G fractions inhibited the LPS-induced nitric oxide production. MC1G was obtained as single compound and identified as syringol dimer (compound I). MC1A was subjected through Diaion® HP-20 column chromatography and catechol (compound II) was obtained from 20% and 30% MeOH column fraction. Four compounds, 4-hydroxybenzaldehyde (compound III), vanillin (compound IV), 4-hydroxyacetophenone (compound V) and apocynin (compound VI), were isolated from MC1B fraction by combining HPCCC (hexane-ethyl acetate-methanol-water system 2:5:1:4 v/v) and preparative HPLC. Ethyl acetate fraction was subjected to Diaion® HP-20 column chromatography and 20% MeOH column fraction was separated using high performance counter-current chromatography (hexane-ethyl acetate-methanol- water system 2:5:2:5 v/v) to obtain protocatechuic acid (compound VII) and 4-hydroxybenzoic acid (compound VIII). All isolated compounds were examined and the result suggested that catechol might be the primary contributing active compound to the suppression of LPS-induced NO production by Arecae Pericarpium.

Keywords: Arecae Pericarpium, *Areca catechu* (L.), HPCCC, phenols, bioassay-guided isolation, nitric oxide inhibition

Student number: 2013-23937

TABLE OF CONTENTS

LIST OF FIGURES

LIST OF TABLES

I. INTRODUCTION

1. Bioassay-guided Isolation

Bioassay-guided isolation is a procedure of compounds separation from an extract by combining various analytical methods, led by biological test results. As shown in Figure 1, after an extract is subjected to bioassay to confirm its activity, crude separation is carried out and the obtained fractions are tested for biological activity. Further separation is performed on the active fractions. The process is repeated several times until a single biologically active compound is obtained. The structure of the pure compound is identified or elucidated with various spectroscopic methods. [1, 2].

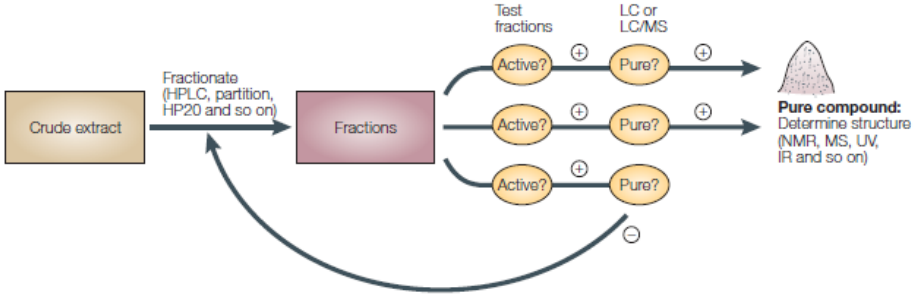

Figure 1. General scheme of bioassay-guided fractionation [1]

2. Inflammation

Inflammation is an essential defense mechanism that takes place following exposure to harmful stimuli. Acute inflammation rapidly occurs in response to tissue injury or infection in which several key agents, such as antibodies and leukocytes, are released to the infection site to repair the damaged tissue. When the initial inflammatory trigger is removed, the process is terminated; however, if harmful stimuli remain, or if healing processes are impaired, acute inflammation can progress to chronic inflammation. Chronic inflammation is a long-term condition characterized by tissue injury and restorative measures occurring simultaneously and it is considered a pivotal driver of countless major diseases, including atherosclerosis, fatty liver disease, type 2 diabetes mellitus, rheumatoid arthritis, psoriasis, Alzheimer's disease (AD) and even cancer [3].

Inflammation is marked by heat, pain, redness, and swelling. The symptoms reflect the effects of cytokines and other inflammatory mediators on the local blood vessels. The redness and heat result from an increase in blood flow, which is caused by local vasodilatation, first involving arterioles and then capillaries and venules. Swelling is the result of alterations in vascular permeability. The endothelial cells become leaky, leading to exudation of fluid, plasma proteins and white blood cells (inflammatory edema) [4].

3. Inducible Nitric Oxide Synthase and Nitric Oxide

Nitric oxide (NO) is a molecule which in mammals, including humans, has been implicated in a wide variety of physiological regulatory mechanisms ranging from vasodilatation and blood pressure control to neurotransmission. It is also involved in nonspecific immunity and in the complex mechanism of tissue injury as a major mediator of inflammatory processes and apoptosis [4].

NO is biosynthesized endogenously from L-arginine in a reaction catalyzed by various nitric oxide synthase (NOS) enzymes, however the enzyme primarily responsible for the roles of NO in inflammatory processes is the inducible NOS (iNOS; NOS2; or type II NOS). NO released by iNOS is not typically expressed in resting cells and must be induced by certain cytokines such as interleukin-1 (IL-1), tumor necrosis factor-α (TNF-α) and interferon-γ (IFN-γ) or microbial products, such as lipopolysaccharide (LPS) and dsRNA [4, 5].

NO is rapidly oxidized to nitrite and/or nitrate by oxygen in biological systems. Integrated nitric oxide production can be estimated from determining the concentrations of nitrite and nitrate end products. The measurement of nitrate/nitrite concentration or of total nitrate and nitrite concentration (NOx) is routinely used as an index of NO production [6].

4. High Performance Counter-current Chromatography (HPCCC)

Counter-current chromatography (CCC) was developed in the early 1970s by Yoichiro Ito. The method provides an advantage over the conventional column chromatography by eliminating the use of a solid support where the amount of stationary phase is limited and dangers of irreversible adsorption from the support are inevitably present [7]. Among CCC instruments, high-performance countercurrent chromatography (HPCCC) is used to generate high *g*-levels up to 240 × *g* to retain a higher proportion of the stationary phase even at a higher mobile-phase flow-rate. It has been shown that *g*-level is one of the most important parameters affecting the stationary phase retention. Higher *g*-level leads to higher stationary phase retention and hence better separation performance. Therefore, faster and more efficient separation is possible compared to conventional CCC methods [8].

An effective CCC separation relies on the selection of a suitable biphasic solvent system, based on the partition coefficient (*K* value) of the target compounds between the two phases. There are various appropriate biphasic solvent systems available with one of the most commonly used is a mixture of *n*-hexane-ethyl acetate-methanol-water (HEMWat) [9]. The selection of the most appropriate solvent system in CCC is crucial and has been the major setback in the employment of CCC separations. Compared to the far more popular solid-support chromatography, the selection of CCC solvent systems is equivalent to choosing both the column and the eluent at once [10].

5. Areca catechu L.

Areca catechu, especially the seed, is used traditionally in different regions for different purposes. In China, it is used as main herb in TCM for the treatment of gastrointestinal diseases (including abdominal distension, dysentery, dyspepsia, and constipation), parasitic diseases, and edematous diseases. In Ayurveda, it is used as digestive, astringent, and emmenagogue agent. In Southeast Asia region, it is used to treat gastrointestinal diseases, parasitic diseases, and liver diseases. The seed of *A. catechu* is a popular chewable item used in traditional herbal medicine as mild stimulant [11].

The phytochemical constituents in this plant include alkaloids, flavonoids, tannins, triterpenes and steroids, phenolic compounds, fatty acids, and anthraquinones, which were isolated mostly from the seed since it is the most commonly used part in traditional medicine. Alkaloids are the characteristic components of *A. catechu* with arecoline being the main alkaloid (content 0.3 – 0.6%). Other alkaloids found in areca nut are arecaidine, guavacoline, guavacone, arecolidine, etc. It has been reported that *A. catechu* is the only plant containing alkaloids of the Arecaceae family. Tannin is the next characteristic component of *A. catechu*. Catechin and epicatechin are the main class of tannins in *A. catechu*. The specific tannin compounds of A.catechu include procyanidin A1, procyanidin B1, procyanidin B2, arecatannin A1, arecatannin B1, arecatannin C1, arecatannin A2, arecatannin A3, and arecatannin B2 [11].

The seed and leaf of *A. catechu* have been reported to have anti-inflammatory activities. The seed extracts showed dose-dependent analgesic and anti-inflammatory effect in animal model [11, 12]. Specifically, the acetone extract of

the seed which contain procyanidins inhibited TPA-induced COX-2 expression through ERK signaling pathway in oral cavity squamous cancer SAS cell line at low dose [11, 13]. The ethanolic leaf extract inhibited iNOS and COX-2 expression dose-dependently with highest inhibition exhibited at 3 µg/mL. The leaf extract was also able to reduce carrageenan-induced paw edema in rats with highest effect shown at 10 mg/kg [14].

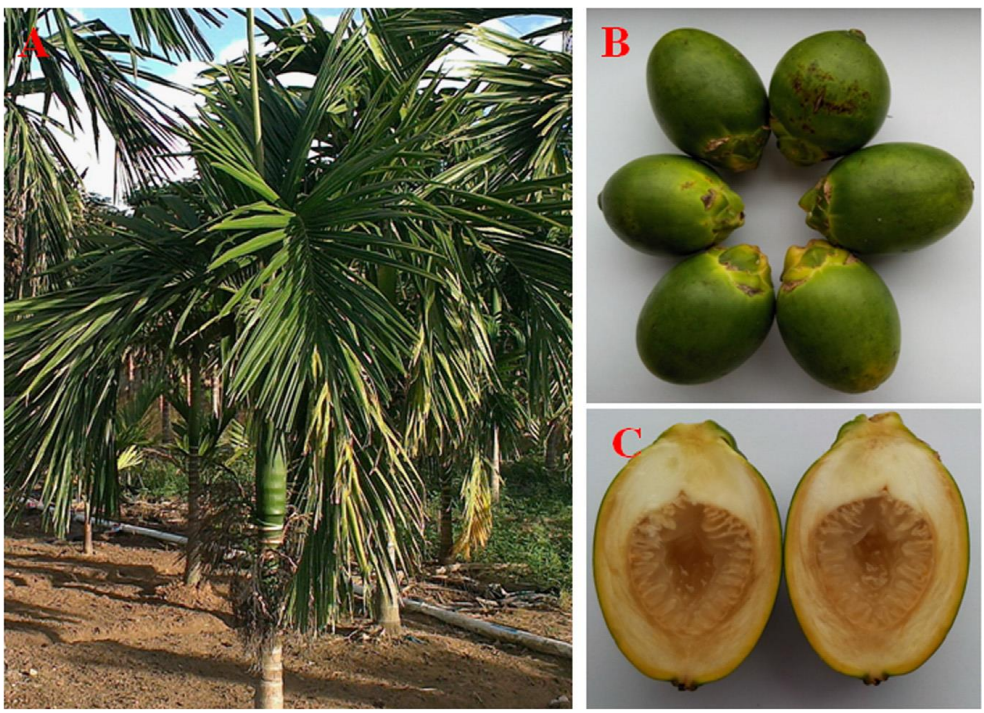

Figure 2. Areca catechu L. (A) Whole *Areca catechu* plant. (B) and (C) The fresh fruit of *Areca catechu* (areca nut) [11]

6. Purpose of This Study

Arecae Pericarpium, the nut (fruit) peel of *Areca catechu* L. (Arecaceae), commonly called betelnut, according to *Compendium of Materia Medica,* is used in Traditional Chinese Medicine (TCM) for abdominal distension, constipation, and edema treatment. Its combination with other herbs in Huo Xiang Zheng Qi formula is used to treat summerheat-dampness diseases and gastrointestinal cold, to cure abdominal distension, vomiting, and diarrhea [11]. In Korea, Arecae Pericarpium is used in Gami-Jeonggisan formula to treat vascular diseases, including atherosclerosis and ischemic stroke [15]. Arecae Pericarpium was reported to have fungicidal activity against *Colletotrichum gloeosporioides* Penz. *in vitro* and in mango fruit medium with fernenol showing highest inhibitory activity [16]. Areca Pericarpium also showed dose-dependent antioxidant activity in human hepatocarcinoma $HepG_2$ cell line and the methanol extract showed the strongest antioxidant activity compared to other parts of the *Areca catechu* (L.) plant [17].

Despite of its traditional usage, studies on anti-inflammatory activity and active compounds from Arecae Pericarpium has not been reported yet. Reported studies on *in vitro* and *in vivo* anti-inflammatory activity of other parts of the plant, such as seed and leaf, lead to hypothesis that Arecae Pericarpium may exhibit anti-inflammatory activity as well [12, 13, 14]. Thus, the purpose of this study is to investigate the anti-inflammatory activity of Arecae Pericarpium and to identifiy the active compounds by applying bioassay-guided isolation scheme.

II. MATERIALS AND METHODS

1. MATERIALS

1.1 Plant Materials

Arecae Pericarpium was purchased from local herb market in Seoul, South Korea and identified by Professor Suh Young Bae of Seoul National University. Voucher specimen was deposited at Faculty of Pharmacy, Seoul National University.

1.2 Chemicals and Reagents

All organic solvents used for extraction, column chromatography and HPCCC were of analytical grade and were purchased from Seoduk Chemical Co. in South Korea. HPLC-grade acetonitrile and methanol for preparative HPLC and HPLC analysis were obtained from J. T. Baker (Phillipsburg, NJ) and Fisher Scientific (Pittsburg, PA). Formic acid (FA) was purchased from Sigma-Aldrich (St. Louis, MO, USA). Distilled water (NANO pure Diamond, Barnstead, USA) was used for all solutions and dilutions. Silica gel 60 (0.063-0.200 mm) was purchased from Merck KGaA (Darmstadt, Germany). Silica gel 60 F_{254} 20x20 cm for thin layer chromatography was purchased from Merck KGaA (Darmstadt, Germany). Diaion®-HP20 (polystyrene adsorption resin) was purchased from Mitsubishi Chemical (Tokyo, Japan).

Dulbecco's phosphate buffered saline (D-PBS, pH 7.4), Dulbecco's Modified Eagle Medium (DMEM), lipopolysaccharide (LPS), Trypan Blue, dimethylsulfoxide (DMSO), penicillin-streptomycin, sulfanilamide, naphtylethylendiamine dihydrochloride, 2-amino-5-mercapto-1,3,4-thiadiazole

(AMT), *N*-*p*-tosyl-L-pheylalanine chloromethyl ketone (TPCK), 4-methylumbelliferyl phosphate (MUP), HEPES were purchased from Sigma Chemical Co. Ltd (St. Louis, MO). Fetal bovine serum (FBS) was purchased from South Pacific (New Zealand). Apocynin, vanillic aldehyde, 4-hydroxybenzoic acid and 4-hydroxybenzaldehyde were purchased from Sigma Chemical Co. Ltd (St. Louis, MO).

1.3 Instruments

HPLC analyses were carried out on Hitachi L-6200 instrument equipped with Sedex 75 Evaporative Light Scattering Detector (ELSD) and UV detector system and SIL-9A auto injector (Shimadzu, Japan) and Agilent 1100 equipped with PDA UV detector. Low resolution electrospray ionization source (ESI) LC/MS data were recorded on Agilent Technologies 6130 Quadrapole mass spectrometer coupled with Agilent Technologies 1200 series HPLC. Columns used for analysis are iNNO C18 column (150 mm x 4.6 mm id, 5µm particle size) from Young Jin Biochrom Co. Ltd (Seongnam, South Korea), LUNA C18 column (150 mm x 4.6 mm id, 3µm particle size) from Phenomenex Inc. (Torrance, CA, USA) and Zorbax SB-C18 column (75 mm x 4.6 mm id, 3.5µm particle size).

Spectrum HPCCC from Dynamic Extractions Ltd (Slough, UK) with tubing id 1.6 mm, total volume 135.5 mL, and sample loop 6 mL was used for CCC separation. The revolution speed was adjusted with a controller to an optimum speed of 1,600 rpm. Hitachi L-6200 intelligent Pump (Tokyo, Japan) was used to fill the CCC apparatus with the stationary phase and

elute the mobile phase. The effluent was continuously monitored by Dynamax UV Absorbance Detector from Rainin Instrument, LLC (California, USA).

Preparative HPLC separation was performed using Hitachi JP/L-7100 equipped with Hitachi L-4000 UV detector. Column used for separation was RSil C18 column (250 mm x 10 mm id, 10µm particle size) from Alltech (Deerfield, IL).

The NMR analyses were recorded on Bruker Avance 500 and 600 spectrometers. ^{1}H and ^{13}C NMR spectra were measured in a DMSO-d6 solution at 500 and 125 MHz or 600 and 150 MHz.

Instruments used for cell culture are as follow: CO_2 incubator, clean bench (Vision Scientific, South Korea), centrifuge (Hanil Scientific, South Korea), multiplate reader (Molecular Devices, Emax, Sunnyvale, CA, US) and multiplate fluorometer (Molecular Devices, Gemini XS, Sunnyvale, CA, US).

2. METHODS

2.1 Cell Culture

RAW 264.7 murine macrophage cells were obtained from American Type Culture Collection (ATCC). Cells were maintained at sub-confluence in 95% air and 5% CO_2 humidified atmosphere at 37°C. Medium used for routine subculture was DMEM supplemented with 10% FBS, penicillin (100 units/mL) and streptomycin (100 µg/mL). Cells were counted with hemocytometer and the number of viable cells was determined by trypan blue dye exclusion.

2.2 Griess Reagent Nitrite Assay

RAW 264.7 macrophages were plated at density of 1 x 10^5 cells/well in a 24-well plate with 500 µL of culture medium and incubated at 37°C for 24 h. Culture medium was changed and cells were treated with samples in various concentration for 2 h and then stimulated with LPS (1 µg/mL) for 18 h. An aliquot of cell-free medium (100 µL/well) was removed to 96-well plate and Griess reagent (100 µL/well) was added. Griess reagent was made from 1% sulfanilamide in 5% phosphoric acid and 0.1% naphtylethylenediamine dihydrochloride in distilled water. To quantify nitrite concentration, standard nitrite solutions were prepared and absorbance of the mixture was determined with microplate fluorometer (Molecular Devices) at wavelength 540 nm. AMT, an iNOS inhibitor, or TPCK, a known NF-κB inhibitor, was used as positive control with concentration of 10 µM. Cells treated with vehicle alone was used as control.

2.3 Cell Viability

The measurement of cell viability was performed using MTT (4,5-dimethylthiazol-2-yl)-2,5-diphenyl tetrazolium bromide) assay concurrently with nitrite assay. RAW 264.7 macrophages were plated at density of 1 x 10^5 cells/well in a 24-well plate with 500 µL of culture medium and incubated at 37°C for 24 h. Culture medium was changed and cells were treated with samples in various concentration for 2 h and stimulated with LPS (1 µg/mL) for 18 h. After 100 µL of media was taken for nitrite assay, 40 µL of MTT solution (2 mg/mL in saline) was added to each well and incubated at 37°C for 2 h. Mitochondrial succinate dehydrogenase in living cells will convert MTT into visible formazan crystals during incubation. The formazan crystals were then solubilized in DMSO and the absorbance was measured at wavelength 595 nm using microplate fluorometer.

2.4 Determination of PGE_2 detection

The amount of PGE_2 produced from activated macrophages was quantified using an enzyme immunoassay (EIA) kit for PGE_2 (Cayman Chemical, Ann Arbor, MI). Briefly, 1×10^5 cells were seeded in 24-well plate and incubated for 24 h. After changing to new media, the cells were pre-treated with several concentrations of MC1A fraction or a vehicle for 2 h and then activated by LPS (1 µg/ml) to express COX-2 for an additional 18 h. These media were diluted 2 times with PBS and transferred to a PGE_2 antibody-coated 96-well culture plate in the EIA kit. Further treatment was according to the manufacturer's instructions. The produced PGE_2 in the specimen was quantified to determine

COX-2 expression using a PGE_2 standard curve. Absorbance at 405 nm was recorded using a microplate reader (Molecular Devices, Emax, Sunnyvale, CA). For comparison, 10 μM TPCK was used as a positive control.

2.5 NF-κB Secretory Alkaline Phosphatase (SEAP) Reporter Gene Assay

Reporter enzyme activity was measured by cell-based assay system for NF-κB activity monitoring. The pNF-κB-SEAP-NPT plasmid that permits expression of the SEAP reporter gene in response to the NF-κB activity and contains the neomycin phosphotransferase (NPT) gene for geneticin resistance in host cells was constructed and transfected into murine macrophages. Transfected RAW 264.7 cells were plated at density of 1 x 10^5 cells/well in a 24-well plate with 500 μL of geneticin-added culture medium and incubated at 37°C for 24 h. Cells were treated with samples in various concentrations for 2 h and stimulated with LPS (1μg/mL) for 18 h. Aliquots of cell-free medium (120 μL) of each treatment was transferred to 1.5 mL vial and heated at 65°C for 6 min and given an assay buffer (2 M diethanolamine, 1 mM $MgCl_2$, 500 μM 4-methylumbelliferyl phosphate (MUP)) in the dark at 37°C for 1 h. The fluorescence from the product of the SEAP/MUP was measured using a 96-well microplate fluorometer at an excitation of 360 nm and emission of 449 nm. TPCK (20 μM) was used as positive control.

2.6 Extraction

Dried Arecae Pericarpium was purchased from a local herb market in Seoul, South Korea. 5 kg of Arecae Pericarpium was macerated in 28 L of methanol

(MeOH) for 3 days. This process was repeated for three times. The extract was dried with rotary evaporator under 50ºC. Subsequently, dried extract was suspended in 10% MeOH and liquid-liquid extraction was performed with hexane, methylene chloride (MC), ethyl acetate (EtOAc) and n-butanol (BuOH) at 1:1 ratio for three times. The obtained fractions were evaporated to dryness under vacuum and stored in desiccator until further use. Each fraction was tested for its inhibition activity against LPS-stimulated NO production in RAW 264.7 macrophage cells. Since methylene chloride and ethyl acetate fraction showed higher NO inhibition activity than other fractions, further separation was performed on those fraction.

2.7 Silica column chromatography

Silica column chromatography separation of MC fraction was performed using an open column with diameter 5 cm and length 58 cm. 500 g of silica gel was activated and packed into the column to separate 18 g of sample. Sample was eluted with a gradient elution of chloroform – ethyl acetate (9:1, 7:3, 5:5, 3:7, 1:9 v/v) continued with ethyl acetate – methanol (9:1, 7:3, 5:5 v/v). Each ratio was collected in 2 bottles of 500 mL and collected fractions were analyzed with TLC.

Silica column chromatography separation of MC1A fraction was performed in an open column (75 x 3 cm). 100 g of silica gel was used to separate 3.3 g of sample. Sample was eluted with 2 L of hexane-ethyl acetate-*n*-butanol with ratio (3:2:0.05) and (2.75:2.25:0.05). Fifteen fractions with volume of 125 mL were collected and analyzed with TLC and HPLC.

2.8 Diaion® HP-20 resin column chromatography

MC1A fraction (1.3 g) and ethyl acetate fraction (17.1 g) were separated with Diaion® HP-20 resin open column chromatography (75 x 3 cm for MC1A and 58 x 5 cm for ethyl acetate fraction). Sample was made into suspension with 10% methanol and poured into the column. Elution began with distilled water as washing step and sequentially eluted with a methanol gradient beginning from 20% to 100% methanol, 3 times of packed column volume for each gradient. Fractions were collected, evaporated, and stored in a refrigerator or desiccator until further use.

2.9 Selection of the two-phase solvent system and measurement of the partition coeffient (*K)* and settling times

The solvent system was selected based on the *K* values of the target compounds. The values were measured based on the peak area shown in HPLC chromatogram. The two-phase solvent system was prepared in a separating funnel flask, shaken vigorously to allow the solvents mix and settle it for 1.5 hours to allow the solvent system separate and equilibrate. The lower phase and upper phase were collected in separated tubes. Approximately 2 mg of crude extract was dissolved in equal volumes of lower and upper phases of the equilibrated two-phase solvent system in test tube. The tube was shaken vigorously to equilibrate the sample between the two phases. The phases were separated and evaporated to dryness under nitrogen (N_2) gas. The residue was dissolved in methanol and analyzed with HPLC. The *K* value was expressed as the peak area of the target compound in the upper phase divided by that in the lower phase. The settling time, which is highly correlated to the retention of the

stationary phase, was expressed as the time to form a clear layer between the two phases after mixing.

2.10 HPCCC Separation

In each separation run, the multi-layered coiled column was filled with the upper phase to form the stationary phase. The first step was performed in reverse phase mode at 25ºC. The preparative column (total 135.5 mL) was filled with upper phase as the stationary phase. The mobile phase (lower phase) was pumped to the system at a flow rate of 3 mL/min while the columns were rotating at a speed of 1600 rpm. Sample was dissolved in same ratio of upper and lower phase with total volume of 6 mL and injected into the HPCCC system.

2.11 Preparative HPLC Separation

MC1B fraction separation was carried out with preparative HPLC technique. The mobile phase used was 0.05% formic acid in distilled water (solvent A) and 0.05% formic acid in methanol (solvent B). Isocratic mode of 18% solvent B was chosen to separate peaks with flow rate of 2.5 mL/min for 120 minutes and monitored with UV detector at 246 nm. For each run, not more than 10 mg of sample dissolved in 200 µL of HPLC grade methanol was injected to sample valve. Peaks observed on chromatogram were collected as fractions, dried under vacuum and analyzed with HPLC to determine their purity.

2.12 Identification of isolated compounds

All isolated compounds were analyzed with HPLC coupled with low resolution electrospray ionization source (LR-ESI/MS) for molecular weight determination and their structure were identified by comparing the ^{1}H and ^{13}C NMR spectra in DMSO-d_6 with references.

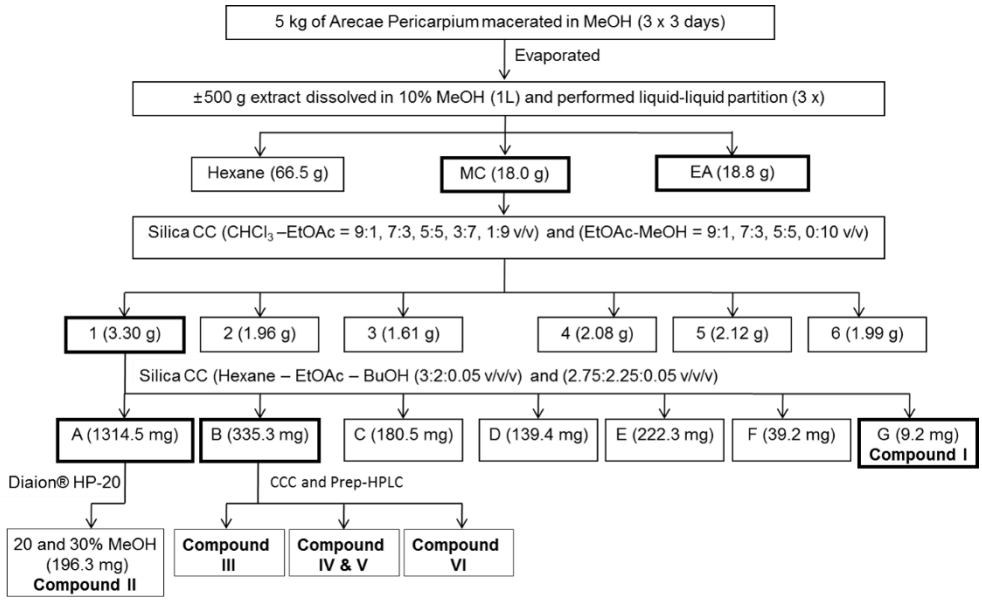

Figure 3. Isolation scheme of Arecae Pericarpium methylene chloride fraction

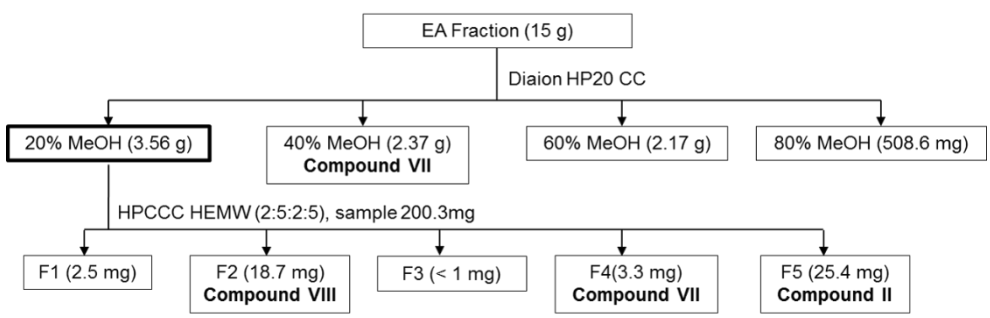

Figure 4. Isolation scheme of Arecae Pericarpium ethyl acetate fraction

III. RESULTS

1. Preliminary study

Fractions obtained from solvent partition (hexane, methylene chloride, ethyl acetate, *n*-butanol, and water fraction) were tested with Griess reagent nitrite assay to screen active fractions in suppressing LPS-stimulated NO production in RAW 264.7 cells. All fractions were tested with increasing concentration from 10, 25, to 50 µg/mL and compared with a positive control, AMT (10 µM).

The cell viability decreased at the highest concentration tested but it is still in the acceptance range (≥80%), except for ethyl acetate fraction which its cell viability decreased until 74% at 50 µg/mL. The methylene chloride fraction suppressed LPS-induced NO production with IC_{50} value 8.89 µM, which is the highest among all tested fractions. The ethyl acetate fraction was the second fraction that showed suppression on NO production with IC_{50} value 13.60 µM. Hexane fraction inhibited NO production with IC_{50} value 31.94 µM while IC_{50} value of *n*-butanol and water fraction were more than 50 µM. Hence, a further separation was performed on methylene chloride and ethyl acetate fractions.

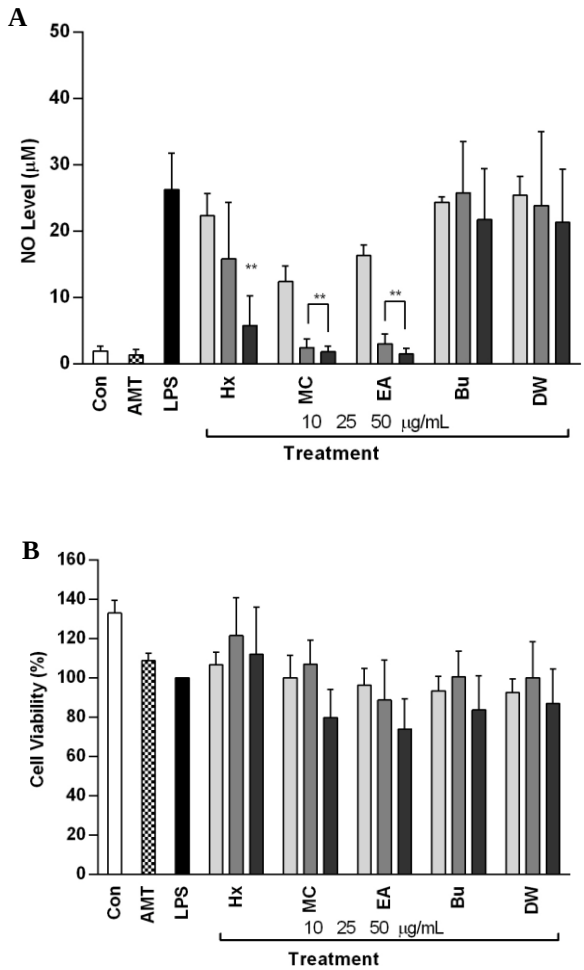

Figure 5. Effect of Arecae Pericarpium on (A) NO production and (B) cell viability of LPS-stimulated RAW 264.7 murine macrophage cell

Dose-dependent suppression of LPS-induced NO production by Arecae Pericarpium fractions in RAW 264.7 macrophages. Data were derived from three independent experiments and are expressed as mean ± standard deviation (S.D). (**) *P<0.01* indicates a significant difference from the LPS-stimulated group.

Control (vehicle), AMT (positive control), LPS (LPS + vehicle)-treated cells alone, HX (hexane fraction), MC (methylene chloride fraction), EA (ethyl acetate fraction), Bu (*n*-butanol fraction), and DW (distilled water fraction).

2. Separation of methylene chloride fraction

The methylene chloride fraction was subjected to silica gel open column chromatography and 17 fractions were obtained. These fractions were analyzed with TLC. The TLC mobile phase system used was methylene chloride-ethyl acetate-*n*-butanol with ratio 9:10:1 v/v, respectively. After elution, TLC plate was dried and observed under room light and UV light (254 nm and 366 nm). The spots showed fluorescence under 254 nm but did not show any phosphorescence under 366 nm. The spots were also not distinguishable when observed under room light. Thus, fractions showing similar spots pattern under 254 nm UV light were combined. Based on the TLC analysis, total of 6 fractions were obtained with the following yields: MC1 (3.30 g), MC2 (1.96 g), MC3 (1.61 g), MC4 (2.08 g), MC5 (2.12 g), and MC6 (1.99 g).

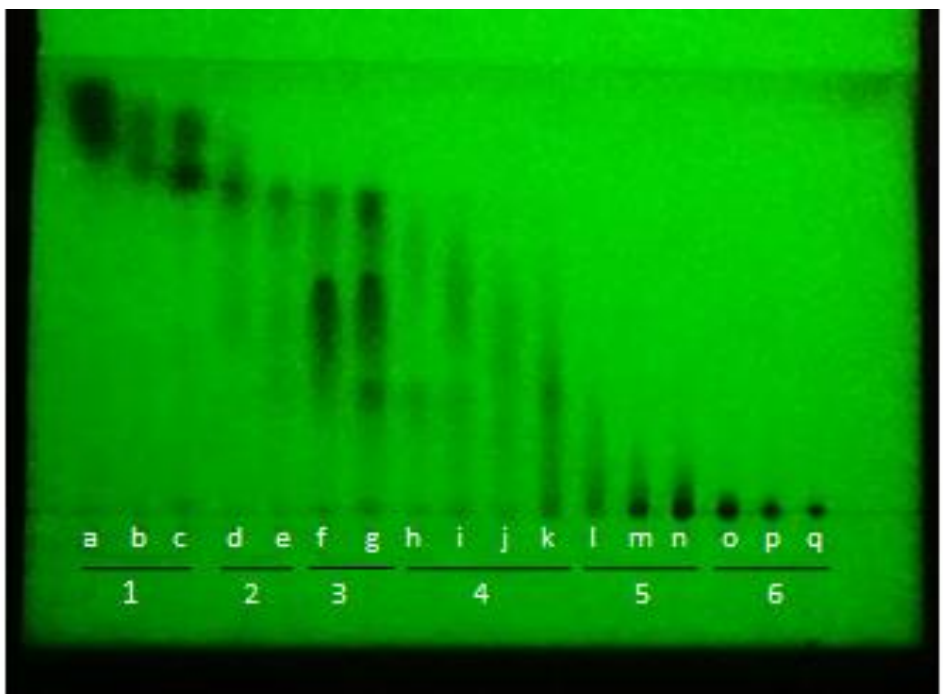

Figure 6. TLC analysis of Arecae Pericarpium methylene chloride fraction under 254 nm UV light

Seventeen eluents obtained from silica gel open column chromatography were grouped into six fractions based on their spots similarity on TLC plate.

3. Suppression of LPS-induced NO production and cell viability assay by silica CC fractions from methylene chloride fraction

The inhibition effect of MC1 to MC6 fractions on LPS-induced NO production in RAW264.7 macrophages were tested with Griess reagent assay and compared to MC fraction and positive control, AMT. All fractions were tested dose-dependently at 5, 10, 25, and 50 μg/mL.

Most fractions showed cytotoxicity at 50 μg/mL, so the NO inhibition activity was compared at lower concentrations. MC1 fraction inhibited NO production with IC_{50} value lower than 5 μg/mL. IC_{50} value of other fractions were 8.56 μg/mL (MC2 fraction), 9.36 μg/mL (MC3 fraction), 8.91 μg/mL (MC4 fraction), and more than 50 μg/mL (MC5 and MC6 fractions). Based on this result, further separation was performed on MC1 fraction.

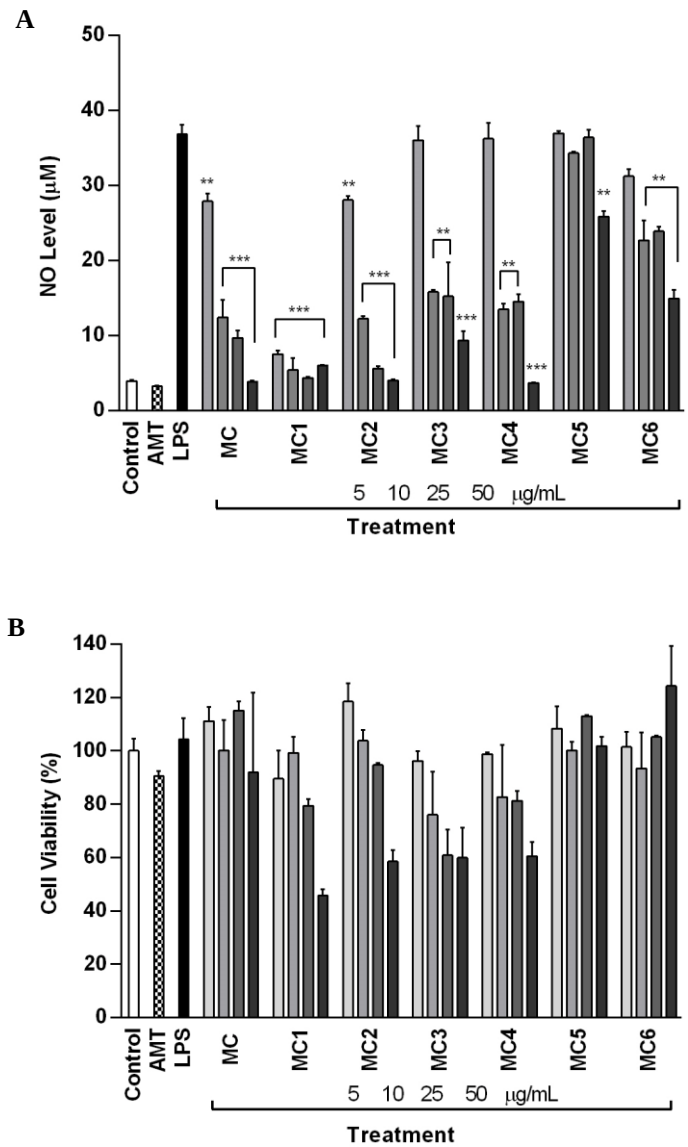

Figure 7. Effect of silica CC fractions from methylene chloride fraction on (A) NO production and (B) Cell viability

Data were derived from three independent experiments and are expressed as mean ± SD. (**) *P<0.01* and (***) *P<0.001* indicate significant difference from the LPS-stimulated group.

4. Separation of MC1 fraction

MC1 fraction was subjected to silica gel open column chromatography. Hexane-ethyl acetate-*n*-butanol with ratio (3:2:0.05 v/v) and (2.75:2.25:0.05 v/v) were selected as mobile phase. Fifteen fractions with volume of 125 mL each were collected and analyzed with TLC. After elution, the TLC plate was dried and observed under day light and UV light (254 nm and 366 nm). The spots showed fluorescence under 254 nm but did not show any phosphorescence under 366 nm. After 2 hours, yellow spots were detected under day light.

Except for the last 4 spots on TLC plate, it was difficult to decide which fractions to combine due to the different Rf of the spots. All fractions were analyzed with HPLC. HPLC condition was as follows: eluents water (A) and acetonitrile (B); gradient program: 0-5 min (5-20% B), 5-25 min (20-51% B), 25-30 min (51-55% B), 30-35 min (55-68% B), 35-40 min (68-100% B) in 1 mL/min. Samples were prepared in 500 µg/mL and 10 µL was injected to HPLC system. The HPLC run was detected by ELSD and UV detector set at 254 nm. Fractions that exhibited similar chromatogram in both ELSD and UV detection mode were combined. Seven fractions in total were obtained as described in below figure and labeled as MC1A – MC1G with following yield: 1314.5 mg, 335.3 mg, 180.5 mg, 139.4 mg, 222.3 mg, 39.2 mg, and 9.2 mg, respectively.

A

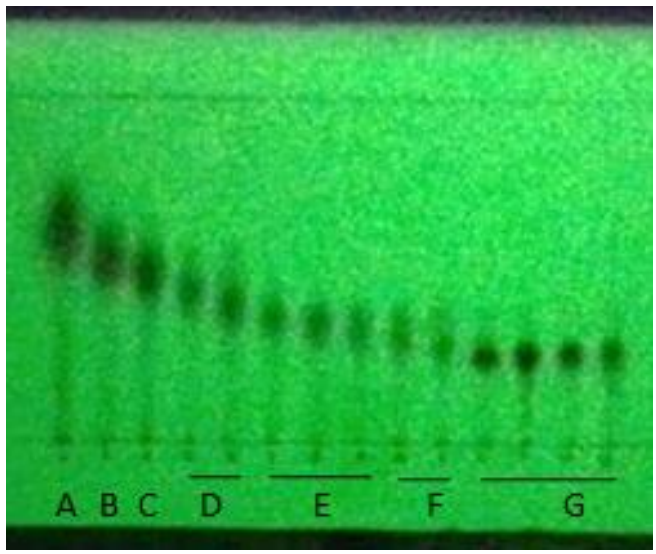

B

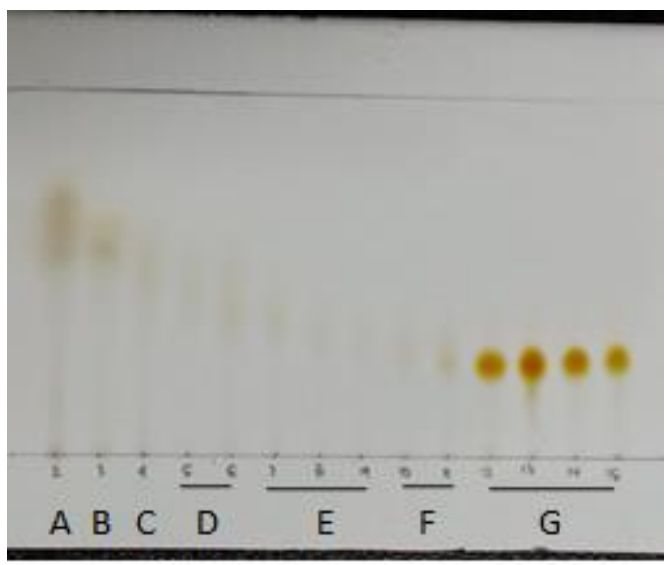

Figure 8. TLC chromatogram of silica CC fractions from MC1 fraction under (A) UV 254 nm and (B) day light

MC1G fraction was obtained as single compound and labeled as compound I. MC1A fraction was subjected through Diaion® HP-20 open column chromatography and compound II was obtained from 20 and 30% methanol elution.

5. Suppression of MC1A – MC1G fraction on LPS-induced NO production in RAW 264.7 macrophages

MC1A-MC1G obtained from silica column chromatography separation were monitored for their suppression effect on LPS-induced NO production in RAW 264.7 macrophages. All fractions were tested at 2.5, 5, and 10 µg/mL and compared to MC1 fraction. MC1A fraction showed the strongest inhibition of LPS-induced NO production with IC_{50} value 1.16 µg/mL, followed by MC1G with IC_{50} value 3.92 µg/mL and MC1B with IC_{50} value 7.13 µg/mL. The IC_{50} values of MC1C, MC1D, and MC1E fractions were more than 10 µg/mL. Cell viability were in accepted range (> 80%) for all fractions, except for MC1G fraction which showed cytotoxicity at 10 µg/mL.

MC1A fraction was able to inhibit LPS-stimulated PGE_2 production as well as shown in Figure 9C. Cells treated with 0.5 µg/mL of MC1A fraction showed more than 50% reduction of PGE_2 production. Other concentrations inhibited PGE_2 production to lower level than the positive control, TPCK (10 µM).

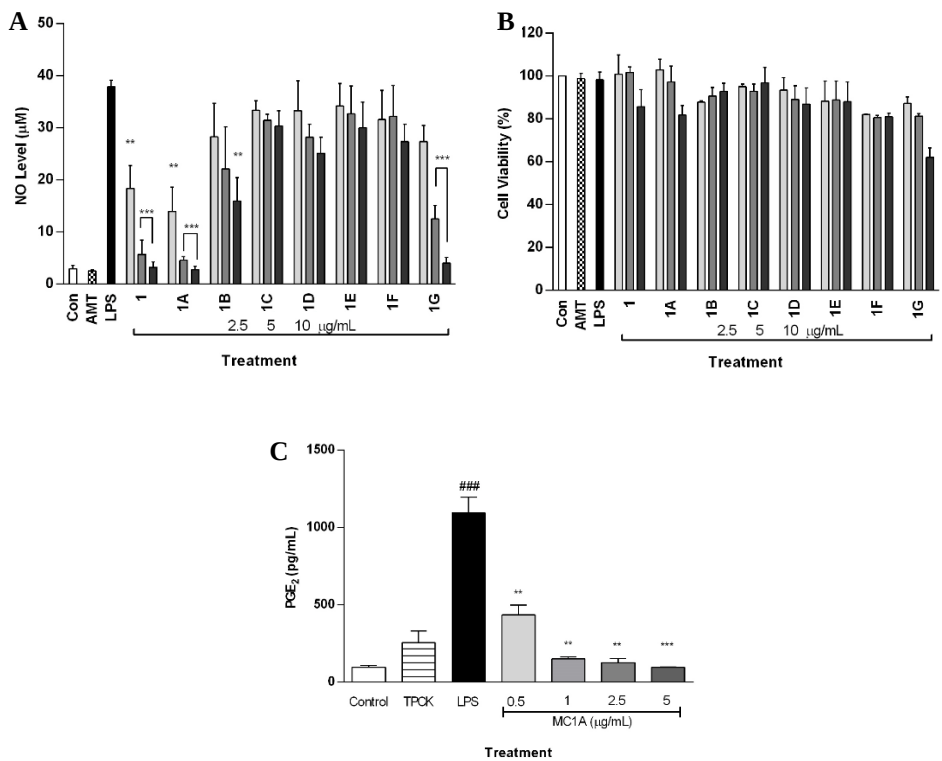

Figure 9. Effect of MC1 silica CC fractions on (A) NO production and (B) Cell Viability. (C) Effect of MC1A fraction on PGE_2 production

Data were derived from three independent experiments and are expressed as mean ± SD. (**) *P<0.01* and (***) *P<0.001* indicate significant difference from the LPS-stimulated group. (###) *P<0.001* indicates significant difference from the unstimulated control group. Control (vehicle), LPS (LPS + vehicle)-treated cells alone, 1 (MC1 fraction), 1A – 1G (MC1A – MC1G fraction). AMT and TPCK 10 μM were used as control positive.

6. Separation of MC1B fraction

The separation of MC1B fraction was initiated with HPLC analysis. HPLC condition was set as following: eluents water + 0.1% FA (A) and methanol + 0.1% FA (B); gradient program: 0-25 min (18% B), 25-35 min (18-100% B), 35-43 min (100 % B), 45-55 min (saturation with 18% B) in 0.3 mL/min. Sample was prepared in methanol with concentration of 100 µg/mL and 5 µL was injected. The column used for analysis was Zorbax SB-C18 column (75 mm x 4.6 mm id, 3.5 µm particle size).

Based on the HPLC chromatogram which showed nine peaks, HPCCC was selected to separate and isolate major peaks. Several solvent system were tested to investigate the optimum partition coefficient (*K*) as shown in Table 1 and HEMW solvent system (2:5:1:4 v/v/v/v) was selected for HPCCC operation. This solvent system was chosen because the peak no 6 and 8 as shown in Figure 10, which are the major peaks in this fraction, could be separated from other peaks.

The HPCCC operation was conducted as described in methods section. However, the target compounds could not be separated from other peaks. It might be caused by the UV detection wavelength selection which detected all compounds at their maximum absorption so all of the peaks were overlapped. The HPCCC chromatogram of MC1B fraction is shown in Figure 11. The yield of the target peak was 40.2 mg.

The peak was further isolated by preparative HPLC as described in methods section. Compound III, mixture of compound IV and V, and compound VI were obtained with yield 1.0 mg, 5.0 mg, and 0.6 mg, respectively. The representative HPLC chromatogram is shown in Figure 12.

Table 1. Solvent system screening for MC1B fraction separation

HEMW	*K* Value								
Ratio	1	2	3	4	5	6	7	8	9
2:5:2:5	1.48	2.94	1.87	5.80	2.66	5.64	5.68	3.37	3.75
2:5:1:4	0.42	2.11	1.49	7.26	2.19	**4.15**	**4.27**	**4.18**	2.08
2:4:2:4	0.89	1.37	1.85	1.95	2.44	2.72	2.79	3.66	4.07
3:4:2:4	0.89	1.61	1.10	2.83	1.53	2.08	2.59	1.62	2.04

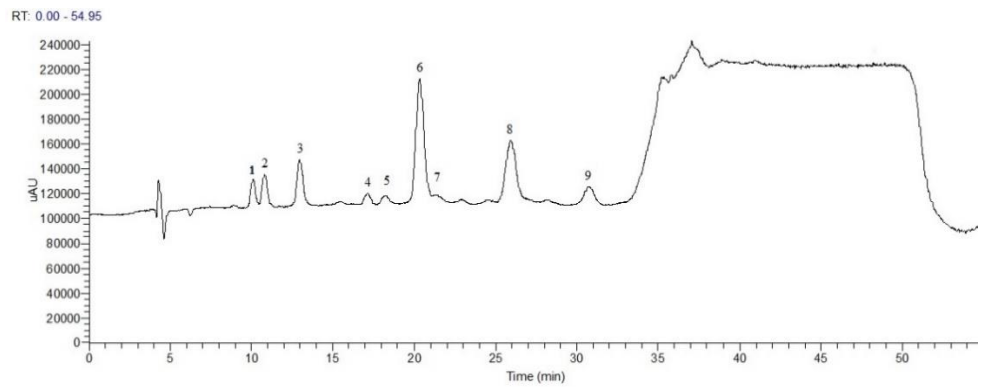

Figure 10. HPLC chromatogram of MC1B fraction

HPLC chromatogram of MC1B fraction analysis. Sample injection 5 µL from 100 µg/mL in methanol solution. Diode array detector was used for peak detection.

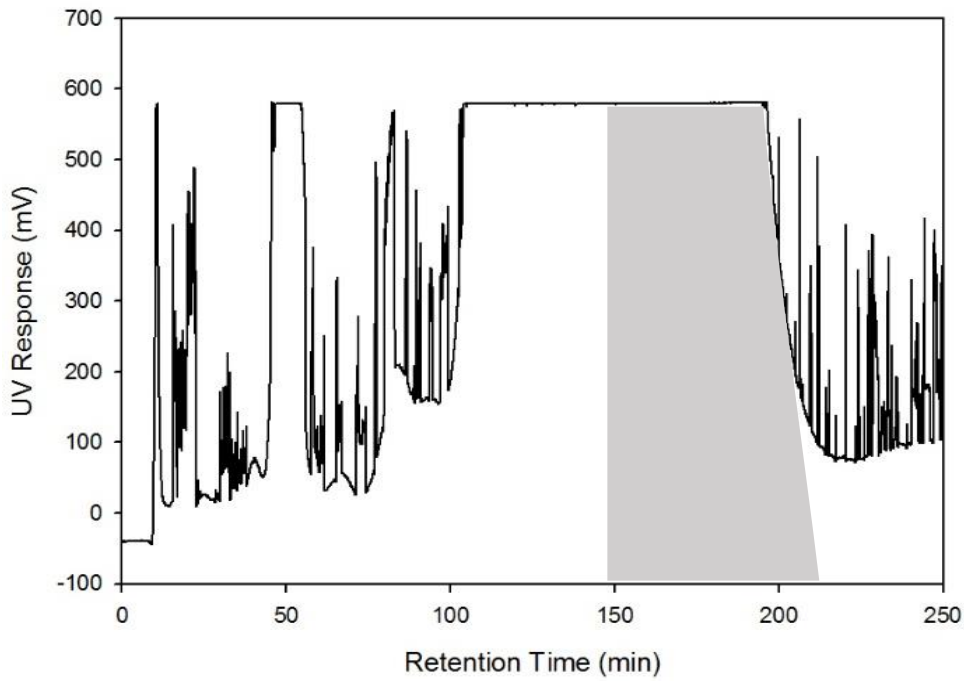

Figure 11. HPCCC chromatogram of MC1B fraction

HPCCC chromatogram of MC1B fraction is shown in above figure. The stationary phase retention was 70.11%. Sample injection was 130.3 mg in 6 mL of solvent system mixture and detected with UV detector at 280 nm for 200 minutes. The gray area marks the target peaks (149 min – 210 min). Peaks were detected with UV detector set at 280 nm.

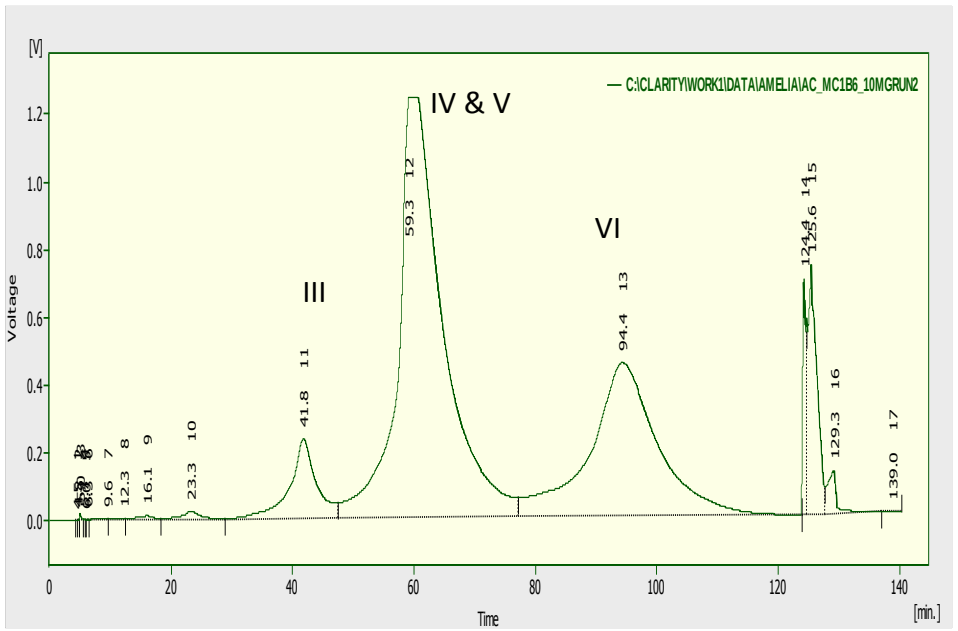

Figure 12. Preparative HPLC chromatogram of MC1B fraction after HPCCC separation

Target peaks separated from other peaks with HPCCC were isolated using preparative HPLC method. Separation was performed in isocratic mode (18% of MeOH with 0.05% FA) with UV detector set at 246 nm.

7. Separation of Ethyl Acetate Fraction

The ethyl acetate fraction was subjected to Diaion® HP-20 resin column chromatography and eluted with aqueous methanol in increasing concentration from 20%, 40%, 60%, and 80% methanol. The 20% MeOH fraction showed NO inhibition activity and was further separated with HPCCC. Several solvent system was tested to estimate the optimum *K* values and HEMW system (2:5:2:5 v/v/v/v) was selected for HPCCC operation.

The operation of HPCCC separation was conducted with UV detection set at 280 nm. The sample was weighed for 200.3 mg and dissolved in 6 mL of upper phase and lower phase mixture. The operation was performed for 200 minutes. Compound VII, VIII, and II were obtained with yield 18.7 mg, 3.3 mg, and 25.4 mg, respectively. The HPCCC chromatogram is shown in Figure 14.

Table 2. Solvent system evaluation for EA-20% MeOH fraction separation

Solvent system	*K* Value				
	1	2	3	4	5
BuOH - DW (5:5)	-	-	-	-	8.70
BuOH - MeOH - DW (5:1:5)	-	3.89	-	11.75	2.35
BuOH - MeOH - DW (5:1:3)	-	3.00	-	6.00	1.90
HEMW (2:5:2:5)	**1.61**	**0.75**	**1.15**	**2.83**	**3.48**
HEMW (2:5:2:10)	1.42	1.34	0.41	5.34	5.80

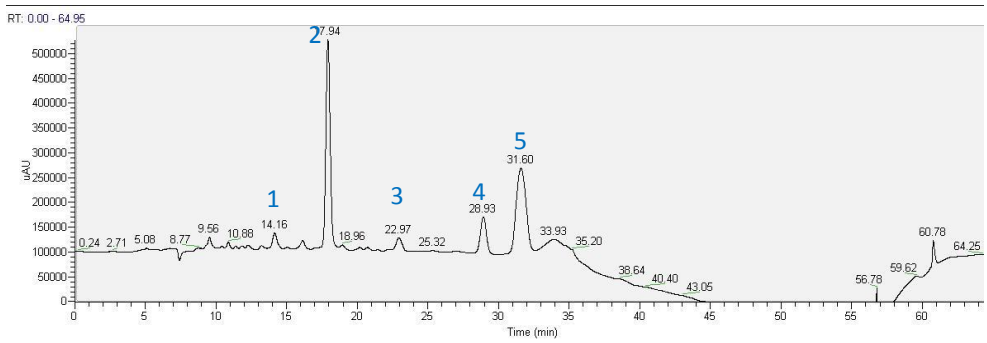

Figure 13. HPLC chromatogram of EA-20% MeOH fraction

The 20% MeOH fraction obtained from Diaion® HP-20 resin open column chromatography was analyzed with HPLC using LUNA C18 column (150 mm x 4.6 mm id, 3µm particle size). The mobile phase used was 0.1% FA in water (A) and acetonitrile (B) The separation was performed in gradient elution as following condition: 0 – 20 min (10% B), 20 – 40 min (10 – 100% B), 40 – 48 min (washing with 100% B), 50 – 60 min (column saturation with 10% B). The sample injection volume was 10 µL from 500 µg/mL concentration. Peaks were detected with diode array detector.

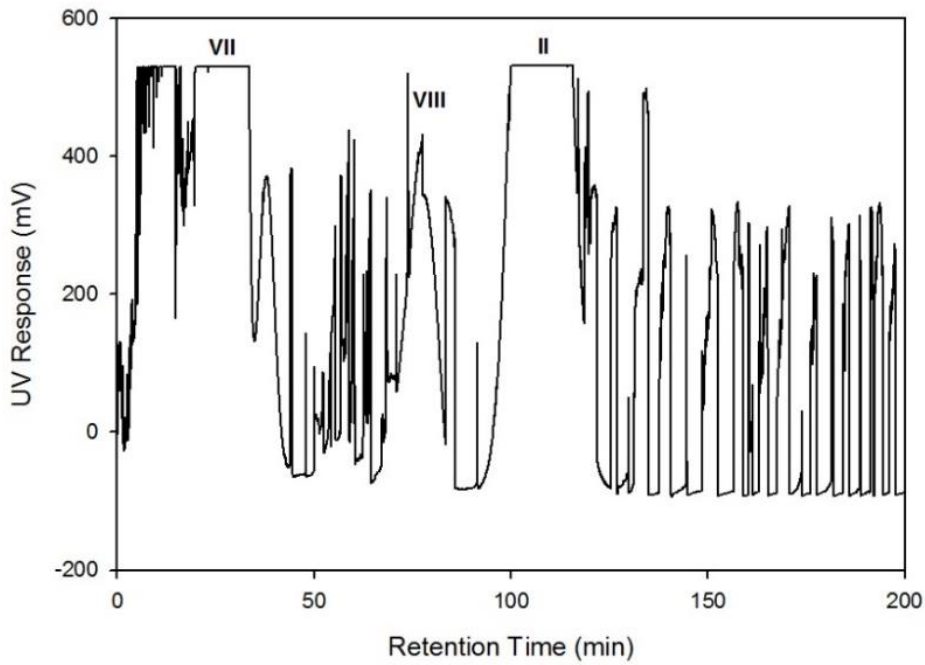

Figure 14. HPCCC chromatogram of EA-20% MeOH fraction

The HPCCC chromatogram of 20% MeOH fraction obtained from Diaion® HP-20 resin open column chromatography. Sample injection volume was 200.3 mg and detected with UV detector at 280 nm. The HPCCC separation was operated for 200 hours at 3 mL/min and 1600 rpm.

8. Suppression of LPS-induced NO production by ethyl acetate fractions obtained from Diaion® HP-20 resin column chromatography separation

Fractions obtained from Diaion® HP-20 resin column chromatography were tested at 5, 10, and 25 µg/mL. 20% MeOH fractions suppressed the LPS-induced NO production to lower level than other fractions. As shown in Figure 15, EA20 fraction showed the highest NO inhibition activity among all tested fractions with IC_{50} value 9.53 µg/mL. The IC_{50} values of other fractions were more than 25 µg/mL. The EA20 fraction might be rich of active compounds in inhibiting NO production, thus this fraction was subjected to further separation.

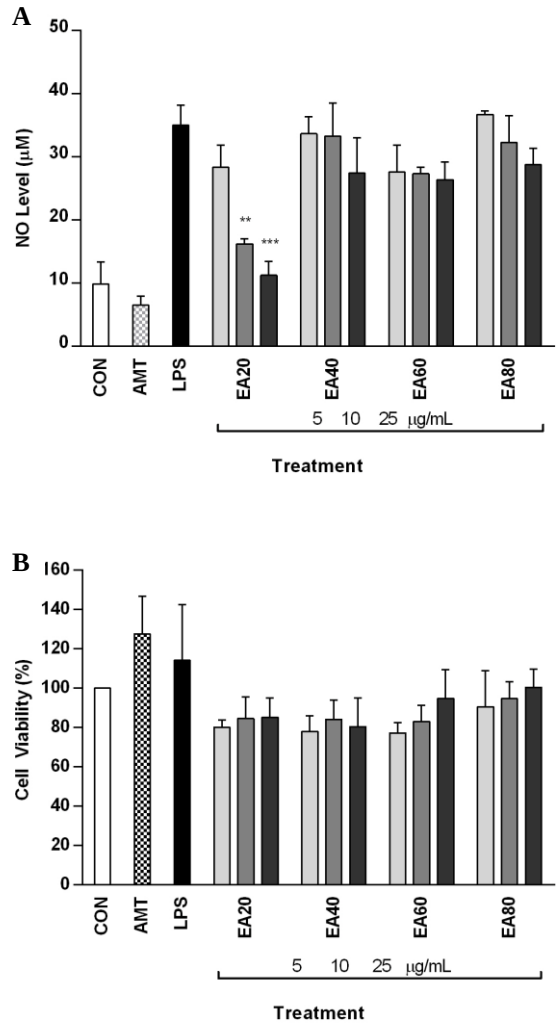

Figure 15. Effect of EA Diaion® HP-20 column fractions on (A) LPS-induced NO production and (B) cell viability

Data were derived from three independent experiments and are expressed as mean ± standard deviation (S.D). (**) *P<0.01* and (***) *P<0.001* indicate significant difference from the LPS-stimulated group. Control (vehicle), LPS (LPS + vehicle)-treated cells alone, EA20, 40, 60, and 80 (% of MeOH eluting the EA fraction). AMT 10 μM was used as positive control.

9. Structure Identification of Isolated Compounds

9.1 Identification of compound I

Compound I (MC1G fraction) was obtained as amorphous powder with slightly yellow color with >95% purity. When analyzed with HPLC-DAD detector, the UV spectrum of this compound showed maximum absorption at 218 and 280 nm. The positive-ion mode of ESI-MS showed molecular ion peak $[M+H]^+$ at m/z 307.1 and its negative-ion ESI-MS showed $[M-H]^-$ at m/z 305.1 (Figure 16).

^{1}H NMR spectrum of compound I showed signals at δ 8.35 (2H, s), 6.81 (4H, s), and 3.83 (12H, s) ppm. The ^{13}C NMR spectrum of compound I showed signal at δ 148.25 (C-2, C-6, C-9 and C-11), 134.92 (C-1 and C-10), 131.43 (C-4 and C-7), 104.37 (C-3, C-5, C-8, and C-12) and 56.25 ppm (methoxy carbons). The ^{13}C NMR spectrum of compound I was compared with ^{13}C NMR spectrum of monomer syringol [18] and almost all peaks are similar except for the peak at 131.43 ppm. Comparing the ESI-MS with another literature [19], it is proposed that this compound is a C-C dimeric syringol which has molecular weight 306 Da. The peak at 131.43 ppm is probably the attachment point of the other ring. The proposed structure is shown in Figure 18.

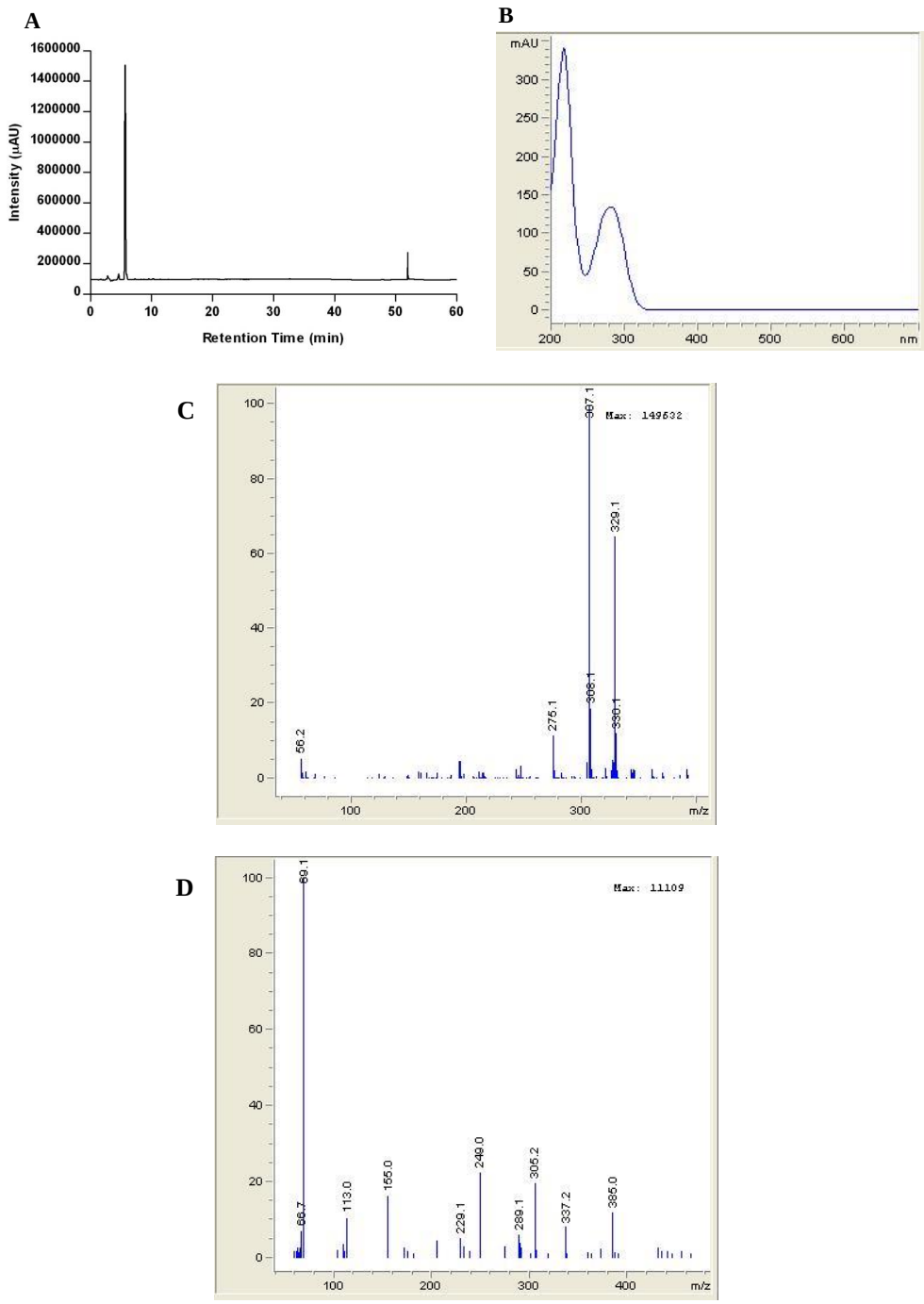

Figure 16. HPLC and ESI-MS analysis of compound I. (A) HPLC chromatogram (B) UV spectrum (C) ESI-MS positive-ion mode (D) ESI-MS negative-ion mode

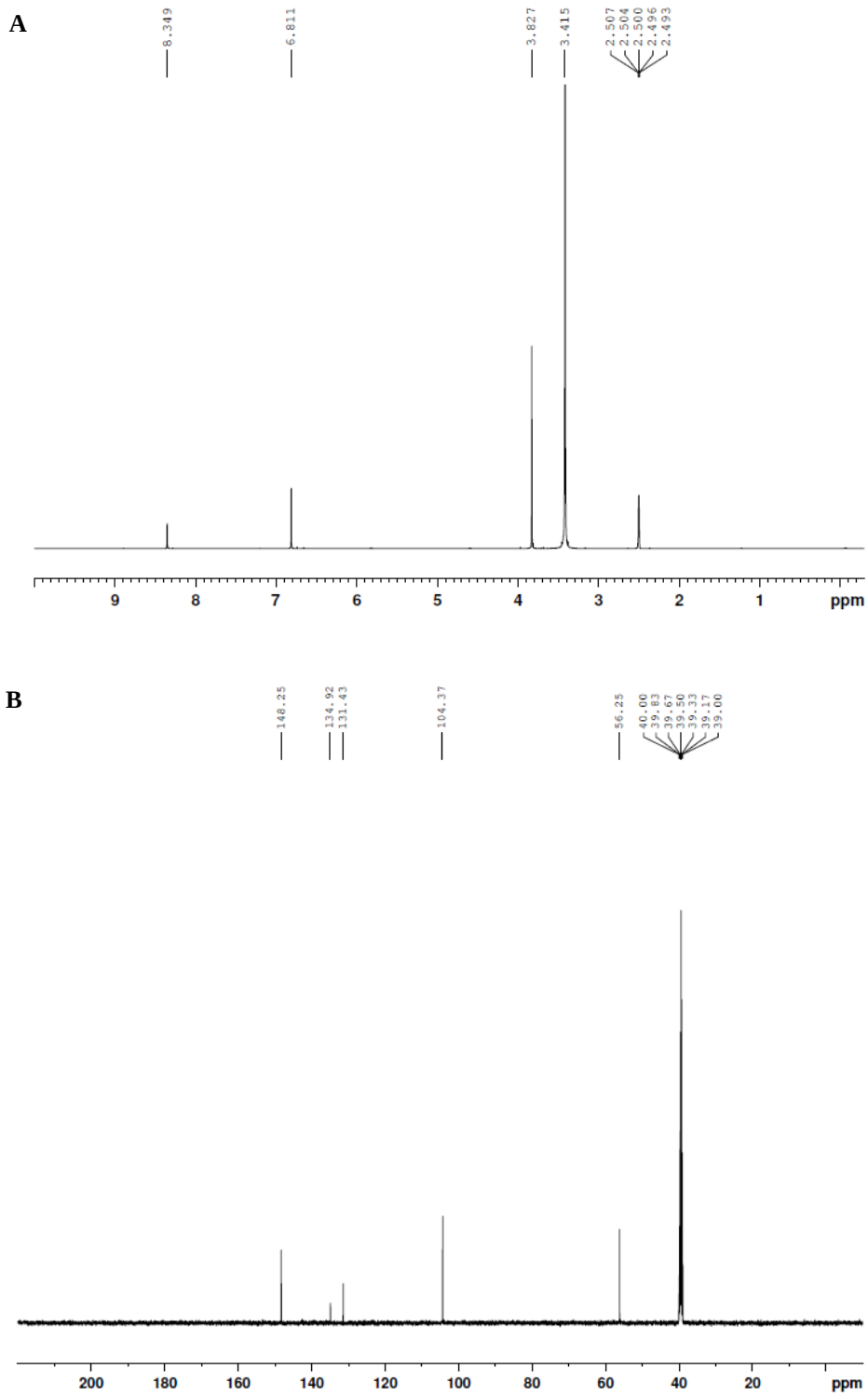

Figure 17. (A) ^{1}H NMR and (B) ^{13}C NMR spectrum of compound I at 500 MHz in DMSO-d_6

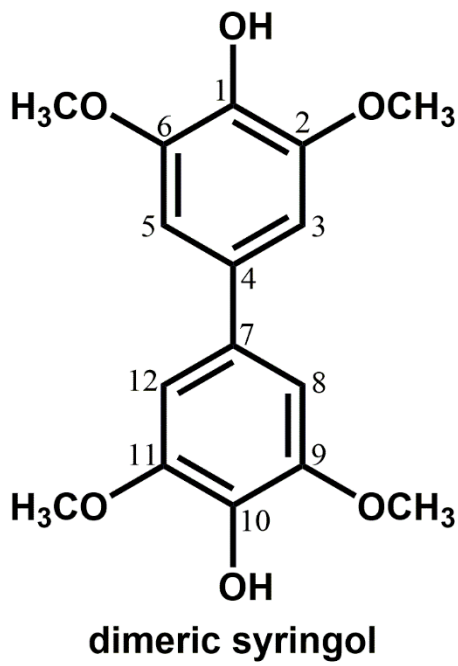

Figure 18. Proposed structure of compound I

9.2 Identification of compound II

Compound II was isolated from MC1A fraction eluted with 20% MeOH and 30% MeOH in Diaion® HP-20 resin open column chromatography. It was obtained as white to slightly gray amorphous powder. Compound II showed maximum absorption at 204, 218 and 276 nm in HPLC-DAD analysis and the negative-ion ESI-MS showed molecular ion peak $[M-H]^-$ at m/z 109.1 (Figure 19).

^{1}H NMR spectrum of compound II showed signals for aromatic ring group at δ 6.74 (2H, m, *J* = 9.5 Hz, 3.5 Hz) and 6.58 (2H, m, *J* = 9.5 Hz, 3.5 Hz) and hydroxyl group at δ 8.82 ppm (1H, br s). The ^{13}C NMR spectrum of compound II showed signal at δ 145.34 (C-1 and C-2), 119.39 (C-4 and C-5) and 115.77 (C-3 and C-6). The NMR spectral data were in alignment with reference data [20] thus compound II was assigned as catechol.

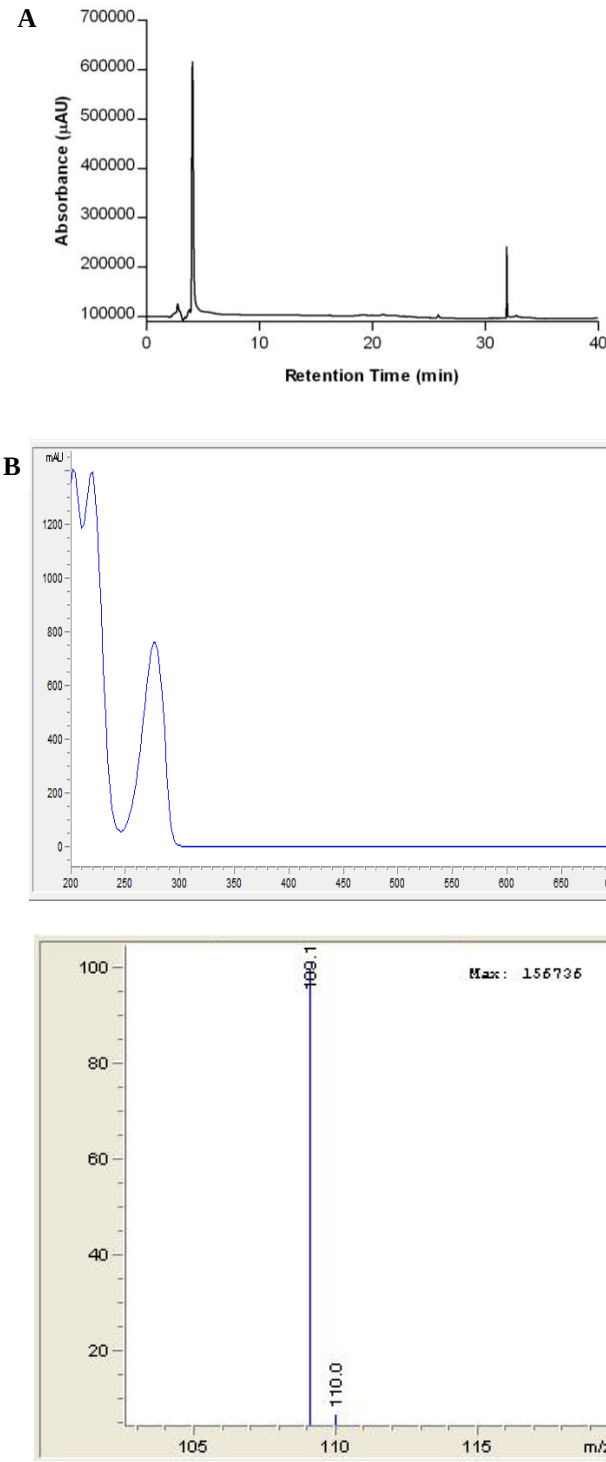

Figure 19. HPLC and ESI-MS analysis of compound II (A) HPLC chromatogram (B) UV spectrum (C) ESI-MS negative-ion mode spectrum

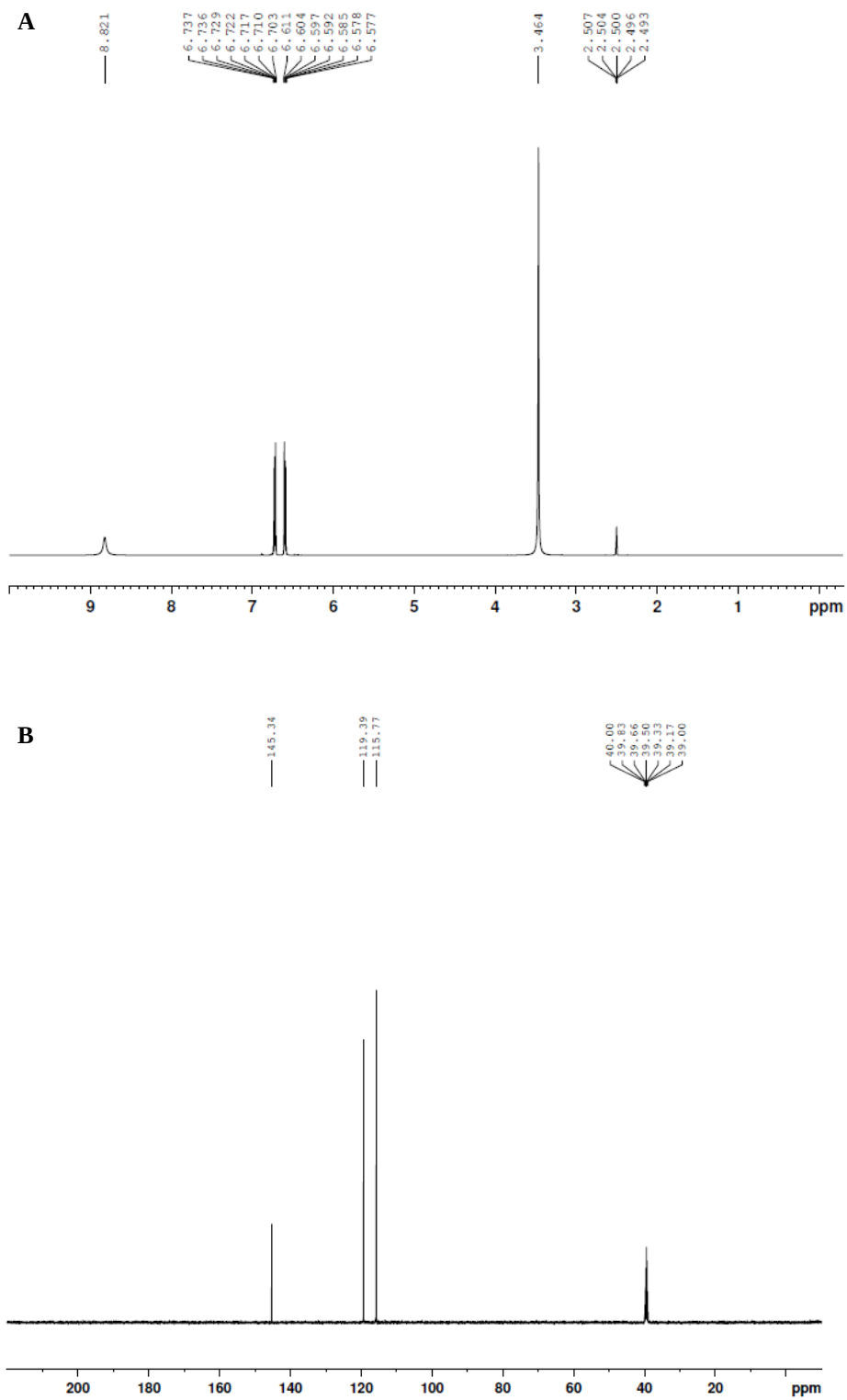

Fig 20. (A) ^{1}H NMR and (B) ^{13}C NMR spectrum of compound II at 500 MHz in DMSO-d6

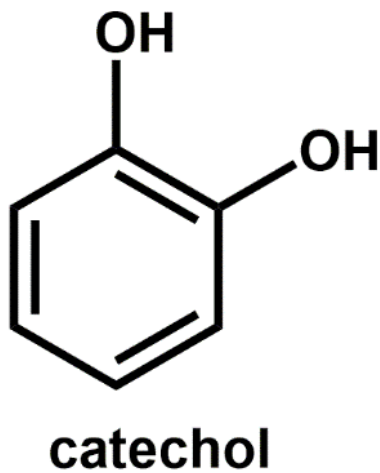

Figure 21. Structure of catechol

9.3 Identification of compound III

Compound III was obtained as white amorphous powder from separation of MC1B fraction. The UV detection of compound III showed maximum absorption at 196, 220, and 284 nm. The ESI-MS negative-ion mode spectra showed base ion peak at m/z 407.0 and an ion peak at m/z 121.1. Observing the NMR spectra, the molecular weight of the compound is most probably 122 Da.

^{1}H NMR spectrum of compound III showed signals for aldehyde proton attached to aromatic ring at δ 9.76 (1H, s), aromatic ring group at δ 7.75 (2H, d, J = 8.5 Hz) and 6.92 ppm (2H, d, J = 8.5 Hz). Due to the low yield of compound III, the ^{13}C NMR spectrum was not available. Instead, 2D NMR (COSY, HSQC, and HMBC) analysis was performed. Based on the HSQC and HMBC NMR spectra, the carbon signals detected at δ 191.11 (C-7), 163.95 (C-4), 132.33 (C-1), 128.28 (C-2 and C-6) and 116.03 ppm (C-3 and C-5) were correlated with the proton NMR and summarized in Table 3. The NMR spectral data of compound III were in alignment with reference [21] thus this compound was assigned as 4-hydroxybenzaldehyde.

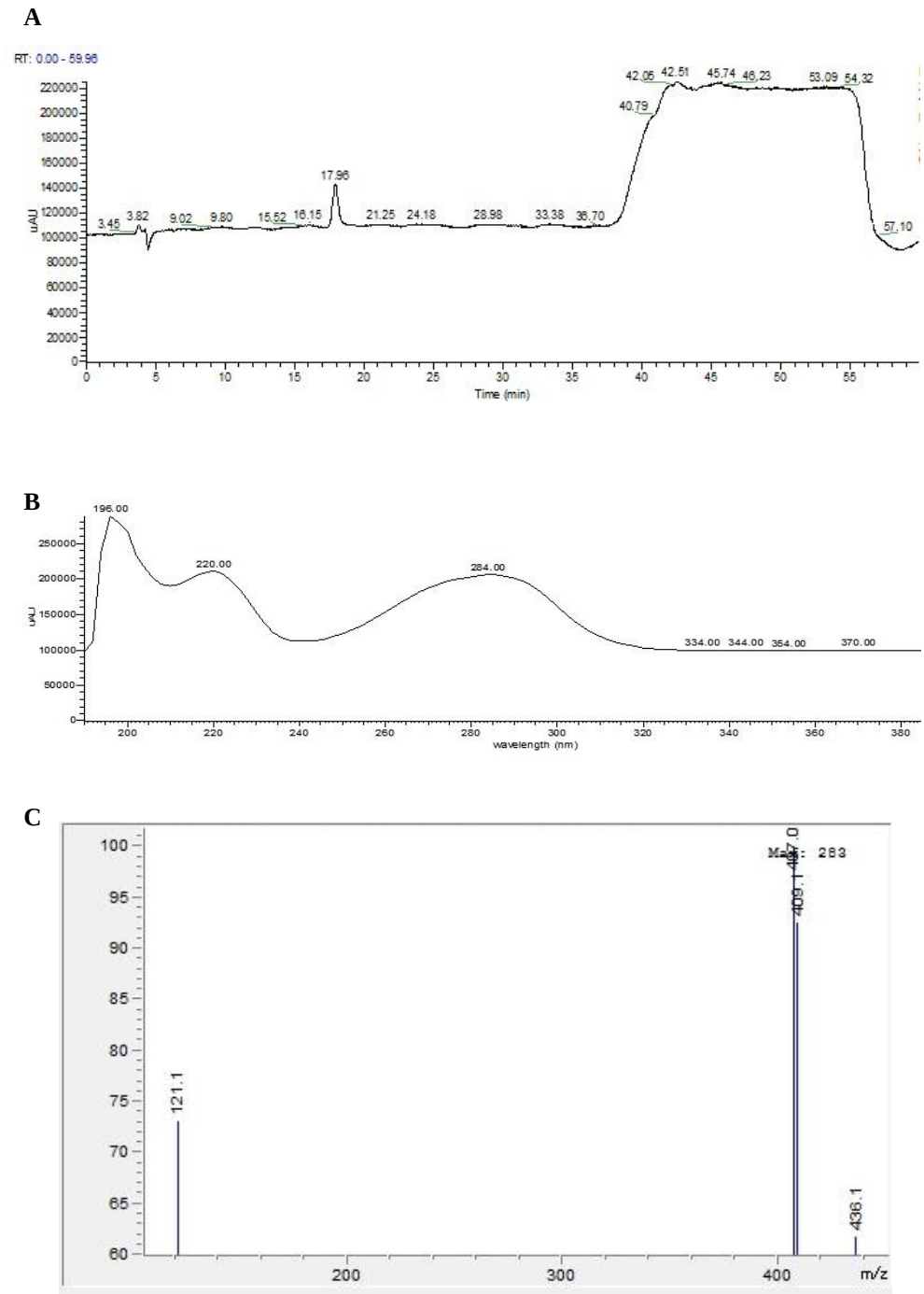

Figure 22. HPLC and ESI-MS analysis of compound III (A) HPLC chromatogram (B) UV spectrum (C) ESI-MS negative-ion mode spectrum

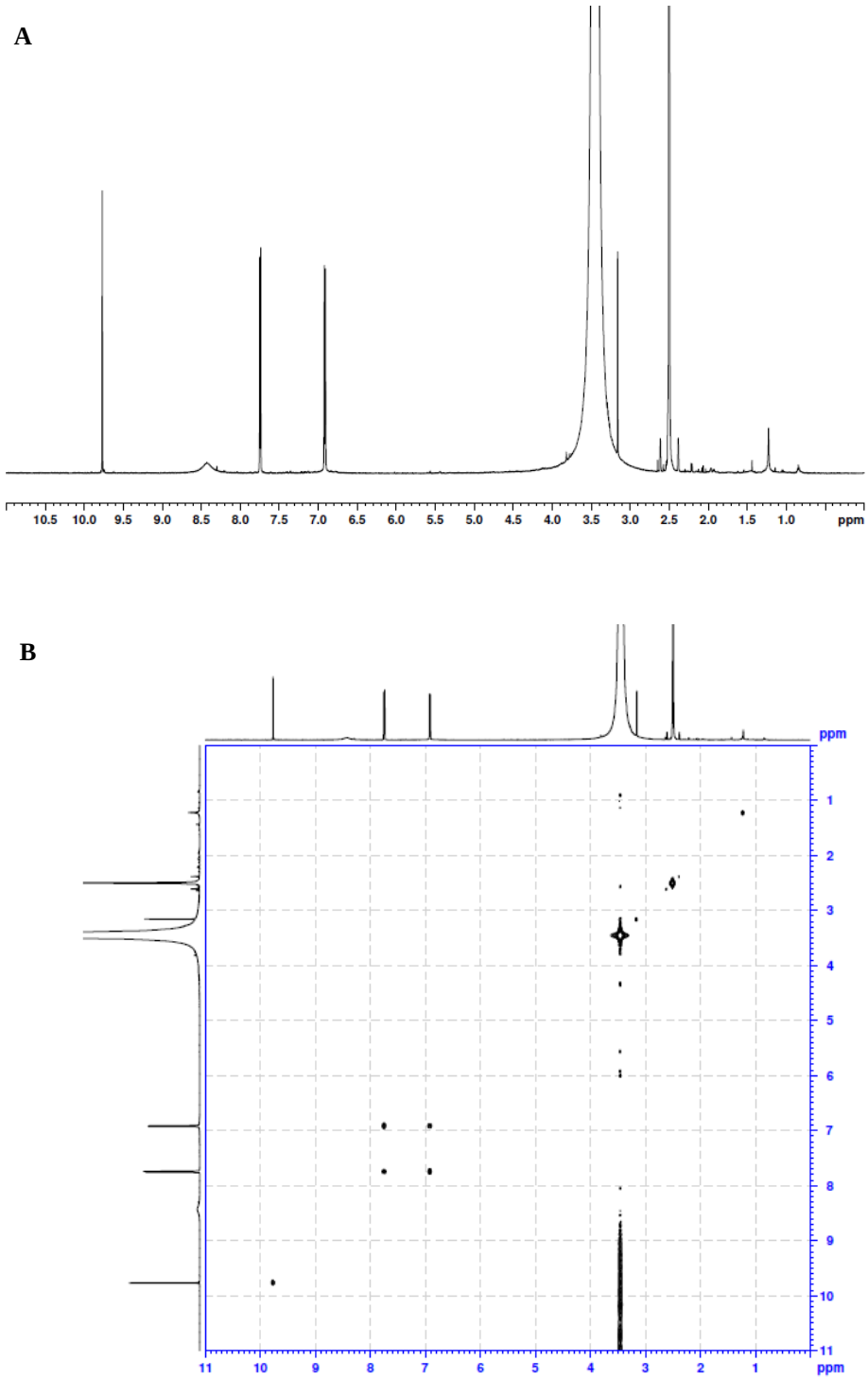

Figure 23. NMR spectra of compound III (A) ^{1}H NMR spectrum (B) ^{1}H-^{1}H COSY spectrum 600 MHz in DMSO-d_6

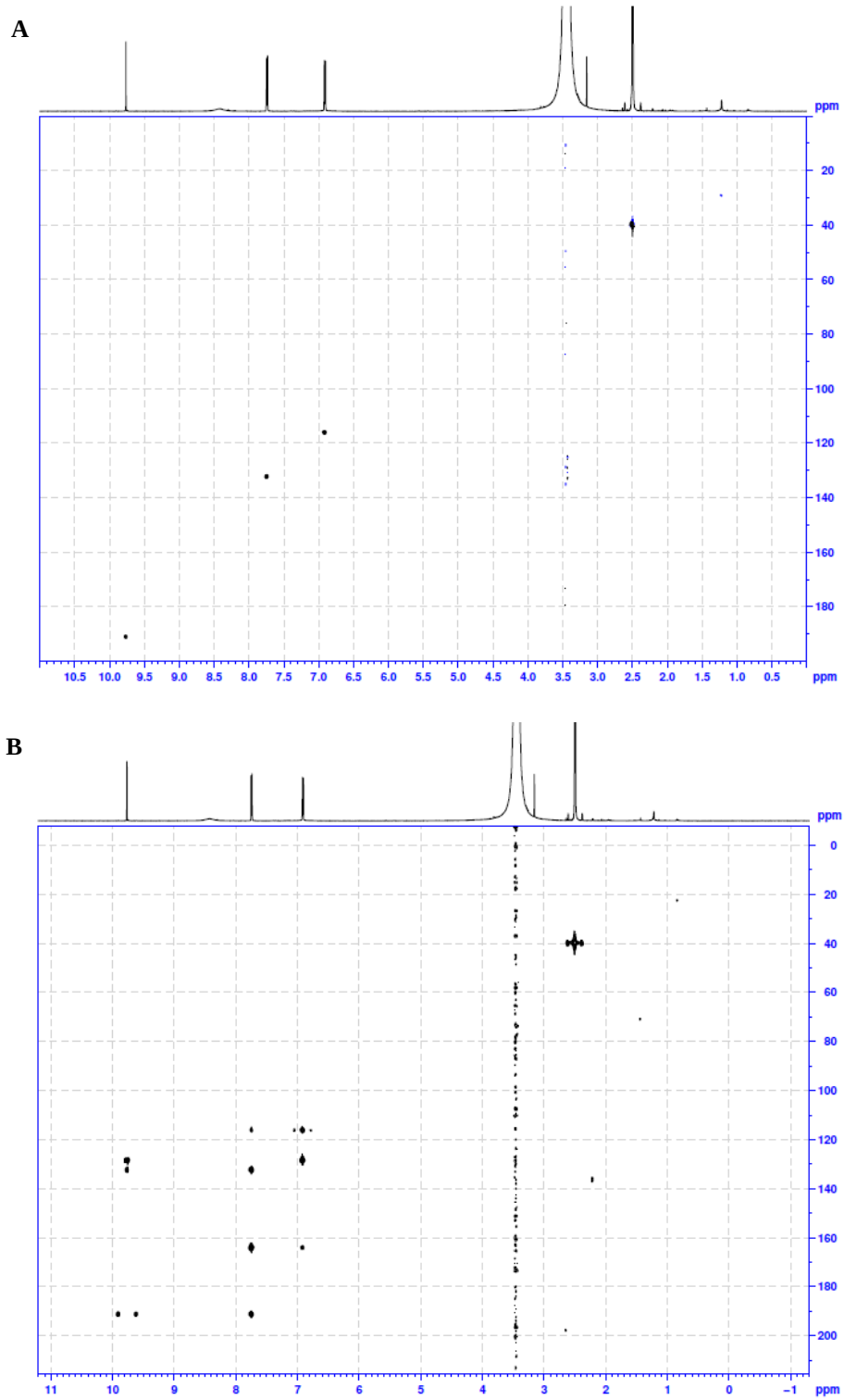

Figure 24. NMR spectra of compound III (A) ^{1}H-^{13}C HSQC NMR spectrum (B) ^{1}H-^{13}C HMBC spectrum 600 MHz in DMSO-d_6

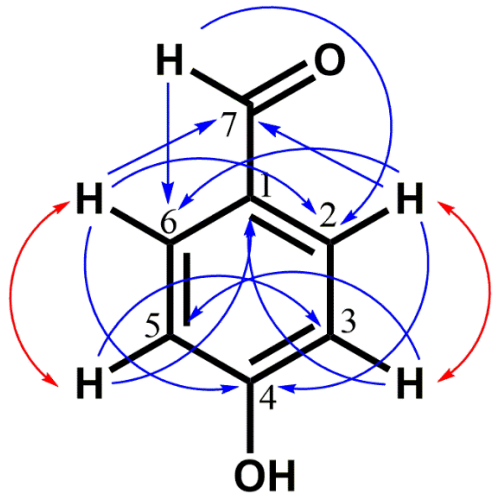

4-hydroxybenzaldehyde

Figure 25. Structure of compound III

9.4 Identification of compound IV and V

Compound IV and V were identified as a mixture. When it was analyzed with LC-ESI/MS, the compounds showed different molecular ion peaks in positive and negative-ion mode. The NMR spectra also showed that there were two different structures in the sample. The UV spectra showed maximum absorption at 198, 222, 276, and 304 nm. The positive-ion mode of ESI-MS showed molecular ion peak at m/z 282.3 while the negative-ion mode at m/z 476.9. Peaks that might relate to each other are peaks at m/z 137.0 and 153.1 in positive-ion mode and m/z 134.8 and 151.0 in negative-ion mode.

^{1}H NMR spectrum of compound IV and V mixture showed signals for aldehyde proton attached to aromatic ring at δ 9.73 (1H, s), aromatic ring group at δ 7.82 (2H, d, *J* = 8.5 Hz), 7.40 (1H, d, *J* = 7.6 Hz), 7.35 (1H, s), 6.92 (1H, d, *J* = 7.6 Hz) and 6.84 ppm (2H, d, *J* = 8.5 Hz). Due to the low yield of obtained compounds, the ^{13}C NMR spectrum was not available. 2D NMR (^{1}H-^{1}H COSY, ^{1}H-^{13}C HSQC, and ^{1}H-^{13}C HMBC) was performed. Observing the HSQC and HMBC NMR spectra, the carbon signals were detected at δ 190.9 (C-7 of compound IV), 154.0 (C-4 of compound IV), 148.5 (C-3 of compound IV), 128.0 (C-1 of compound IV), 126.3 (C-6 of compound IV), 110.32 (C-2 of compound IV), 26.1 ppm (methyl at ketone group); 196. 3 (C-7 of compound V), 162.1 (C-4 of compound V), 130.7 (C-2 and C-6 of compound V), 128.5 (C-1 of compound V), 115.4 (C-5 of compound IV), 115.0 (C-5 of compound V), and 55.3 (methoxy carbon). The NMR spectra data were compared with reference [22, 23] thus compound IV was assigned as vanilic aldehyde and compound V as 4-hydroxyacetophenone. The data are summarized in Table 3.

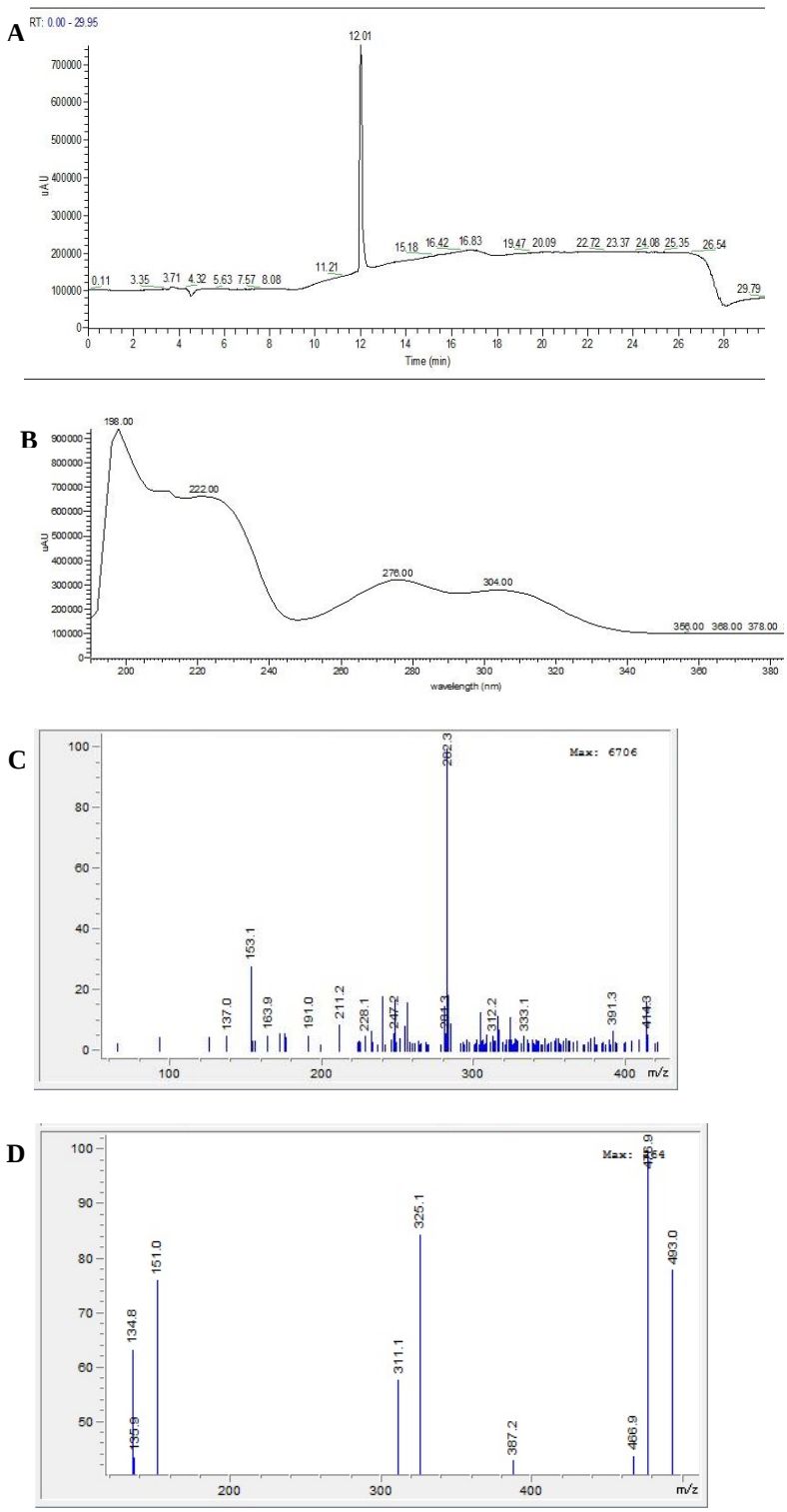

Figure 26. HPLC and ESI/MS analysis of compound IV and V mixture. (A) HPLC chromatogram (B) UV spectrum (C) ESI-MS positive-ion mode (D) ESI-MS negative-ion mode

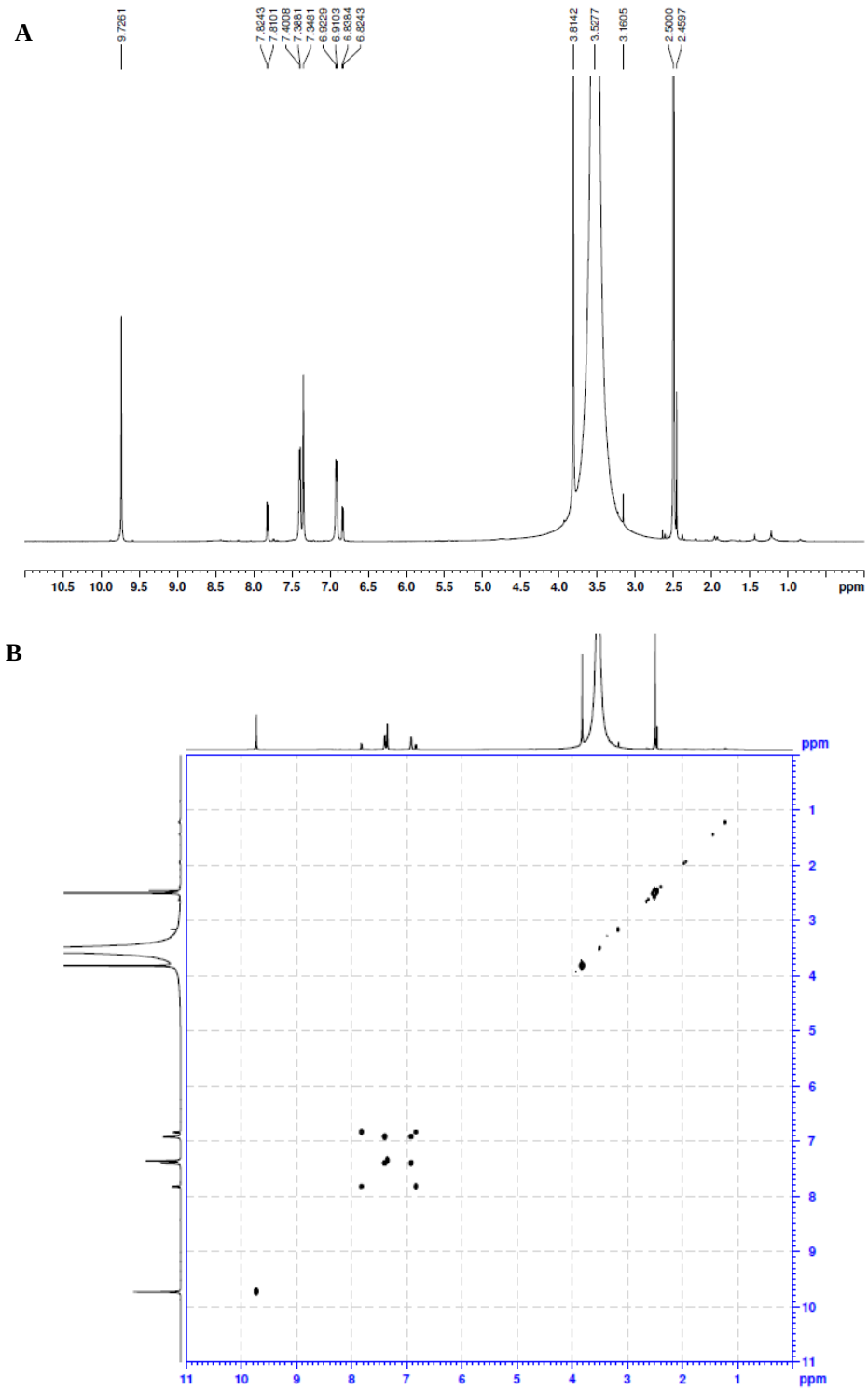

Figure 27. NMR spectra of Compound IV and V mixture at 600 MHz in DMSO-d_6 (A) ^{1}H NMR spectrum (B) ^{1}H-^{1}H COSY spectrum

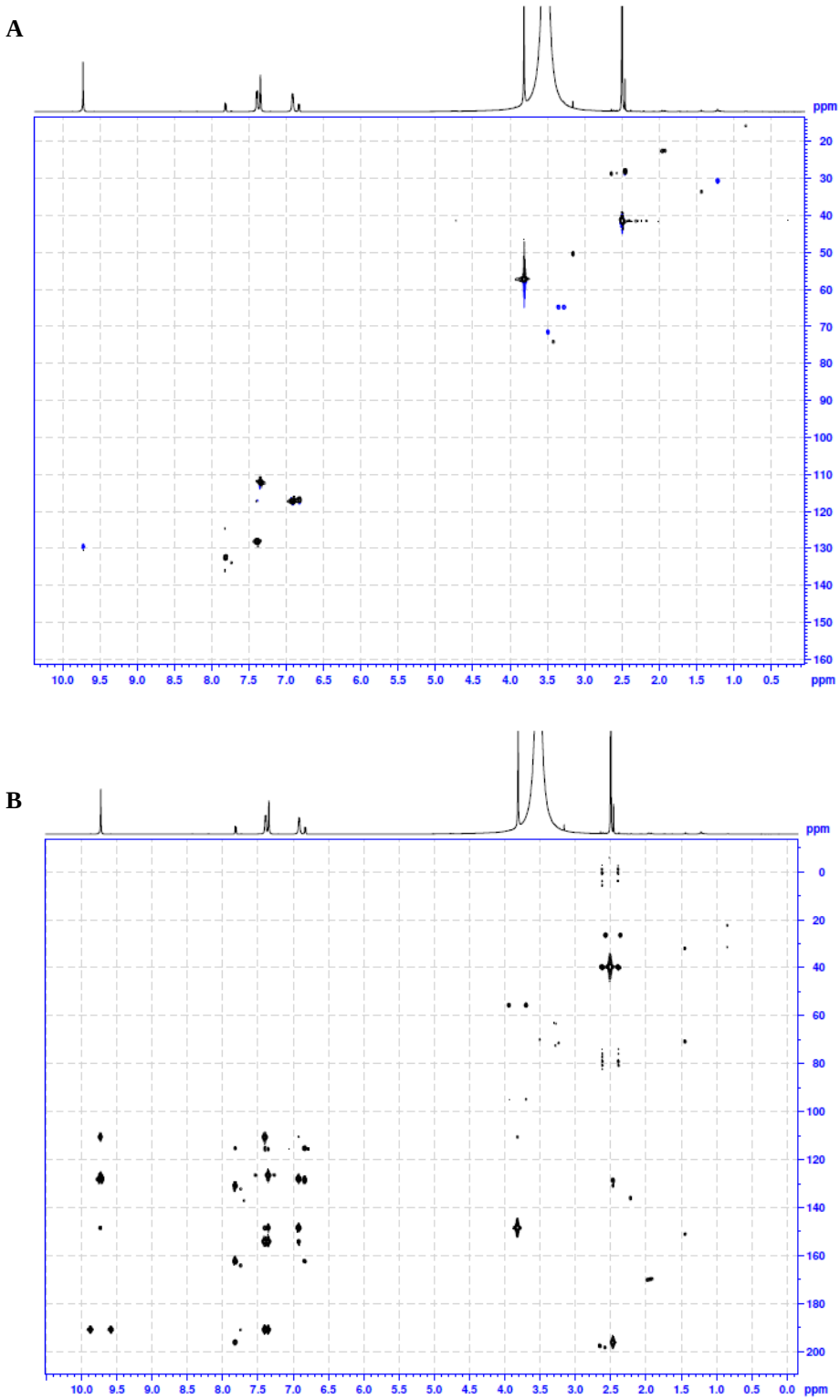

Figure 28. NMR spectra of Compound IV and V mixture at 600 MHz in DMSO-d_6 (A) ^{1}H-^{13}C HSQC spectrum (B) ^{1}H-^{13}C HMBC spectrum

A

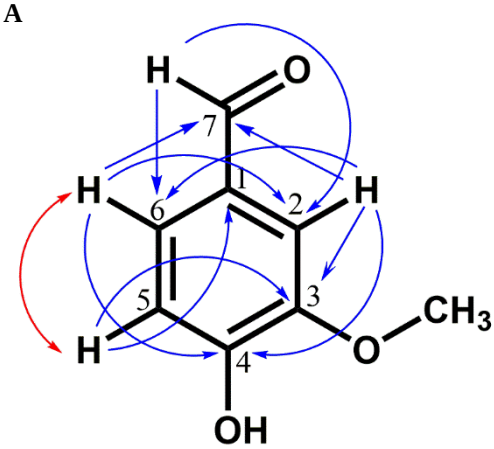

vanillic aldehyde

B

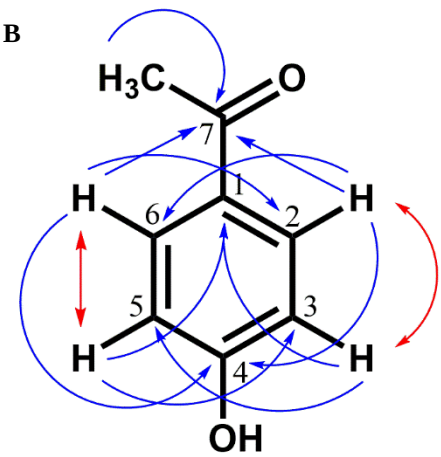

4-hydroxyacetophenone

Figure 29. Structure of (A) compound IV and (B) compound V with HMBC and COSY correlation

9.5 Identification of compound VI

Compound VI was isolated from MC1B fraction and obtained as off white solid. It has maximum absorption at 200, 214, 232, 280, and 310 nm. The ESI-MS positive-ion mode spectrum showed molecular ion peak at m/z 167.1 and the negative-ion mode spectrum showed molecular ion peak at m/z 165.1.

^{1}H NMR spectrum of compound VI showed signals of aromatic ring protons at δ 7.49 (1H, dd, *J* = 8.2 Hz, 1.9 Hz), 7.42 (1H, d, *J* = 1.7 Hz), 6.85 (1H, d, *J* = 8.2 Hz), methoxy proton at 3.81 (3H, s) and ketone proton at 2.48 ppm (3H, s). Due to the low yield of obtained compound, the ^{13}C NMR spectrum was not available so 2D NMR (^{1}H-^{1}H COSY, HSQC, and HMBC) was performed to determine the carbon peaks. Observing the HSQC and HMBC NMR spectra, the carbon signals were detected at δ 196. 3 (C-1), 152.0 (C-4), 147.7 (C-3), 123.4 (C-6), 114.7 (C-5), 110.8 (C-2), 55.3 (methoxy carbon), 26.1 ppm (methyl at ketone group). One impurity peak was found at δ 8.44 ppm attached to δ 165.9 ppm. It is assumed to be trace of formic acid used in preparative HPLC separation solvent system which might not completely evaporated. The summary of the spectral data is shown in Table 3. The NMR spectral data were in alignment with reference data [24]. Thus, compound VI was assigned as apocynin.

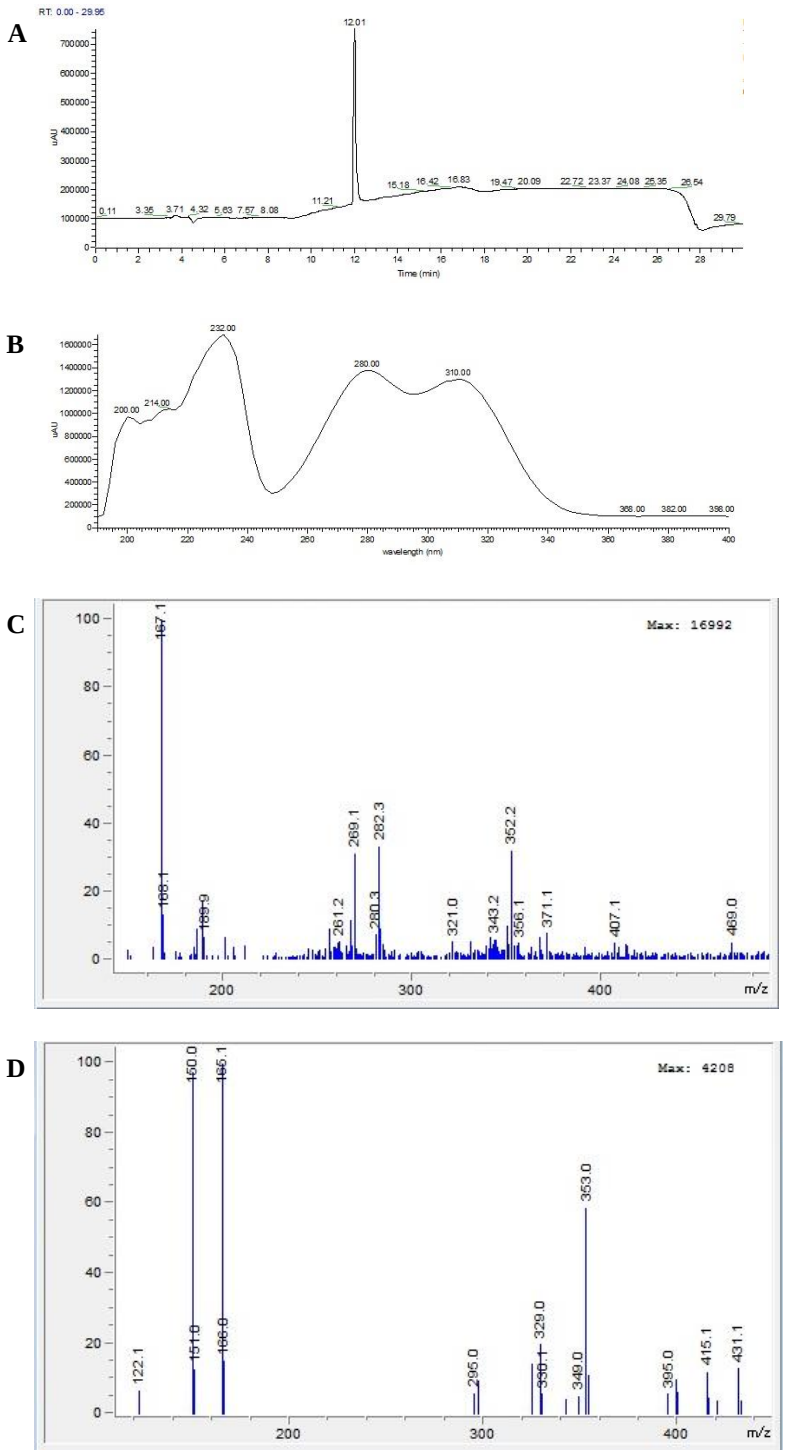

Figure 30. HPLC and ESI/MS analysis of compound VI. (A) HPLC chromatogram (B) UV spectrum (C) ESI-MS positive-ion mode (D) ESI-MS negative-ion mode

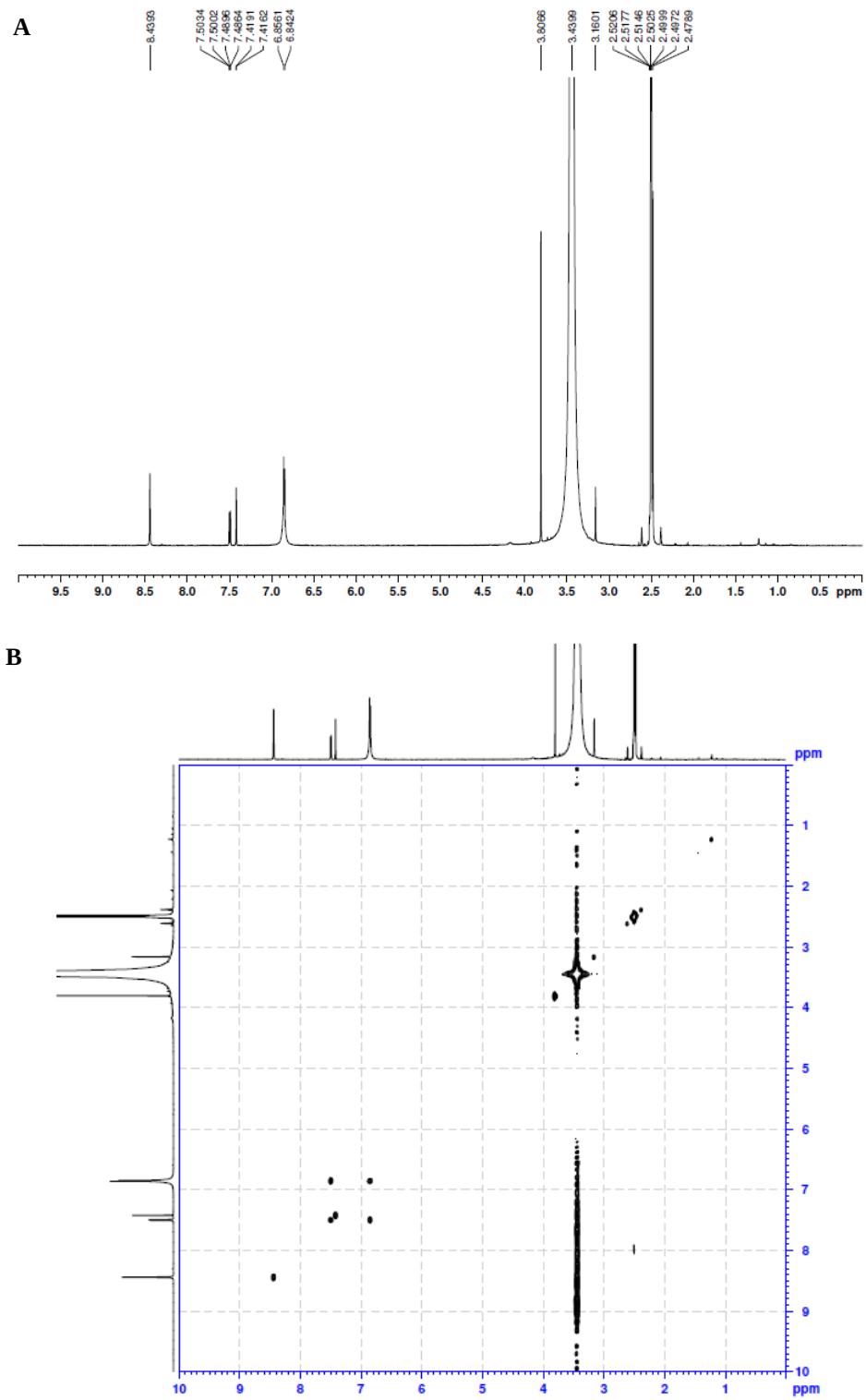

Figure 31. NMR spectra of Compound VI at 600 MHz in DMSO-d_6 (A) ^{1}H NMR spectrum (B) ^{1}H-^{1}H COSY spectrum

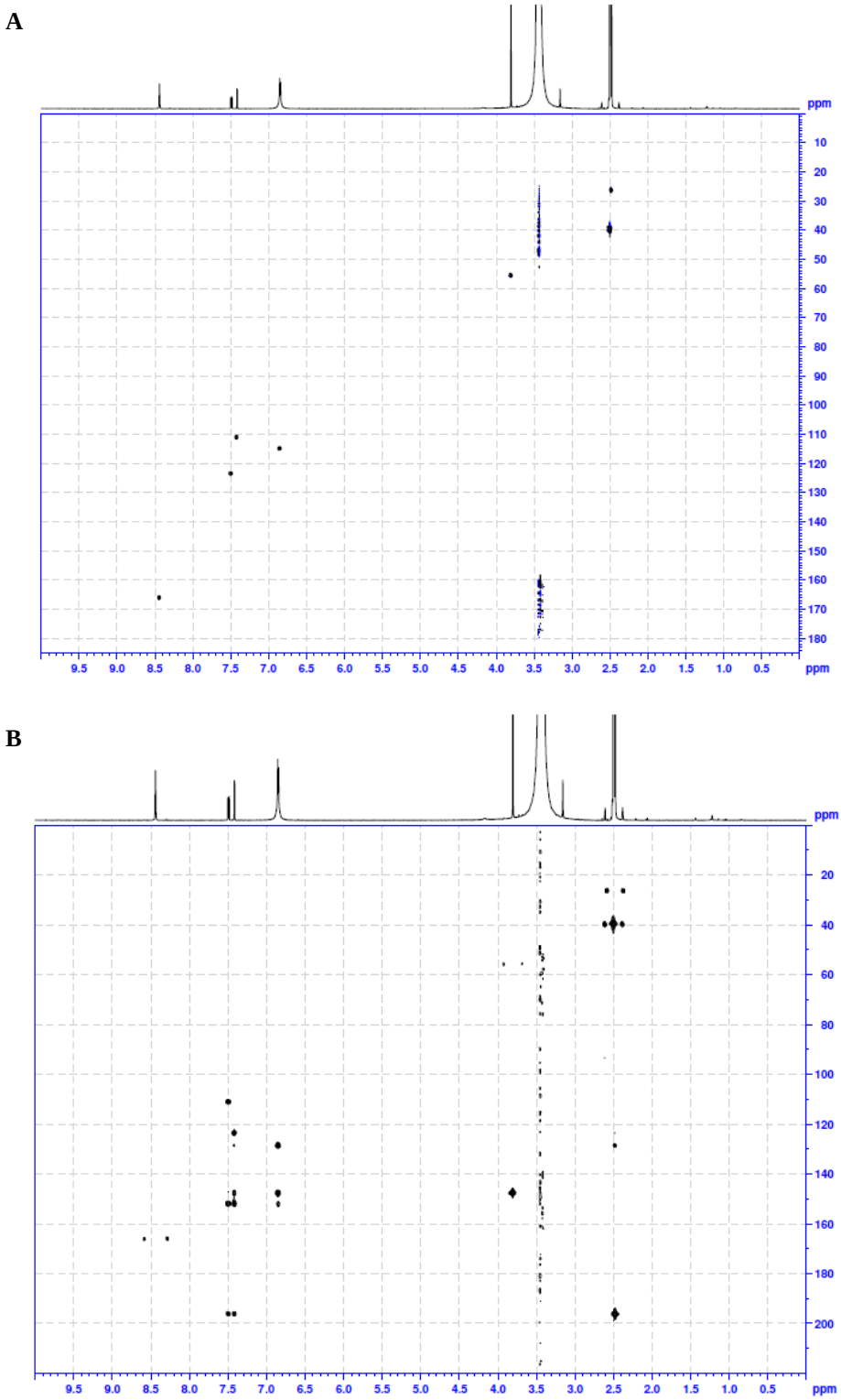

Figure 32. NMR spectra of Compound VI at 600 MHz in DMSO-d_6 (A) ^{1}H-^{13}C HSQC spectrum (B) ^{1}H-^{13}C HMBC spectrum

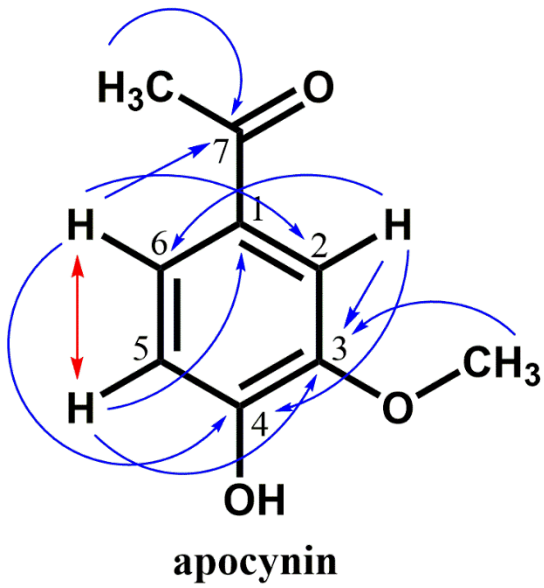

Figure 33. Structure of compound VI

Table 3. ^{1}H and ^{13}C NMR data of compound III, IV, V and VI

No	Compound III		Compound IV		Compound V		Compound VI	
	δH (mult; *J* in Hz)	δC	δH (mult; *J* in Hz)	δC	δH (mult; *J* in Hz)	δC	δH (mult; *J* in Hz)	δC
1		132.3		128.0		128.5		128.5
2	7.75 (2H, d, 8.5)	128.3	7.35 (1H, s)	110.3	7.82 (2H, d, 8.6)	130.7	7.42 (1H, d, 1.7)	110.8
3	6.92 (2H, d, 8.5)	116.0		148.5	6.83 (2H, d, 8.6)	115.0		147.7
4		164.0		154.0		162.1		152.0
5	6.92 (2H, d, 8.5)	116.0	6.92 (1H, d, 7.6)	115.4	6.83 (2H, d, 8.6)	115.0	6.85 (1H, d, 8.2)	114.7
6	7.75 (2H, d, 8.5)	128.3	7.39 (1H, d, 7.6)	126.3	7.82 (2H, d, 8.6)	130.7	7.49 (1H, dd, 8.2, 1.9)	123.4
7	9.76 (1H, s)	191.1	9.73 (1H, s)	190.9		196.3		196.3
	OCH3		3.79 (3H, s)	55.3			3.81 (3H, s)	55.3
	CH3				2.46 (3H, s)	26.1	2.48 (3H, s)	26.1

9.6 Identification of compound VII

Compound VII was obtained as white with slightly brown colored solid. It has maximum absorption at 205, 220, 260 and 296 nm. The ESI-MS positive-ion mode spectrum showed base ion peak at m/z 137.1. However, another peak at m/z 155.1 corresponds well with the negative-ion mode spectrum which showed base ion peak at m/z 153.1. Thus, the molecular weight of the compound was assumed to be 154.1 Da.

^{1}H NMR spectrum of compound VII showed signals of two hydroxyl groups attached to aromatic ring at δ 9.66 (1H, br s), 9.34 (1H, br s) and aromatic ring protons at 7.32 (1H, d, *J* = 2 Hz), 7.28 (1H, dd, *J* = 8 Hz, 2 Hz) and 6.78 ppm (1H, d, *J* = 8 Hz). The ^{13}C NMR spectra showed signals at δ 167.40 (C-7), 150.06 (C-4), 144.93 (C-3), 121.95 (C-2 and C-6), 121.71 (C-1), 116.59 (C-H aromatic ring), and 115.20 ppm (C-H aromatic ring. The NMR spectral data were in alignment with reference data [25] thus compound VII was assigned as protocatechuic acid.

Several other peaks were also detected in ^{1}H and ^{13}C NMR spectra. The ^{1}H NMR spectra showed peaks at δ 3.58 ppm whereas the ^{13}C NMR spectra showed peaks at δ 173.50, 51.46, 28.74 and 28.58 ppm. However, these peaks were not correlated to the peaks of compound VII based on the HSQC and HMBC NMR spectra. Thus, these peaks were concluded to be impurities.

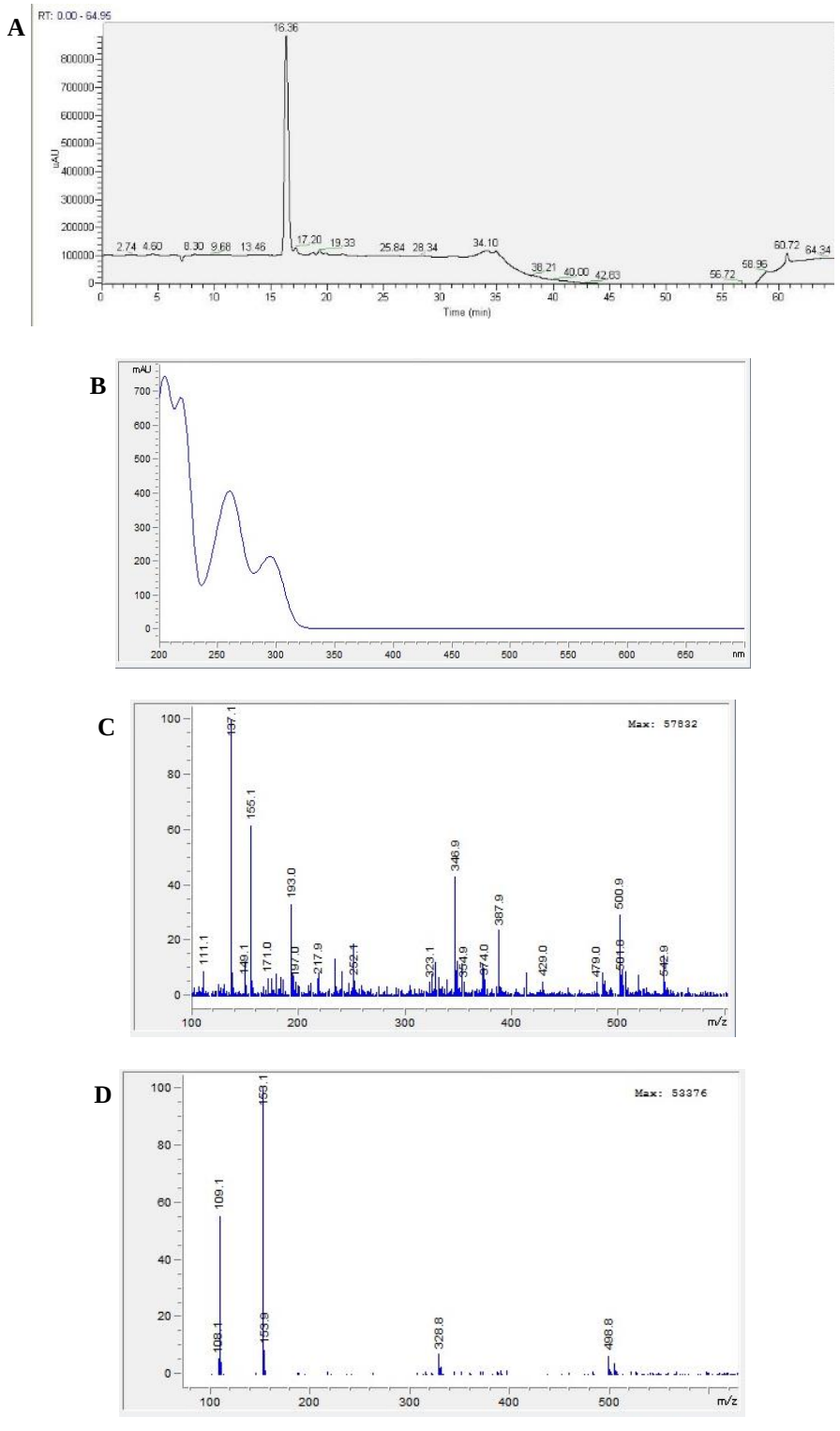

Figure 34. HPLC and ESI-MS spectrum of compound VII. (A) HPLC chromatogram (B) UV spectrum (C) ESI-MS positive-ion mode (D) ESI-MS negative-ion mode

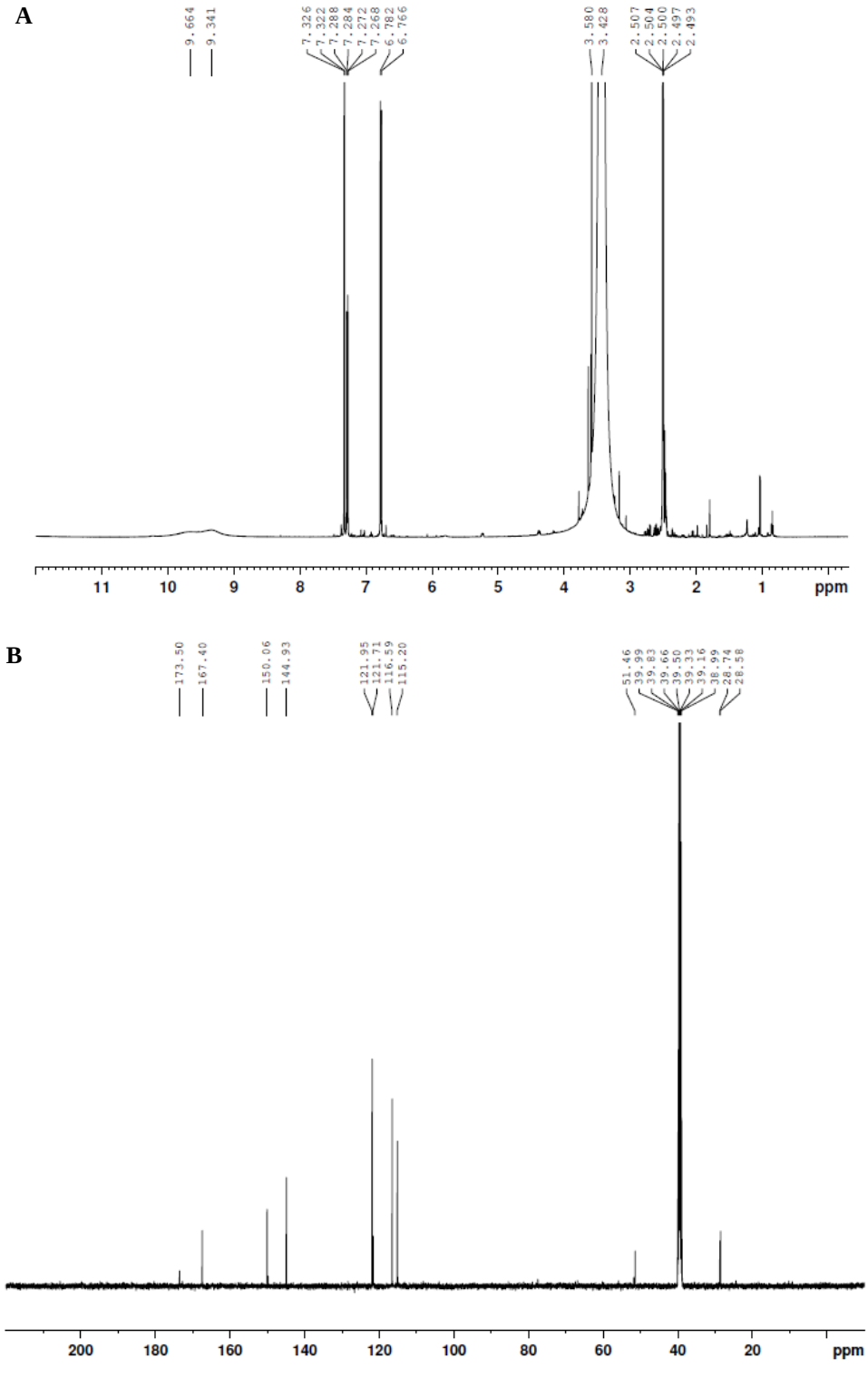

Figure 35. One dimension NMR spectra of compound VII at 500 MHz in DMSO-d_6. (A) ^{1}H NMR (B) ^{13}C NMR

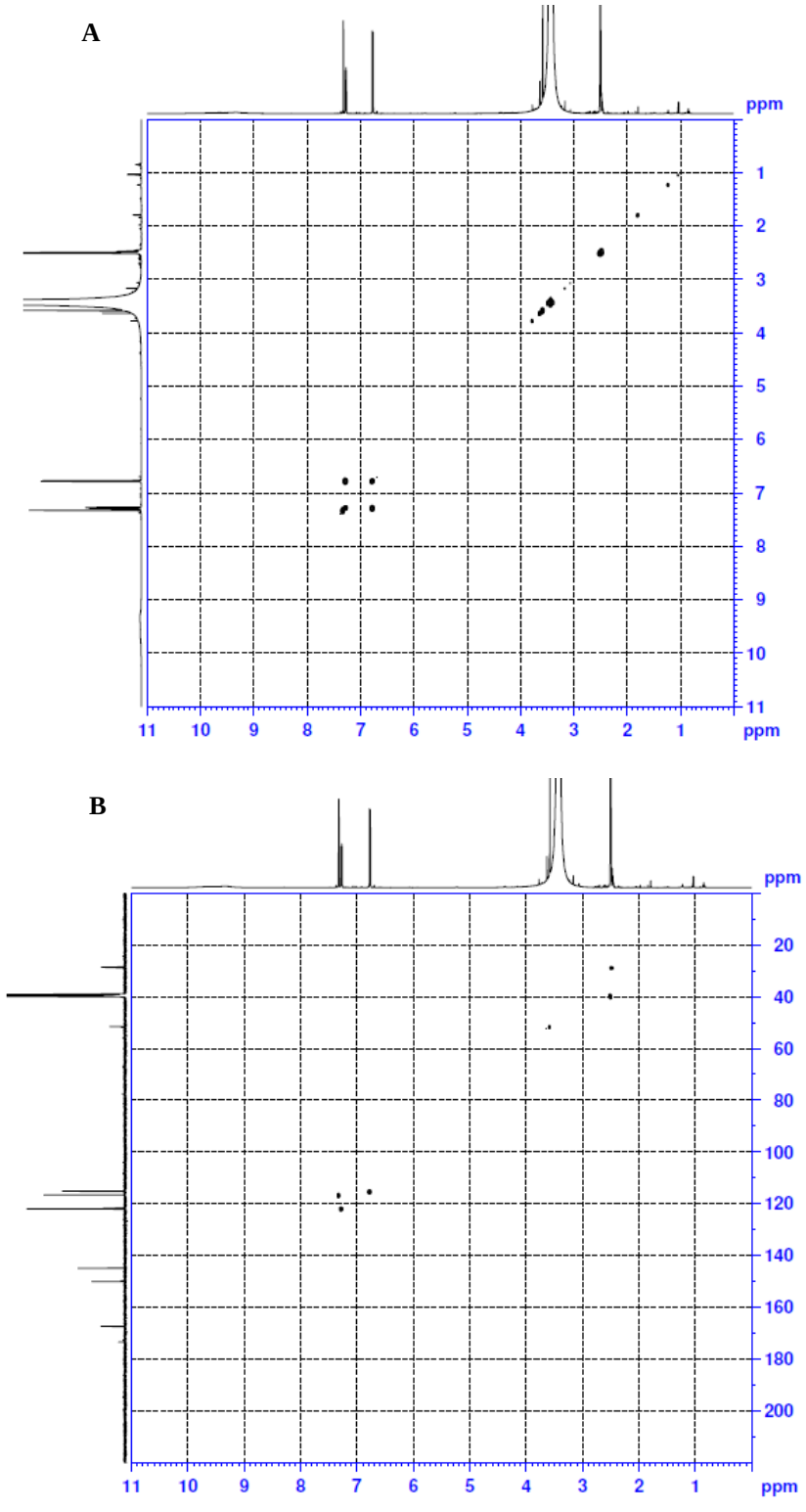

Figure 36. NMR spectra of compound VII at 500 MHz in DMSO-d_6. (A) ^{1}H-^{1}H COSY spectrum and (B) ^{1}H-^{13}C HSQC spectrum

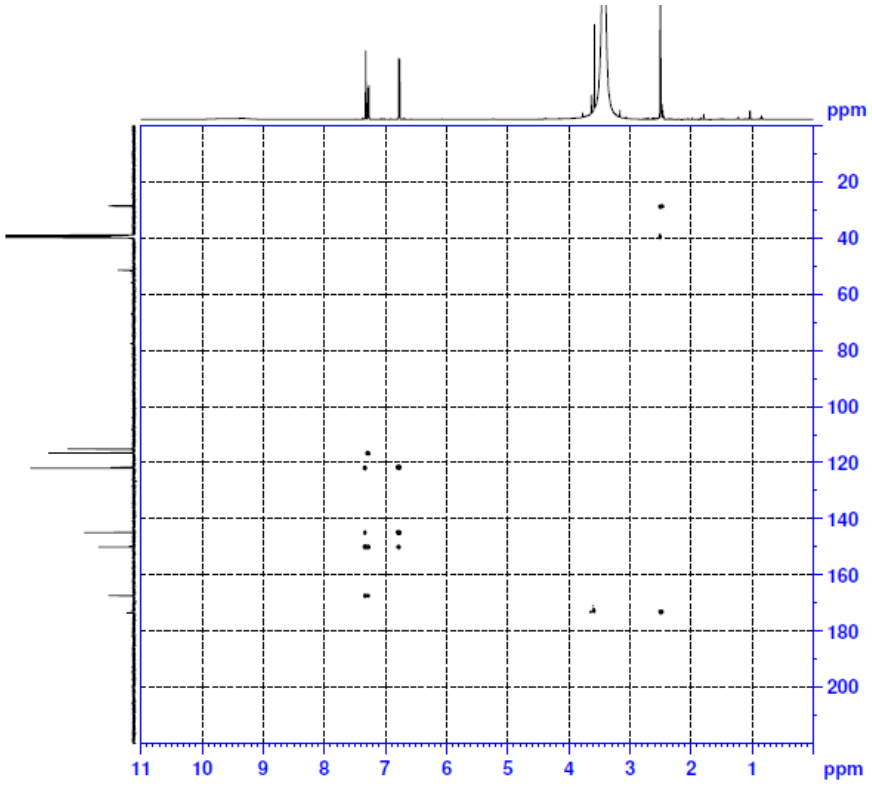

Figure 37. ^{1}H-^{13}C HMBC spectrum of compound VII at 500 MHz in DMSO-d_6

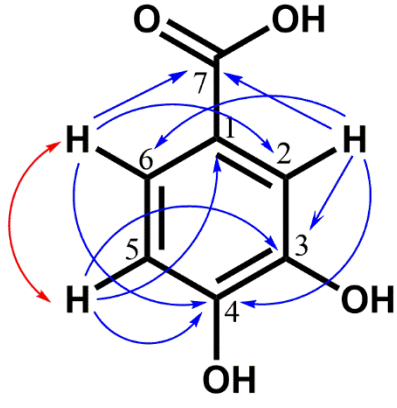

protocatechuic acid

Figure 38. Structure of compound VII

9.7 Identification of compound VIII

Compound VIII was obtained as white solid. It has maximum absorption at 252 nm. The ESI-MS positive-ion mode spectrum showed base ion peak at m/z 139.1 and the negative-ion mode spectrum which showed base ion peak at m/z 137.0.

^{1}H NMR spectrum of compound VIII showed peaks of hydroxyl group attached to aromatic ring at δ 10.26 (1H, br s) and aromatic ring protons at 7.79 (2H, dt, *J* = 10 Hz, 5 Hz, 3Hz) and 6.82 ppm (2H, dt, *J* = 10 Hz, 5 Hz, 3 Hz). The ^{13}C NMR spectra showed peaks at δ 167.31 (C-7), 161.69 (C-4), 131.65 (C-2 and C-6), 121.44 (C-1), and 115.23 ppm (C-3 and C-5). The NMR spectral data were in alignment with reference [26] and it is concluded that compound VIII is 4-hydroxybenzoic acid. This compound was also found in the 40% MeOH elution of EA fraction in Diaion HP-20 column chromatography.

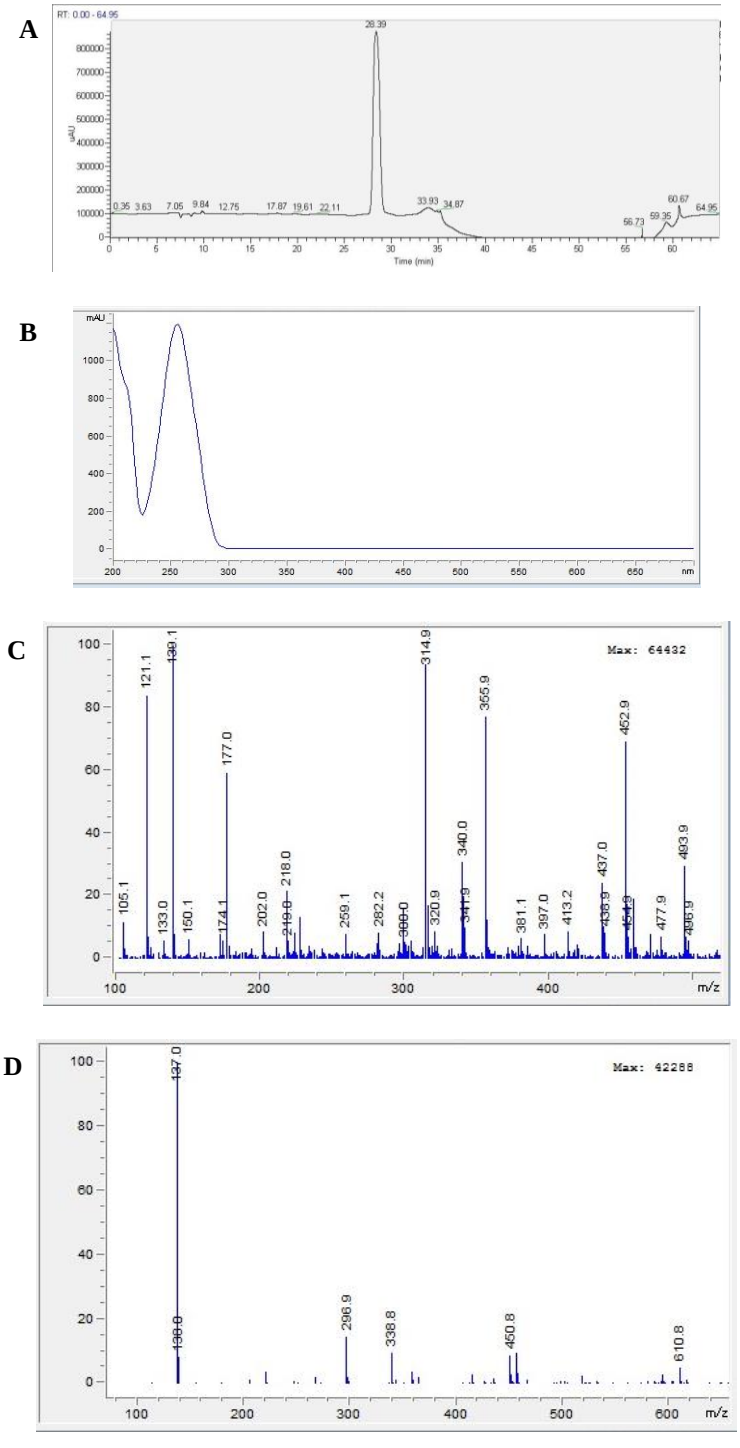

Figure 39. HPLC and ESI-MS spectrum of compound VIII. (A) HPLC chromatogram (B) UV spectrum (C) ESI-MS positive-ion mode (D) ESI-MS negative-ion mode

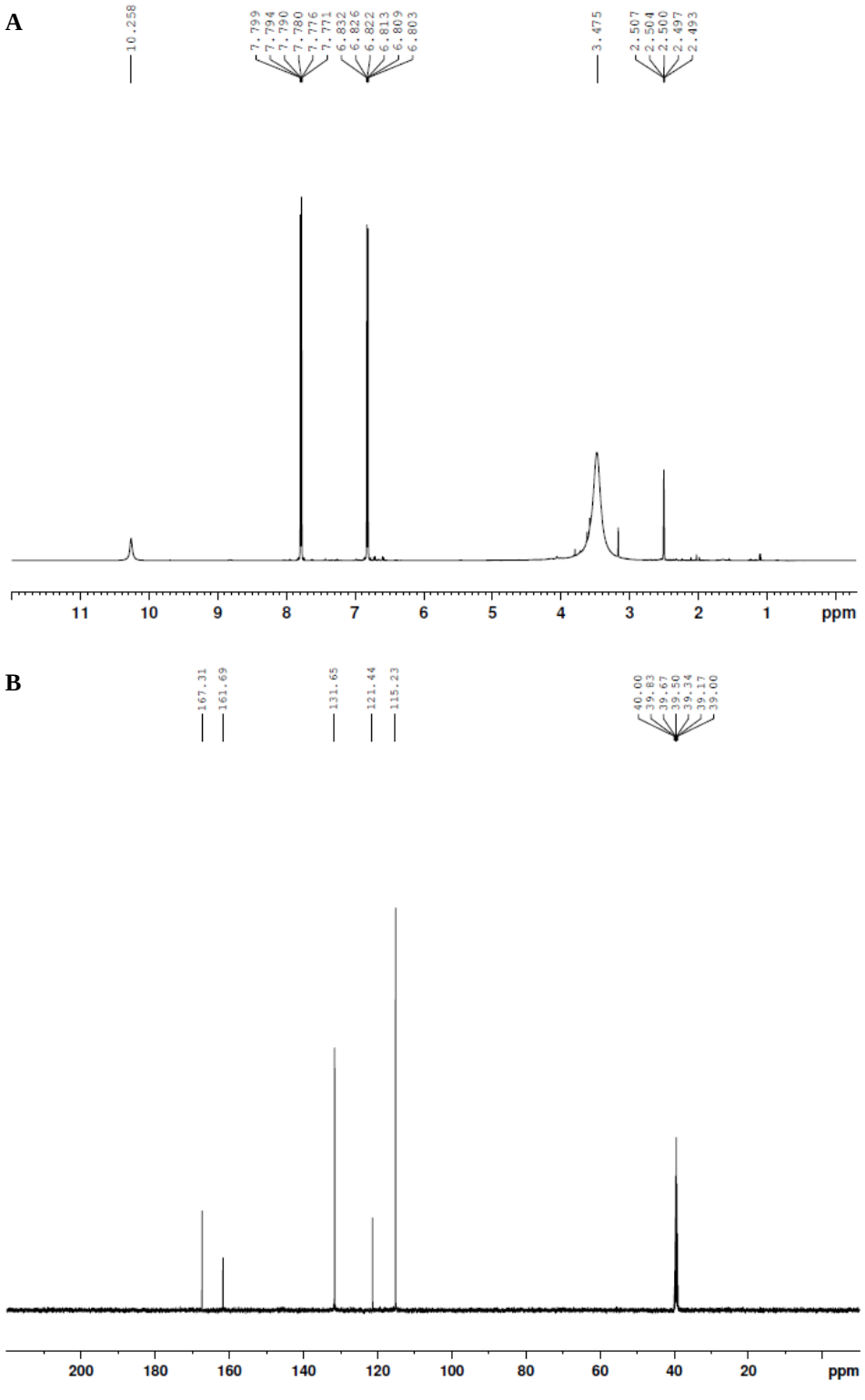

Figure 40. NMR spectra of compound VIII at 500 MHz in DMSO-d_6. (A) ^{1}H NMR (B) ^{13}C NMR

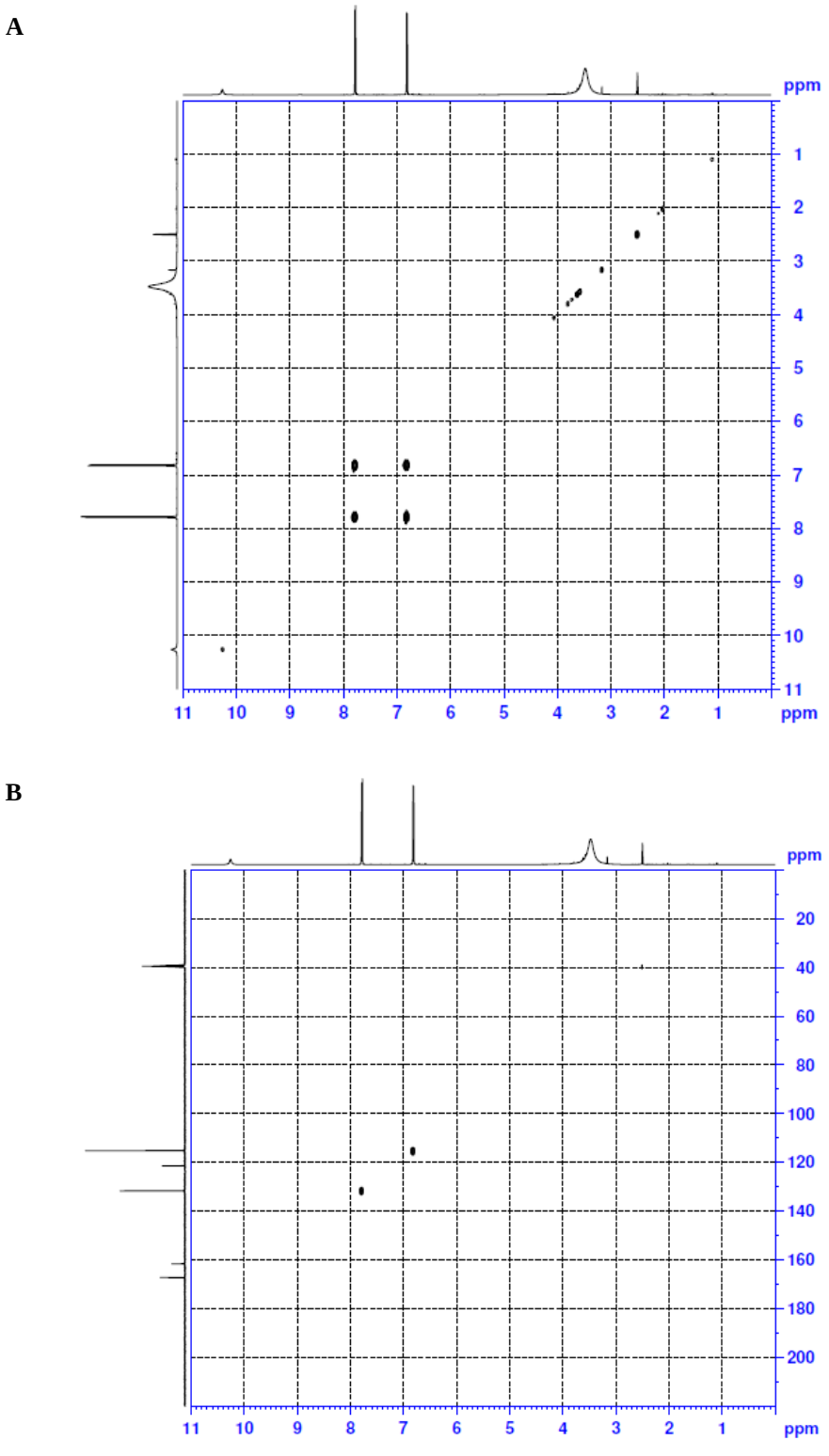

Figure 41. NMR spectra of compound VIII at 500 MHz in DMSO-d_6. (A) ^{1}H-^{13}C HSQC spectrum (B) ^{1}H-^{13}C HMBC spectrum

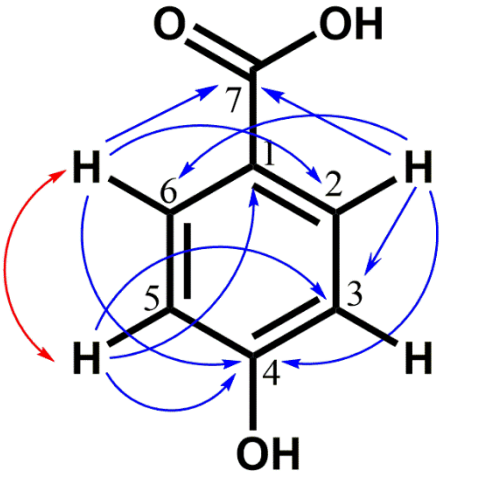

Figure 42. Structure of compound VIII

Table 4. ^{1}H and ^{13}C NMR data of compound VII and VIII

No	Compound VII		Compound VIII	
	δH (mult; *J* in Hz)	δC	δH (mult; *J* in Hz)	δC
1		121.7		121.4
2	7.32 (1H, d, 2.1)	116.6	7.79 (2H, d, 10, 5, 3)	131.6
3		144.9		115.2
4		150.1	10.26 (1H, s)	161.7
5	6.77 (1H, d, 8)	115.2	6.77 (2H, d, 10, 5, 3)	115.2
6	7.27 (1H, d, 2.1)	122.0	7.79 (2H, d, 10, 5, 3)	131.6
7		167.4		167.4

10. Suppression of LPS-induced NO activity of isolated compounds

The ability of the isolated compounds to inhibit LPS-induced NO production were examined. The compounds were tested at 5, 10, 20 and 40 µM for syringol and catechol because above 40 µM both compounds showed cytotoxicity. The remaining compounds were tested at 10, 50 and 100 µM. Among all tested compounds, only syringol and catechol showed dose-dependent NO inhibition activity with catechol showing the most potent inhibition activity.

Further on, NF-κB SEAP assay was performed for catechol and syringol to examine their ability to inhibit NF-κB expression. The result showed that catechol was able to decrease NF-κB expression significantly with IC_{50} value 13.56 µM while the IC_{50} value of syringol was more than 40 µM.

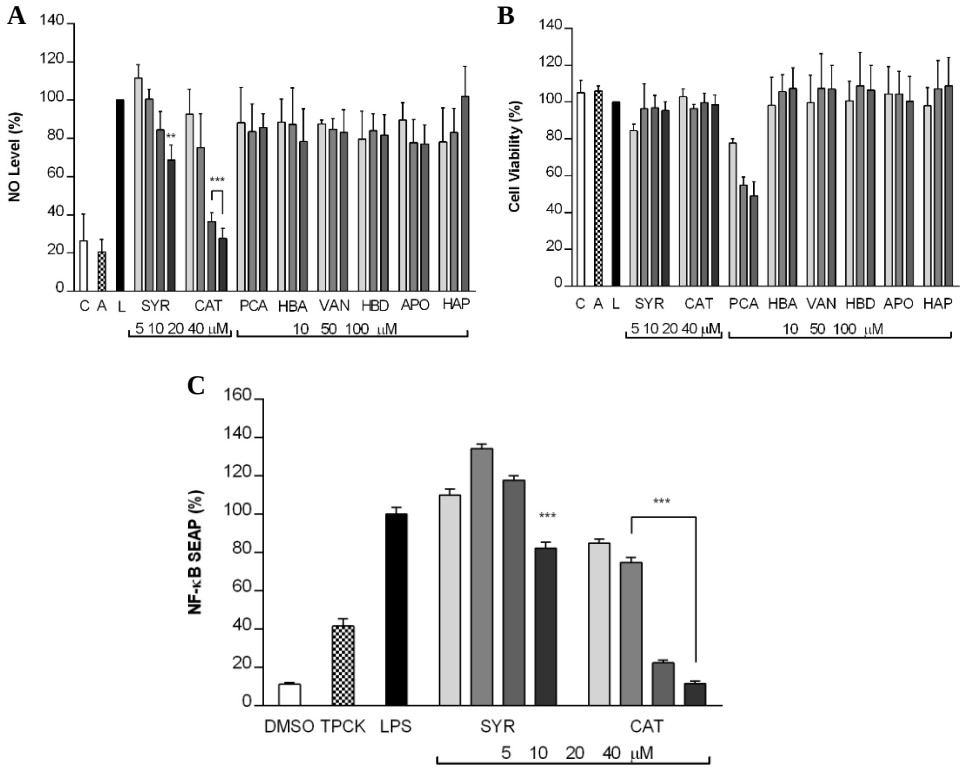

Figure 43. Effect of isolated compounds on (A) NO production and (B) cell viability and (C) NF-κB inhibition activity of syringol and catechol

Data were derived from three independent experiments and are expressed as mean ± SD. (***) *P<0.001* indicates significant difference from the LPS-stimulated group. C is control (vehicle), L is (LPS + vehicle)-treated cells alone, A is AMT 10 µM used as positive control. TPCK (20 µM) was used as positive control for NF-κB SEAP assay. SYR: syringol, CAT: catechol, PCA: protocatechuic acid, HBA: 4-hydroxybenzoic acid, VAN: vanillic aldehyde, HBD: 4-hydroxybenzaldehyde, APO: apocynin, and HAP: 4-hydroxyacetophenone.

IV. DISCUSSION

The search of new drugs from natural products have been continuously conducted to treat human diseases. Basically, the ethnopharmacology use of a natural product is employed as the basis of its drug discovery research where the separation process is performed in order to "find and follow" the supposed pharmacological activity with the final aim to isolate and identify the bioactive compounds, especially if information on the secondary metabolite is limited [27]. In the current study, Arecae Pericarpium, which has been used in TCM to treat edematous diseases, was examined to elucidate its potential anti-inflammatory effect and to discover the active compound contributing to this activity.

The potential anti-inflammatory activity of Arecae Pericarpium is screened by examining the ability of tested fractions to suppress LPS-induced NO production in murine macrophage cells. Macrophage play a central role in a host's defense against bacterial infection through phagocytosis, cytotoxicity, and intracellular killing [28, 29]. Stimulation of murine macrophages by LPS results in the expression of iNOS and increased NO production which plays a critical role in macrophage activation and is associated with acute and chronic inflammations [29]. The increased NO production is examined with Griess reaction by quantifying the nitrite level in the conditioned medium of RAW264.7 cells treated with LPS. This cell-based assay system has been used for drug screening and the evaluation of potential inhibitors of the pathways leading to the induction of iNOS and NO production. Due to its reliability and simplicity, this method is commonly employed in bioassay-guided isolation of anti-inflammatory agent scheme [30].

The result of preliminary study in this research indicated that Arecae Pericarpium was able to suppress LPS-induced NO production in murine macrophages with methylene chloride and ethyl acetate fractions showing the strongest inhibition compared to other fractions. Thus, it is confirmed that Arecae Pericarpium has the potential anti-inflammatory activity and the active compounds are present in these fractions.

The potential anti-inflammatory activity of the methylene chloride fraction was further supported with the PGE_2 assay result of MC1A fraction which was able to reduce the PGE_2 level with IC_{50} less than 0.5 μg/mL. This result suggested that the methylene chloride fraction of Arecae Pericarpium might exert potential anti-inflammatory activity also through the inhibition of COX-2 enzyme.

The methylene chloride fraction was separated with combination of column chromatography, HPCCC, and preparative HPLC. Through column chromatography separation process, dimeric syringol (9.2 mg) and catechol (196.3 mg) were isolated. After column chromatography separation, combination of HPCCC and preparative HPLC was needed to isolate 4-hydroxybenzaldehyde (1.0 mg), mixture of vanillic aldehyde and 4-hydroxyacetophenone (5.0 mg), and apocynin (0.6 mg). The length of the separation process might contribute to the low yield of these compounds.

Ethyl acetate fraction was subjected to Diaion HP-20 resin column chromatography. From 3.2 g of active fraction obtained, 200 mg was separated by HPCCC and protocatechuic acid (18.7 mg), 4-hydroxybenzoic acid (3.3 mg) and catechol (25.4 mg) were isolated.

All of the isolated compounds were tested to compare their activity. Among all of the isolated compounds, catechol exhibited highest inhibition activity of LPS-stimulated NO production, followed by syringol. Other compounds did not or only slightly inhibited the NO production.

NF-κB transcription factor has been shown to play a significant role in LPS-induced expression of pro-inflammatory mediators, including iNOS and COX-2. To investigate the molecular mechanism of inhibition of iNOS and COX-2 transcription mediated by catechol and syringol, NF-κB transcriptional activity was investigated using a reporter gene assay system. The result showed that only catechol was able to inhibit NF-κB transcription with IC_{50} value 13.56 μM while the IC_{50} value of syringol was more than 40 μM. Therefore, it is suggested that catechol suppressed the LPS-induced NO production by inhibiting NF-κB transcription.

Based on the yield and the bioassay results, it is suggested that catechol might be the primary contributing compound to the potential anti-inflammatory activity of Arecae Pericarpium. Catechol is a major phenolic compound in areca nut as well. This compound has been reported to have antioxidant activity [31] and anti-inflammatory in BV2 microglial cells and RAW 264.7 cells [32, 33]. It was reported that catechol was able to exhibit anti-inflammatory effect on LPS-stimulated BV2 microglial cells through inhibiting NF-κB and p38 MAPK signaling pathway [33]. The data in the present study support the pharmacological basis of the use of Arecae Pericarpium as a traditional herbal medicine to treat inflammatory diseases.

V. CONCLUSION

This result of this study have showed that Arecae Pericarpium suppressed NO production induced by LPS in RAW 264.6 cells and eight phenolic compounds were isolated from the methylene chloride and ethyl acetate fractions by applying bioassay-guided isolation scheme. The phenolic compounds are dimeric syringol, catechol, 4-hydroxybenzyl aldehyde, vanilic aldehyde, 4-hydoxyacetophenone, apocynin, protocatechuic acid and 4-hydroxybenzoic acid. Catechol was found to be the major compound and might be the primary contributing compound to the inhibition activity of Arecae Pericarpium on LPS-stimulated NO production in RAW 264.7 macrophage cells. The result of this study can enrich the existing study on Arecae Pericarpium and support the further study on the use of Arecae Pericarpium in treating inflammatory diseases.

REFERENCES

1. Rimando, A.M., et al., *Searching for rice allelochemicals: An example of bioassay-guided isolation.* Agronomy Journal, 2001. 93(1): 16-20.
2. Koehn, F.E., and Carter, G.T., *The evolving role of natural products in drug discovery.* Nat Rev Drug Discov, 2005. 4(3): 206-221.
3. Killeen, Matthew J., Linder, Mark, Pontoniere, Paolo, Crea, Roberto, *NF-kb signaling and chronic inflammatory diseases: exploring the potential of natural products to drive new therapeutic opportunities.* Drug Discovery Today, 2014. 19 (4): 373-378.
4. Zamora, Ruben, Vodovotz, Yoram, Billiar, Timothy R., *Inducible nitric oxide synthase and inflammatory diseases.* Molecular Medicine, 2000. 6(5):347-373.
5. Korhonen, Riku, Lahti, Aleksi, Kankaanranta, Hannu, Moilanen, Eeva, *Nitric oxide production and signaling in inflammation*. Current Drug Targets – Inflammation & Allergy, 2005. 4: 471-479.
6. Sun, Jie, Zhang, Xhueji, Broderick, Mark, Fein, Harry. *Measurement of nitric oxide production in biological systems by using Griess reaction assay.* Sensors, 2003. 3: 276-284.
7. Ito, Yoichiro. *Golden rules and pitfalls in selecting optimum conditions for high-speed counter-current chromatography*. J Chromatography A, 2005. 1065: 145-168.
8. Guzlek, H, Wood, P.L, Janaway, Lee. *Performance comparison using the GUESS mixture to evaluate counter-current chromatography instruments*. J Chromatography A, 2009. 1216: 1481-1486.
9. Shehzad, Omer, et al., *Application of stepwise gradients in counter-current chromatography: A rapid and economical strategy for the one-step separation of eight coumarins from Seseli resinosum*. J Chromatography A, 2013. 1310: 66-73.

10. Friesen, J. B., Pauli, G. F., *G.U.E.S.S.- A generally useful estimate of solvent systems for CCC*. Journal of Liquid Chromatography and Related Technologies, 2005. 28 (17): 2777-2806.
11. Peng, Wei, et al., *Areca catechu L. (Arecaceae): A review of its traditional uses, botany, phytochemistry, pharmacology and toxicology*. J Ethnopharmacology, 2015. 164: 340-356.
12. Bhandare, A.M., Kshirsagar, A.D., Vyawahare, N.S., Hadambar, A.A., Thorve, V.S., *Potential analgesic, anti-inflammatory and antioxidant activities of hydroalcoholic extract of Areca catechu L. nut*. Food and Chemical Toxicology, 2010. 48: 3412–3417.
13. Huang, P.L., Chi, C.W., Liu, T.Y., *Effects of Areca catechu L. containing procyanidins on cyclooxygenase-2expression in vitro and in vivo*. Food and Chemical Toxicology, 2010. 48: 306–313.
14. Lee, Kang Pa, et al., *The anti-inflammatory effect of Indonesian Areca catechu leaf extract in vitro and in vivo.* Nutrition Research and Practice, 2014. 8(3): 267-271.
15. Moon, Sang-Kwan et al., *Inhibition of human endothelial cell proliferation by Gami–Jeonggi–San (Jiawei–Zhenqi–San) is accompanied by transcriptional up-regulation of p53 and Waf1 tumor suppressor genes.* J Ethnopharmacology, 2005. 100: 187-192.
16. Yenjit, P., Issarakraisila, M., Intana, W., Chantrapromma, Kan., *Fungicidal activity of compounds extracted from the pericarp of Areca catechu against Colletotrichum gloeosporioides in vitro and in mango fruit.* Postharvest Biology and Technology, 2010. 55: 129-132.
17. Phaechamud, T., Toprasri P., Chinpaisal, C., *Antioxidant activity of Areca catechu extracts in human hepatocarcinoma HepG$_2$ cell lines*. Pharmaceutical Biology, 2009. 47(3): 242–247.
18. Atadana, Frederick W., *Catalytic pyrolysis of cellulose, hemicellulose and lignin model compounds.* Master thesis, 2010.

19. Sun, Y.L., Zhang, Q., Anastasio C., and Sun, J., *Insights into secondary organic aerosol formed via aqueous-phase reactions of phenolic compounds based on high resolution mass spectrometry*. Atmos. Chem. Phys., 2010. 10: 4809–4822.
20. WSS: Spectral data were obtained from Wiley Subscription Services, Inc. (US).
21. Gui, Ren-Yi et al., *Chaetominine, (+)-alantrypinone, questin, isorhodoptilometrin, and 4-hydroxybenzaldehyde produced by the endophytic fungus Aspergillus sp. YL-6 inhibit wheat (Triticum aestivum) and radish (Raphanus sativus) germination*. Journal of Plant Interactions, 2015. 10 (1): 87-92.
22. Stella Christophoridou, Photis Dais. *Detection and quantification of phenolic compounds in olive oil by high resolution 1H nuclear magnetic resonance spectroscopy.* Analytica Chimica Acta, 2009. 633: 283-292.
23. Liu, Qian, et al. *Chemical constituents from Qianliang tea*. Journal of Chinese Pharmaceutical Sciences, 2013. 22 (5): 427–430.
24. ACD: Spectral data were obtained from Advanced Chemistry Development, Inc.
25. Hur, Jong Moon, Park, Jong Cheol, Hwang, Young Hee. *Aromatic Acid and Flavonoids from the Leaves of Zanthoxylum piperitum.* Natural Product Sciences, 2001. 7(1): 23-26.
26. Liang, Yong-hong, et al. *Two new phenolic acids from Drynariae Rhizoma*. Acta Pharm Sin, 2010. 45: 874-878
27. Brusotti, G., et al. *Isolation and characterization of bioactive compounds from plant resources: The role of analysis in the ethnopharmacological approach.* Journal of Pharmaceutical and Biomedical Analysis, 2014. 87: 218-228.
28. Adams, D.O., Hamilton, T.A.. *The cell biology of macrophage activation.* Annual Review of Immunology, 1984. 2: 283-318.
29. Zhou, H.Y., et al. *Anti-inflammatory activity of 4-methoxyhonokiol is a function of the inhibition of iNOS and COX-2 expression in RAW 264.7*

macrophages via NF-κB, JNK and p38 MAPK inactivation. European Journal of Pharmacology, 2008. 586: 340-349.

30. Sae-Wong, Chutha, et al. *Suppresive effects of methoxyflavonoids isolated from Kaempferia parviflora on inducible nitric oxide synthase (iNOS) expression in RAW 264.7 cells.* Journal of Ethnopharmacology, 2011. 136: 488-495.
31. Loo, A. Y., Jain, K., Darah, I. *Antioxidant activity of compounds isolated from the pyroligneous acid, Rhizophora apiculata*. Food Chemistry, 2008. 107: 1151–1160.
32. Zheng, Long Tai, et al. *Anti-inflammatory effects of catechols in lipopolysaccharide-stimulated microglia cells: Inhibition of microglial neurotoxicity*. European Journal of Pharmacology, 2008. 588: 106–113.
33. Kazłowskaa, Katarzyna et al. *Anti-inflammatory properties of phenolic compounds and crude extract from Porphyra dentata*. Journal of Ethnopharmacology, 2010. 128: 123–130.

국문초록

RAW 264.7 세포내 지질다당류로 유도된 산화질소의 생성 억제에 따른 대복피 유래 페놀성 화합물의 분리

Amelia Indriana

서울대학교 대학원

약학과 천연물과학 전공

Arecae Pericarpium는 *Areca catechu* L. (Arecaceae)의 과피이다. 중의학에서는 복부 팽만, 구토증세, 설사를 완화하는 곽향정기산에, 한의학에서는 혈관질환의 치료를 위한 가미정기산에 처방된다. Arecae Pericarpium의 항산화 및 항진균 효과와 그것의 지표물질 추출이 보고된 바 있다. 그러나 Arecae Pericarpium의 항염증 효과는 현재까지 보고된 바가 없어 본 연구에서는 RAW 264.7 대식세포에서 산화질소 생성을 억제하는 Arecae Pericarpium의 항염성분 분리를 목표로 하였다. Arecae Pericarpium 유래 물질의 분리는 RAW 264.7 대식세포에서 LPS 처리에 의해 유도되는 산화질소 생성의 억제 정도에 따라 수행되었다. 건조된 Arecae Pericarpium을 메탄올로 침출하여 농축하고 헥산, 메틸렌클로라이드, 에틸아세테이트, 부탄올을 이용하여 순차적 용매 분획을 시행하였다.

산화질소 생성 억제 활성이 뛰어난 메틸렌클로라이드와 에틸아세테이트 층을 선택하여 물질 분리를 진행하였다. 메틸렌클로라이드 층은 실리카겔 컬럼 크로마토그래피를 통하여 7개의 분획(MC1A~MC1G)으로 나누었다. 그 중 MC1A, MC1B, MC1G 분획이 산화질소 생성 억제 효과를 보였으며 MC1G은 syringol dimer (compound **I**)를 단일 물질로 포함하고 있음을 밝혔다. Diaion® HP-20 수지를 이용한 컬럼크로마토그래피를 통한 MC1A 유래의 20 %, 30 % 메탄올 용출액에서 catechol (compound **II**)을 정제하였다. MC1B에서 유래한 4-hydroxybenzaldehyde (compound **III)**, vanillin (compound **IV**), 4-hydroxyacetophenone (compound **V**), apocynin (compound **VI**) 등 네 개의 물질은 헥산-에틸아세테이트-메탄올-물(2:5:1:4, v/v/v/v)로 구성된 용매계를 이용한 HPCCC(고성능향류크로마토그래피)와 preparative HPLC를 통하여 분리되었다. Ethyl acetate 층은 Diaion® HP-20 수지를 이용한 컬럼크로마토그래피를 통하여 분획하고 그 중 20% 메탄올 용출액을 선택하여 HPCCC를 수행하였다. 헥산-에틸아세테이트-메탄올-물 2:5:2:5(v/v/v/v)의 비율로 조성된 용매계를 통하여 protocatechuic acid (compound **VII)**와 4-hydroxybenzoic acid (compound **VIII**)를 분리하였다. 본 연구에서 분리된 Arecae Pericarpium 유래 화합물들이 중에서 catechol이 LPS에 의해 유도되는 산화질소 생성 억제의 주된 활성에 기여함을 밝혔다.

주요어: 대복피, *Areca catechu* (L.), HPCCC, 페놀성 화합물, 생물학적 검정법, 산화질소 생성의 억제

학번: 2013-23937

Isolation of Phenolic Compounds from Arecae Pericarpium Guided by Inhibition of LPS-Induced Nitric Oxide Production in RAW 264.7 Cells

RAW 264.7 세포내 지질다당류로 유도된 산화질소의 생성 억제에 따른 대복피 유래 페놀성 화합물의 분리

August 2015

Amelia Indriana

Natural Product Science Major
College of Pharmacy
Master Course in Graduate School
Seoul National University

Abstract

Isolation of Phenolic Compounds from Arecae Pericarpium Guided by Inhibition of LPS-Induced Nitric Oxide Production in RAW 264.7 Cells

Amelia Indriana

Natural Products Science Major

College of Pharmacy

Master Course in the Graduate School

Seoul National University

Arecae Pericarpium is the nut husk of *Areca catechu* L. (Arecaceae). In Traditional Chinese Medicine, it is used in Huo Xiang Zheng Qi formula to cure abdominal distension, vomiting, and diarrhea and Gami-Jeonggisan formula in Traditional Korean Medicine to treat vascular diseases. Arecae Pericarpium has been studied for its antioxidative activity, antifungal activity, and phytochemical compounds isolation. However, its antiinflammatory activity has not been reported yet. This study aimed to isolate compounds from Arecae Pericarpium guided by the inhibition of nitric oxide production on RAW 264.7 macrophage cells.

Dried Arecae Pericarpium was macerated in methanol. The macerate was evaporated, dissolved in 10% methanol and partitioned with hexane, methylene chloride, ethyl acetae and *n*-butanol. Methylene chloride and ethyl acetate fraction,

which inhibited nitric oxide production to lower levels compared to other fractions, were further separated. Methylene chloride fraction was subjected to repeated silica gel column chromatography to obtain seven fractions (MC1A to MC1G fraction). MC1A, MC1B and MC1G fractions inhibited the LPS-induced nitric oxide production. MC1G was obtained as single compound and identified as syringol dimer (compound I). MC1A was subjected through Diaion® HP-20 column chromatography and catechol (compound II) was obtained from 20% and 30% MeOH column fraction. Four compounds, 4-hydroxybenzaldehyde (compound III), vanillin (compound IV), 4-hydroxyacetophenone (compound V) and apocynin (compound VI), were isolated from MC1B fraction by combining HPCCC (hexane-ethyl acetate-methanol-water system 2:5:1:4 v/v) and preparative HPLC. Ethyl acetate fraction was subjected to Diaion® HP-20 column chromatography and 20% MeOH column fraction was separated using high performance counter-current chromatography (hexane-ethyl acetate-methanol- water system 2:5:2:5 v/v) to obtain protocatechuic acid (compound VII) and 4-hydroxybenzoic acid (compound VIII). All isolated compounds were examined and the result suggested that catechol might be the primary contributing active compound to the suppression of LPS-induced NO production by Arecae Pericarpium.

Keywords: Arecae Pericarpium, *Areca catechu* (L.), HPCCC, phenols, bioassay-guided isolation, nitric oxide inhibition

Student number: 2013-23937

TABLE OF CONTENTS

LIST OF FIGURES

LIST OF TABLES

I. INTRODUCTION

1. Bioassay-guided Isolation

Bioassay-guided isolation is a procedure of compounds separation from an extract by combining various analytical methods, led by biological test results. As shown in Figure 1, after an extract is subjected to bioassay to confirm its activity, crude separation is carried out and the obtained fractions are tested for biological activity. Further separation is performed on the active fractions. The process is repeated several times until a single biologically active compound is obtained. The structure of the pure compound is identified or elucidated with various spectroscopic methods. [1, 2].

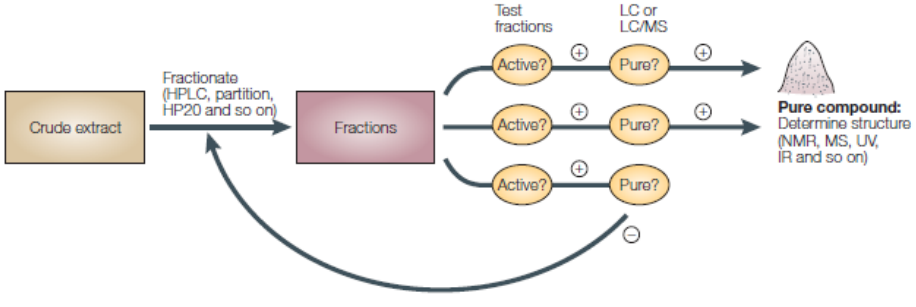

Figure 1. General scheme of bioassay-guided fractionation [1]

2. Inflammation

Inflammation is an essential defense mechanism that takes place following exposure to harmful stimuli. Acute inflammation rapidly occurs in response to tissue injury or infection in which several key agents, such as antibodies and leukocytes, are released to the infection site to repair the damaged tissue. When the initial inflammatory trigger is removed, the process is terminated; however, if harmful stimuli remain, or if healing processes are impaired, acute inflammation can progress to chronic inflammation. Chronic inflammation is a long-term condition characterized by tissue injury and restorative measures occurring simultaneously and it is considered a pivotal driver of countless major diseases, including atherosclerosis, fatty liver disease, type 2 diabetes mellitus, rheumatoid arthritis, psoriasis, Alzheimer's disease (AD) and even cancer [3].

Inflammation is marked by heat, pain, redness, and swelling. The symptoms reflect the effects of cytokines and other inflammatory mediators on the local blood vessels. The redness and heat result from an increase in blood flow, which is caused by local vasodilatation, first involving arterioles and then capillaries and venules. Swelling is the result of alterations in vascular permeability. The endothelial cells become leaky, leading to exudation of fluid, plasma proteins and white blood cells (inflammatory edema) [4].

3. Inducible Nitric Oxide Synthase and Nitric Oxide

Nitric oxide (NO) is a molecule which in mammals, including humans, has been implicated in a wide variety of physiological regulatory mechanisms ranging from vasodilatation and blood pressure control to neurotransmission. It is also involved in nonspecific immunity and in the complex mechanism of tissue injury as a major mediator of inflammatory processes and apoptosis [4].

NO is biosynthesized endogenously from L-arginine in a reaction catalyzed by various nitric oxide synthase (NOS) enzymes, however the enzyme primarily responsible for the roles of NO in inflammatory processes is the inducible NOS (iNOS; NOS2; or type II NOS). NO released by iNOS is not typically expressed in resting cells and must be induced by certain cytokines such as interleukin-1 (IL-1), tumor necrosis factor-α (TNF-α) and interferon-γ (IFN-γ) or microbial products, such as lipopolysaccharide (LPS) and dsRNA [4, 5].

NO is rapidly oxidized to nitrite and/or nitrate by oxygen in biological systems. Integrated nitric oxide production can be estimated from determining the concentrations of nitrite and nitrate end products. The measurement of nitrate/nitrite concentration or of total nitrate and nitrite concentration (NOx) is routinely used as an index of NO production [6].

4. High Performance Counter-current Chromatography (HPCCC)

Counter-current chromatography (CCC) was developed in the early 1970s by Yoichiro Ito. The method provides an advantage over the conventional column chromatography by eliminating the use of a solid support where the amount of stationary phase is limited and dangers of irreversible adsorption from the support are inevitably present [7]. Among CCC instruments, high-performance countercurrent chromatography (HPCCC) is used to generate high *g*-levels up to 240 × *g* to retain a higher proportion of the stationary phase even at a higher mobile-phase flow-rate. It has been shown that *g*-level is one of the most important parameters affecting the stationary phase retention. Higher *g*-level leads to higher stationary phase retention and hence better separation performance. Therefore, faster and more efficient separation is possible compared to conventional CCC methods [8].

An effective CCC separation relies on the selection of a suitable biphasic solvent system, based on the partition coefficient (*K* value) of the target compounds between the two phases. There are various appropriate biphasic solvent systems available with one of the most commonly used is a mixture of *n*-hexane-ethyl acetate-methanol-water (HEMWat) [9]. The selection of the most appropriate solvent system in CCC is crucial and has been the major setback in the employment of CCC separations. Compared to the far more popular solid-support chromatography, the selection of CCC solvent systems is equivalent to choosing both the column and the eluent at once [10].

5. Areca catechu L.

Areca catechu, especially the seed, is used traditionally in different regions for different purposes. In China, it is used as main herb in TCM for the treatment of gastrointestinal diseases (including abdominal distension, dysentery, dyspepsia, and constipation), parasitic diseases, and edematous diseases. In Ayurveda, it is used as digestive, astringent, and emmenagogue agent. In Southeast Asia region, it is used to treat gastrointestinal diseases, parasitic diseases, and liver diseases. The seed of *A. catechu* is a popular chewable item used in traditional herbal medicine as mild stimulant [11].

The phytochemical constituents in this plant include alkaloids, flavonoids, tannins, triterpenes and steroids, phenolic compounds, fatty acids, and anthraquinones, which were isolated mostly from the seed since it is the most commonly used part in traditional medicine. Alkaloids are the characteristic components of *A. catechu* with arecoline being the main alkaloid (content 0.3 – 0.6%). Other alkaloids found in areca nut are arecaidine, guavacoline, guavacone, arecolidine, etc. It has been reported that *A. catechu* is the only plant containing alkaloids of the Arecaceae family. Tannin is the next characteristic component of *A. catechu*. Catechin and epicatechin are the main class of tannins in *A. catechu*. The specific tannin compounds of A.catechu include procyanidin A1, procyanidin B1, procyanidin B2, arecatannin A1, arecatannin B1, arecatannin C1, arecatannin A2, arecatannin A3, and arecatannin B2 [11].

The seed and leaf of *A. catechu* have been reported to have anti-inflammatory activities. The seed extracts showed dose-dependent analgesic and anti-inflammatory effect in animal model [11, 12]. Specifically, the acetone extract of

the seed which contain procyanidins inhibited TPA-induced COX-2 expression through ERK signaling pathway in oral cavity squamous cancer SAS cell line at low dose [11, 13]. The ethanolic leaf extract inhibited iNOS and COX-2 expression dose-dependently with highest inhibition exhibited at 3 µg/mL. The leaf extract was also able to reduce carrageenan-induced paw edema in rats with highest effect shown at 10 mg/kg [14].

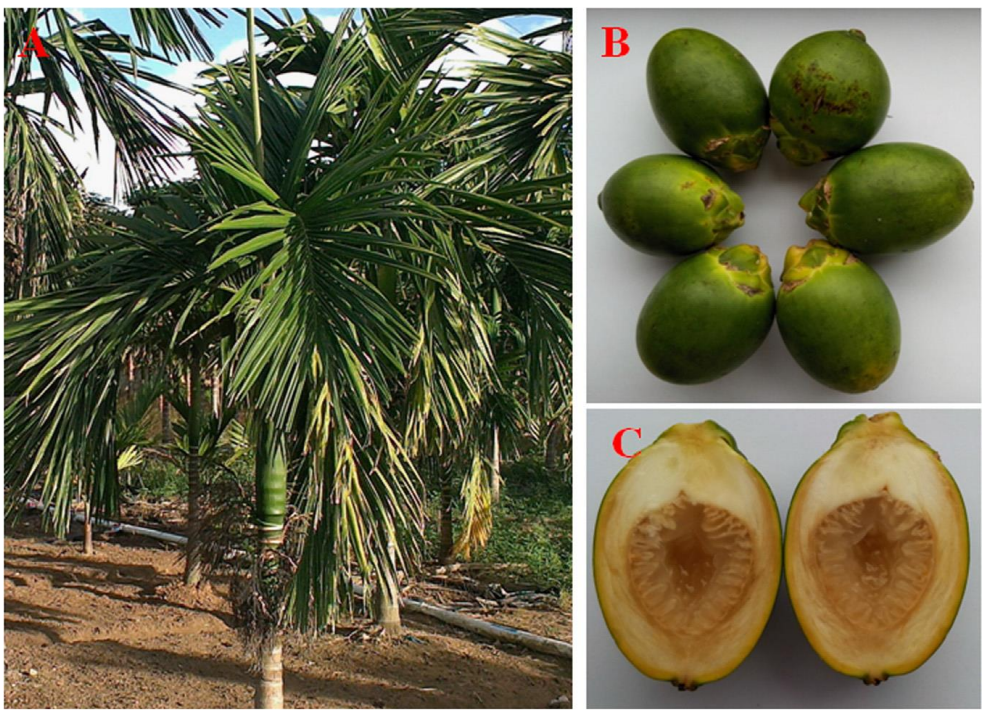

Figure 2. Areca catechu L. (A) Whole *Areca catechu* plant. (B) and (C) The fresh fruit of *Areca catechu* (areca nut) [11]

6. Purpose of This Study

Arecae Pericarpium, the nut (fruit) peel of *Areca catechu* L. (Arecaceae), commonly called betelnut, according to *Compendium of Materia Medica,* is used in Traditional Chinese Medicine (TCM) for abdominal distension, constipation, and edema treatment. Its combination with other herbs in Huo Xiang Zheng Qi formula is used to treat summerheat-dampness diseases and gastrointestinal cold, to cure abdominal distension, vomiting, and diarrhea [11]. In Korea, Arecae Pericarpium is used in Gami-Jeonggisan formula to treat vascular diseases, including atherosclerosis and ischemic stroke [15]. Arecae Pericarpium was reported to have fungicidal activity against *Colletotrichum gloeosporioides* Penz. *in vitro* and in mango fruit medium with fernenol showing highest inhibitory activity [16]. Areca Pericarpium also showed dose-dependent antioxidant activity in human hepatocarcinoma $HepG_2$ cell line and the methanol extract showed the strongest antioxidant activity compared to other parts of the *Areca catechu* (L.) plant [17].

Despite of its traditional usage, studies on anti-inflammatory activity and active compounds from Arecae Pericarpium has not been reported yet. Reported studies on *in vitro* and *in vivo* anti-inflammatory activity of other parts of the plant, such as seed and leaf, lead to hypothesis that Arecae Pericarpium may exhibit anti-inflammatory activity as well [12, 13, 14]. Thus, the purpose of this study is to investigate the anti-inflammatory activity of Arecae Pericarpium and to identifiy the active compounds by applying bioassay-guided isolation scheme.

II. MATERIALS AND METHODS

1. MATERIALS

1.1 Plant Materials

Arecae Pericarpium was purchased from local herb market in Seoul, South Korea and identified by Professor Suh Young Bae of Seoul National University. Voucher specimen was deposited at Faculty of Pharmacy, Seoul National University.

1.2 Chemicals and Reagents

All organic solvents used for extraction, column chromatography and HPCCC were of analytical grade and were purchased from Seoduk Chemical Co. in South Korea. HPLC-grade acetonitrile and methanol for preparative HPLC and HPLC analysis were obtained from J. T. Baker (Phillipsburg, NJ) and Fisher Scientific (Pittsburg, PA). Formic acid (FA) was purchased from Sigma-Aldrich (St. Louis, MO, USA). Distilled water (NANO pure Diamond, Barnstead, USA) was used for all solutions and dilutions. Silica gel 60 (0.063-0.200 mm) was purchased from Merck KGaA (Darmstadt, Germany). Silica gel 60 F_{254} 20x20 cm for thin layer chromatography was purchased from Merck KGaA (Darmstadt, Germany). Diaion®-HP20 (polystyrene adsorption resin) was purchased from Mitsubishi Chemical (Tokyo, Japan).

Dulbecco's phosphate buffered saline (D-PBS, pH 7.4), Dulbecco's Modified Eagle Medium (DMEM), lipopolysaccharide (LPS), Trypan Blue, dimethylsulfoxide (DMSO), penicillin-streptomycin, sulfanilamide, naphtylethylendiamine dihydrochloride, 2-amino-5-mercapto-1,3,4-thiadiazole

(AMT), *N*-*p*-tosyl-L-pheylalanine chloromethyl ketone (TPCK), 4-methylumbelliferyl phosphate (MUP), HEPES were purchased from Sigma Chemical Co. Ltd (St. Louis, MO). Fetal bovine serum (FBS) was purchased from South Pacific (New Zealand). Apocynin, vanillic aldehyde, 4-hydroxybenzoic acid and 4-hydroxybenzaldehyde were purchased from Sigma Chemical Co. Ltd (St. Louis, MO).

1.3 Instruments

HPLC analyses were carried out on Hitachi L-6200 instrument equipped with Sedex 75 Evaporative Light Scattering Detector (ELSD) and UV detector system and SIL-9A auto injector (Shimadzu, Japan) and Agilent 1100 equipped with PDA UV detector. Low resolution electrospray ionization source (ESI) LC/MS data were recorded on Agilent Technologies 6130 Quadrapole mass spectrometer coupled with Agilent Technologies 1200 series HPLC. Columns used for analysis are iNNO C18 column (150 mm x 4.6 mm id, 5µm particle size) from Young Jin Biochrom Co. Ltd (Seongnam, South Korea), LUNA C18 column (150 mm x 4.6 mm id, 3µm particle size) from Phenomenex Inc. (Torrance, CA, USA) and Zorbax SB-C18 column (75 mm x 4.6 mm id, 3.5µm particle size).

Spectrum HPCCC from Dynamic Extractions Ltd (Slough, UK) with tubing id 1.6 mm, total volume 135.5 mL, and sample loop 6 mL was used for CCC separation. The revolution speed was adjusted with a controller to an optimum speed of 1,600 rpm. Hitachi L-6200 intelligent Pump (Tokyo, Japan) was used to fill the CCC apparatus with the stationary phase and

elute the mobile phase. The effluent was continuously monitored by Dynamax UV Absorbance Detector from Rainin Instrument, LLC (California, USA).

Preparative HPLC separation was performed using Hitachi JP/L-7100 equipped with Hitachi L-4000 UV detector. Column used for separation was RSil C18 column (250 mm x 10 mm id, 10µm particle size) from Alltech (Deerfield, IL).

The NMR analyses were recorded on Bruker Avance 500 and 600 spectrometers. ^{1}H and ^{13}C NMR spectra were measured in a DMSO-d6 solution at 500 and 125 MHz or 600 and 150 MHz.

Instruments used for cell culture are as follow: CO_2 incubator, clean bench (Vision Scientific, South Korea), centrifuge (Hanil Scientific, South Korea), multiplate reader (Molecular Devices, Emax, Sunnyvale, CA, US) and multiplate fluorometer (Molecular Devices, Gemini XS, Sunnyvale, CA, US).

2. METHODS

2.1 Cell Culture

RAW 264.7 murine macrophage cells were obtained from American Type Culture Collection (ATCC). Cells were maintained at sub-confluence in 95% air and 5% CO_2 humidified atmosphere at 37°C. Medium used for routine subculture was DMEM supplemented with 10% FBS, penicillin (100 units/mL) and streptomycin (100 µg/mL). Cells were counted with hemocytometer and the number of viable cells was determined by trypan blue dye exclusion.

2.2 Griess Reagent Nitrite Assay

RAW 264.7 macrophages were plated at density of 1 x 10^5 cells/well in a 24-well plate with 500 µL of culture medium and incubated at 37°C for 24 h. Culture medium was changed and cells were treated with samples in various concentration for 2 h and then stimulated with LPS (1 µg/mL) for 18 h. An aliquot of cell-free medium (100 µL/well) was removed to 96-well plate and Griess reagent (100 µL/well) was added. Griess reagent was made from 1% sulfanilamide in 5% phosphoric acid and 0.1% naphtylethylenediamine dihydrochloride in distilled water. To quantify nitrite concentration, standard nitrite solutions were prepared and absorbance of the mixture was determined with microplate fluorometer (Molecular Devices) at wavelength 540 nm. AMT, an iNOS inhibitor, or TPCK, a known NF-κB inhibitor, was used as positive control with concentration of 10 µM. Cells treated with vehicle alone was used as control.

2.3 Cell Viability

The measurement of cell viability was performed using MTT (4,5-dimethylthiazol-2-yl)-2,5-diphenyl tetrazolium bromide) assay concurrently with nitrite assay. RAW 264.7 macrophages were plated at density of 1 x 10^5 cells/well in a 24-well plate with 500 µL of culture medium and incubated at 37°C for 24 h. Culture medium was changed and cells were treated with samples in various concentration for 2 h and stimulated with LPS (1 µg/mL) for 18 h. After 100 µL of media was taken for nitrite assay, 40 µL of MTT solution (2 mg/mL in saline) was added to each well and incubated at 37°C for 2 h. Mitochondrial succinate dehydrogenase in living cells will convert MTT into visible formazan crystals during incubation. The formazan crystals were then solubilized in DMSO and the absorbance was measured at wavelength 595 nm using microplate fluorometer.

2.4 Determination of PGE_2 detection

The amount of PGE_2 produced from activated macrophages was quantified using an enzyme immunoassay (EIA) kit for PGE_2 (Cayman Chemical, Ann Arbor, MI). Briefly, 1×10^5 cells were seeded in 24-well plate and incubated for 24 h. After changing to new media, the cells were pre-treated with several concentrations of MC1A fraction or a vehicle for 2 h and then activated by LPS (1 µg/ml) to express COX-2 for an additional 18 h. These media were diluted 2 times with PBS and transferred to a PGE_2 antibody-coated 96-well culture plate in the EIA kit. Further treatment was according to the manufacturer's instructions. The produced PGE_2 in the specimen was quantified to determine

COX-2 expression using a PGE_2 standard curve. Absorbance at 405 nm was recorded using a microplate reader (Molecular Devices, Emax, Sunnyvale, CA). For comparison, 10 μM TPCK was used as a positive control.

2.5 NF-κB Secretory Alkaline Phosphatase (SEAP) Reporter Gene Assay

Reporter enzyme activity was measured by cell-based assay system for NF-κB activity monitoring. The pNF-κB-SEAP-NPT plasmid that permits expression of the SEAP reporter gene in response to the NF-κB activity and contains the neomycin phosphotransferase (NPT) gene for geneticin resistance in host cells was constructed and transfected into murine macrophages. Transfected RAW 264.7 cells were plated at density of 1 x 10^5 cells/well in a 24-well plate with 500 μL of geneticin-added culture medium and incubated at 37°C for 24 h. Cells were treated with samples in various concentrations for 2 h and stimulated with LPS (1μg/mL) for 18 h. Aliquots of cell-free medium (120 μL) of each treatment was transferred to 1.5 mL vial and heated at 65°C for 6 min and given an assay buffer (2 M diethanolamine, 1 mM $MgCl_2$, 500 μM 4-methylumbelliferyl phosphate (MUP)) in the dark at 37°C for 1 h. The fluorescence from the product of the SEAP/MUP was measured using a 96-well microplate fluorometer at an excitation of 360 nm and emission of 449 nm. TPCK (20 μM) was used as positive control.

2.6 Extraction

Dried Arecae Pericarpium was purchased from a local herb market in Seoul, South Korea. 5 kg of Arecae Pericarpium was macerated in 28 L of methanol

(MeOH) for 3 days. This process was repeated for three times. The extract was dried with rotary evaporator under 50ºC. Subsequently, dried extract was suspended in 10% MeOH and liquid-liquid extraction was performed with hexane, methylene chloride (MC), ethyl acetate (EtOAc) and n-butanol (BuOH) at 1:1 ratio for three times. The obtained fractions were evaporated to dryness under vacuum and stored in desiccator until further use. Each fraction was tested for its inhibition activity against LPS-stimulated NO production in RAW 264.7 macrophage cells. Since methylene chloride and ethyl acetate fraction showed higher NO inhibition activity than other fractions, further separation was performed on those fraction.

2.7 Silica column chromatography

Silica column chromatography separation of MC fraction was performed using an open column with diameter 5 cm and length 58 cm. 500 g of silica gel was activated and packed into the column to separate 18 g of sample. Sample was eluted with a gradient elution of chloroform – ethyl acetate (9:1, 7:3, 5:5, 3:7, 1:9 v/v) continued with ethyl acetate – methanol (9:1, 7:3, 5:5 v/v). Each ratio was collected in 2 bottles of 500 mL and collected fractions were analyzed with TLC.

Silica column chromatography separation of MC1A fraction was performed in an open column (75 x 3 cm). 100 g of silica gel was used to separate 3.3 g of sample. Sample was eluted with 2 L of hexane-ethyl acetate-*n*-butanol with ratio (3:2:0.05) and (2.75:2.25:0.05). Fifteen fractions with volume of 125 mL were collected and analyzed with TLC and HPLC.

2.8 Diaion® HP-20 resin column chromatography

MC1A fraction (1.3 g) and ethyl acetate fraction (17.1 g) were separated with Diaion® HP-20 resin open column chromatography (75 x 3 cm for MC1A and 58 x 5 cm for ethyl acetate fraction). Sample was made into suspension with 10% methanol and poured into the column. Elution began with distilled water as washing step and sequentially eluted with a methanol gradient beginning from 20% to 100% methanol, 3 times of packed column volume for each gradient. Fractions were collected, evaporated, and stored in a refrigerator or desiccator until further use.

2.9 Selection of the two-phase solvent system and measurement of the partition coeffient (*K)* and settling times

The solvent system was selected based on the *K* values of the target compounds. The values were measured based on the peak area shown in HPLC chromatogram. The two-phase solvent system was prepared in a separating funnel flask, shaken vigorously to allow the solvents mix and settle it for 1.5 hours to allow the solvent system separate and equilibrate. The lower phase and upper phase were collected in separated tubes. Approximately 2 mg of crude extract was dissolved in equal volumes of lower and upper phases of the equilibrated two-phase solvent system in test tube. The tube was shaken vigorously to equilibrate the sample between the two phases. The phases were separated and evaporated to dryness under nitrogen (N_2) gas. The residue was dissolved in methanol and analyzed with HPLC. The *K* value was expressed as the peak area of the target compound in the upper phase divided by that in the lower phase. The settling time, which is highly correlated to the retention of the

stationary phase, was expressed as the time to form a clear layer between the two phases after mixing.

2.10 HPCCC Separation

In each separation run, the multi-layered coiled column was filled with the upper phase to form the stationary phase. The first step was performed in reverse phase mode at 25ºC. The preparative column (total 135.5 mL) was filled with upper phase as the stationary phase. The mobile phase (lower phase) was pumped to the system at a flow rate of 3 mL/min while the columns were rotating at a speed of 1600 rpm. Sample was dissolved in same ratio of upper and lower phase with total volume of 6 mL and injected into the HPCCC system.

2.11 Preparative HPLC Separation

MC1B fraction separation was carried out with preparative HPLC technique. The mobile phase used was 0.05% formic acid in distilled water (solvent A) and 0.05% formic acid in methanol (solvent B). Isocratic mode of 18% solvent B was chosen to separate peaks with flow rate of 2.5 mL/min for 120 minutes and monitored with UV detector at 246 nm. For each run, not more than 10 mg of sample dissolved in 200 µL of HPLC grade methanol was injected to sample valve. Peaks observed on chromatogram were collected as fractions, dried under vacuum and analyzed with HPLC to determine their purity.

2.12 Identification of isolated compounds

All isolated compounds were analyzed with HPLC coupled with low resolution electrospray ionization source (LR-ESI/MS) for molecular weight determination and their structure were identified by comparing the ^{1}H and ^{13}C NMR spectra in DMSO-d_6 with references.

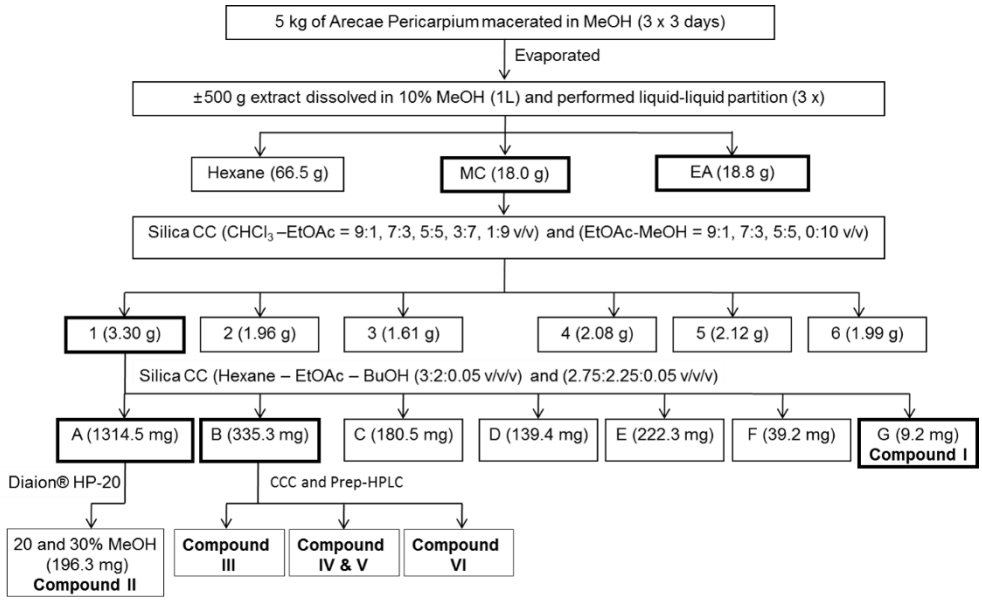

Figure 3. Isolation scheme of Arecae Pericarpium methylene chloride fraction

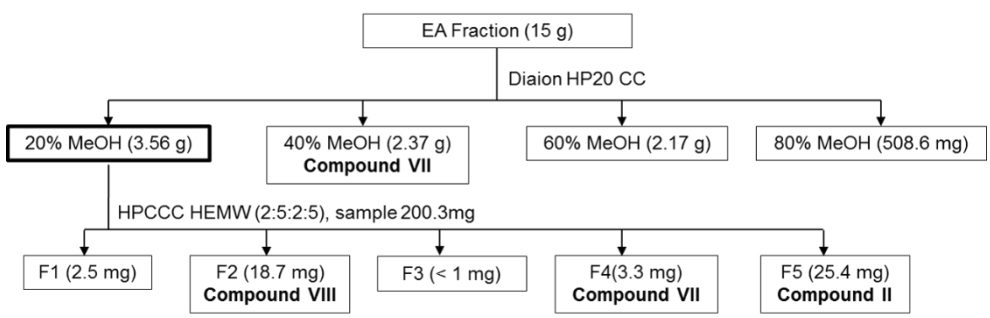

Figure 4. Isolation scheme of Arecae Pericarpium ethyl acetate fraction

III. RESULTS

1. Preliminary study

Fractions obtained from solvent partition (hexane, methylene chloride, ethyl acetate, *n*-butanol, and water fraction) were tested with Griess reagent nitrite assay to screen active fractions in suppressing LPS-stimulated NO production in RAW 264.7 cells. All fractions were tested with increasing concentration from 10, 25, to 50 µg/mL and compared with a positive control, AMT (10 µM).

The cell viability decreased at the highest concentration tested but it is still in the acceptance range (≥80%), except for ethyl acetate fraction which its cell viability decreased until 74% at 50 µg/mL. The methylene chloride fraction suppressed LPS-induced NO production with IC_{50} value 8.89 µM, which is the highest among all tested fractions. The ethyl acetate fraction was the second fraction that showed suppression on NO production with IC_{50} value 13.60 µM. Hexane fraction inhibited NO production with IC_{50} value 31.94 µM while IC_{50} value of *n*-butanol and water fraction were more than 50 µM. Hence, a further separation was performed on methylene chloride and ethyl acetate fractions.

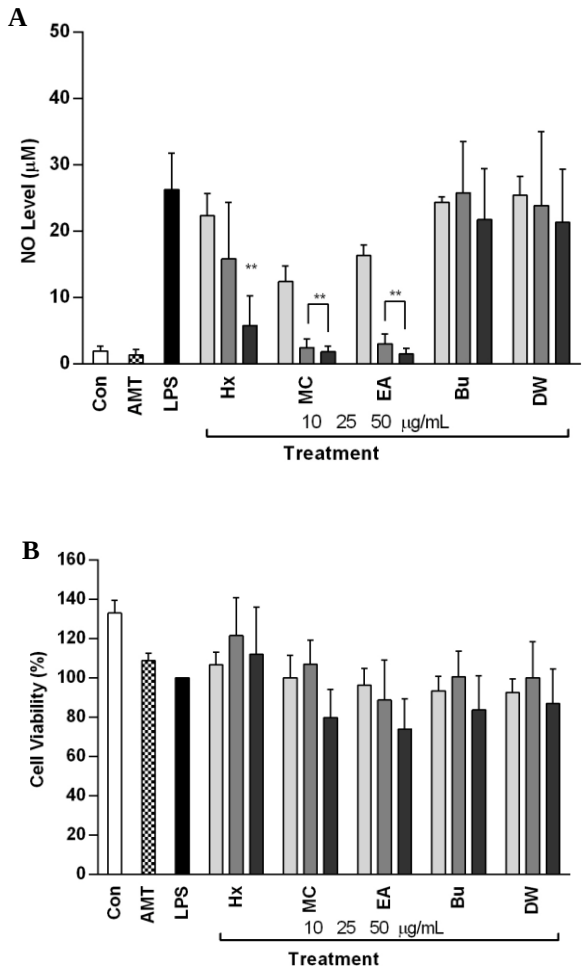

Figure 5. Effect of Arecae Pericarpium on (A) NO production and (B) cell viability of LPS-stimulated RAW 264.7 murine macrophage cell

Dose-dependent suppression of LPS-induced NO production by Arecae Pericarpium fractions in RAW 264.7 macrophages. Data were derived from three independent experiments and are expressed as mean ± standard deviation (S.D). (**) *P<0.01* indicates a significant difference from the LPS-stimulated group.

Control (vehicle), AMT (positive control), LPS (LPS + vehicle)-treated cells alone, HX (hexane fraction), MC (methylene chloride fraction), EA (ethyl acetate fraction), Bu (*n*-butanol fraction), and DW (distilled water fraction).

2. Separation of methylene chloride fraction

The methylene chloride fraction was subjected to silica gel open column chromatography and 17 fractions were obtained. These fractions were analyzed with TLC. The TLC mobile phase system used was methylene chloride-ethyl acetate-*n*-butanol with ratio 9:10:1 v/v, respectively. After elution, TLC plate was dried and observed under room light and UV light (254 nm and 366 nm). The spots showed fluorescence under 254 nm but did not show any phosphorescence under 366 nm. The spots were also not distinguishable when observed under room light. Thus, fractions showing similar spots pattern under 254 nm UV light were combined. Based on the TLC analysis, total of 6 fractions were obtained with the following yields: MC1 (3.30 g), MC2 (1.96 g), MC3 (1.61 g), MC4 (2.08 g), MC5 (2.12 g), and MC6 (1.99 g).

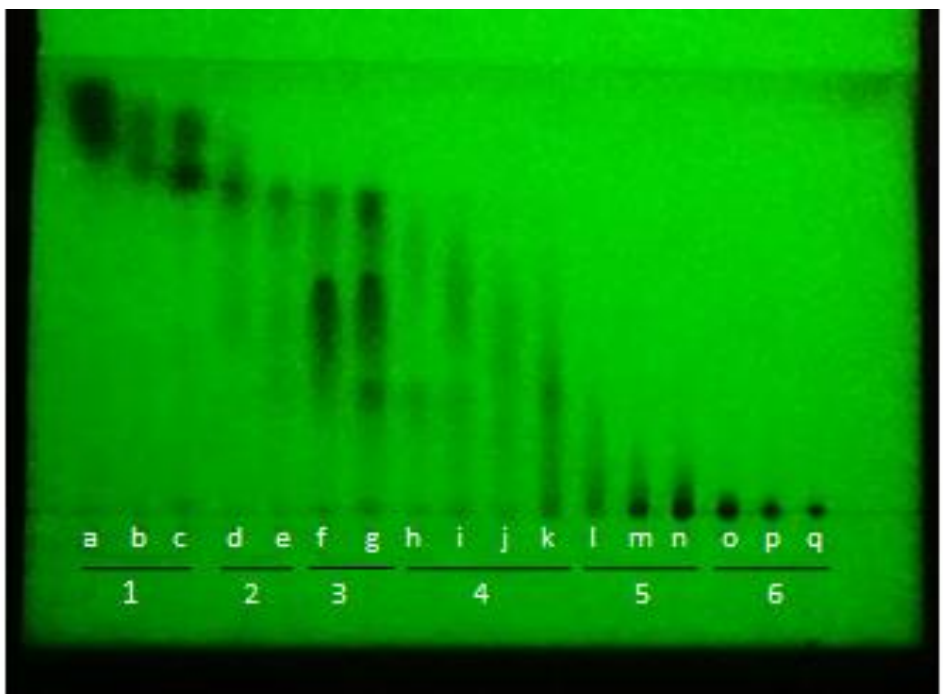

Figure 6. TLC analysis of Arecae Pericarpium methylene chloride fraction under 254 nm UV light

Seventeen eluents obtained from silica gel open column chromatography were grouped into six fractions based on their spots similarity on TLC plate.

3. Suppression of LPS-induced NO production and cell viability assay by silica CC fractions from methylene chloride fraction

The inhibition effect of MC1 to MC6 fractions on LPS-induced NO production in RAW264.7 macrophages were tested with Griess reagent assay and compared to MC fraction and positive control, AMT. All fractions were tested dose-dependently at 5, 10, 25, and 50 μg/mL.

Most fractions showed cytotoxicity at 50 μg/mL, so the NO inhibition activity was compared at lower concentrations. MC1 fraction inhibited NO production with IC_{50} value lower than 5 μg/mL. IC_{50} value of other fractions were 8.56 μg/mL (MC2 fraction), 9.36 μg/mL (MC3 fraction), 8.91 μg/mL (MC4 fraction), and more than 50 μg/mL (MC5 and MC6 fractions). Based on this result, further separation was performed on MC1 fraction.

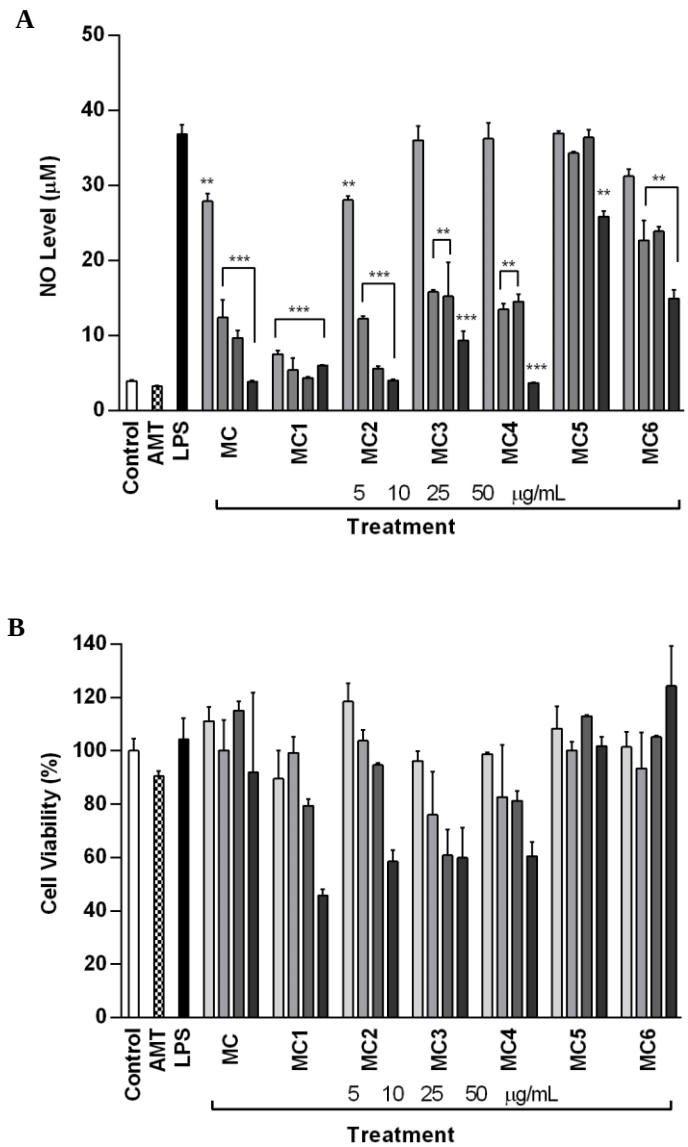

Figure 7. Effect of silica CC fractions from methylene chloride fraction on (A) NO production and (B) Cell viability

Data were derived from three independent experiments and are expressed as mean ± SD. (**) *P<0.01* and (***) *P<0.001* indicate significant difference from the LPS-stimulated group.

4. Separation of MC1 fraction

MC1 fraction was subjected to silica gel open column chromatography. Hexane-ethyl acetate-*n*-butanol with ratio (3:2:0.05 v/v) and (2.75:2.25:0.05 v/v) were selected as mobile phase. Fifteen fractions with volume of 125 mL each were collected and analyzed with TLC. After elution, the TLC plate was dried and observed under day light and UV light (254 nm and 366 nm). The spots showed fluorescence under 254 nm but did not show any phosphorescence under 366 nm. After 2 hours, yellow spots were detected under day light.

Except for the last 4 spots on TLC plate, it was difficult to decide which fractions to combine due to the different Rf of the spots. All fractions were analyzed with HPLC. HPLC condition was as follows: eluents water (A) and acetonitrile (B); gradient program: 0-5 min (5-20% B), 5-25 min (20-51% B), 25-30 min (51-55% B), 30-35 min (55-68% B), 35-40 min (68-100% B) in 1 mL/min. Samples were prepared in 500 µg/mL and 10 µL was injected to HPLC system. The HPLC run was detected by ELSD and UV detector set at 254 nm. Fractions that exhibited similar chromatogram in both ELSD and UV detection mode were combined. Seven fractions in total were obtained as described in below figure and labeled as MC1A – MC1G with following yield: 1314.5 mg, 335.3 mg, 180.5 mg, 139.4 mg, 222.3 mg, 39.2 mg, and 9.2 mg, respectively.

A

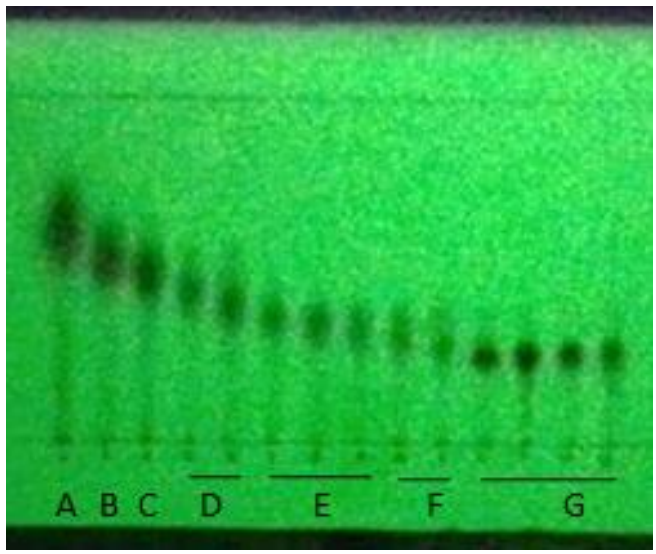

B

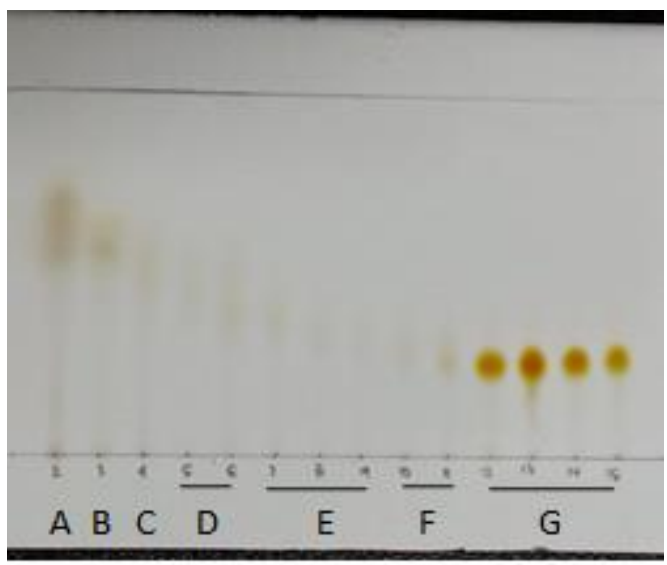

Figure 8. TLC chromatogram of silica CC fractions from MC1 fraction under (A) UV 254 nm and (B) day light

MC1G fraction was obtained as single compound and labeled as compound I. MC1A fraction was subjected through Diaion® HP-20 open column chromatography and compound II was obtained from 20 and 30% methanol elution.

5. Suppression of MC1A – MC1G fraction on LPS-induced NO production in RAW 264.7 macrophages

MC1A-MC1G obtained from silica column chromatography separation were monitored for their suppression effect on LPS-induced NO production in RAW 264.7 macrophages. All fractions were tested at 2.5, 5, and 10 µg/mL and compared to MC1 fraction. MC1A fraction showed the strongest inhibition of LPS-induced NO production with IC_{50} value 1.16 µg/mL, followed by MC1G with IC_{50} value 3.92 µg/mL and MC1B with IC_{50} value 7.13 µg/mL. The IC_{50} values of MC1C, MC1D, and MC1E fractions were more than 10 µg/mL. Cell viability were in accepted range (> 80%) for all fractions, except for MC1G fraction which showed cytotoxicity at 10 µg/mL.

MC1A fraction was able to inhibit LPS-stimulated PGE_2 production as well as shown in Figure 9C. Cells treated with 0.5 µg/mL of MC1A fraction showed more than 50% reduction of PGE_2 production. Other concentrations inhibited PGE_2 production to lower level than the positive control, TPCK (10 µM).

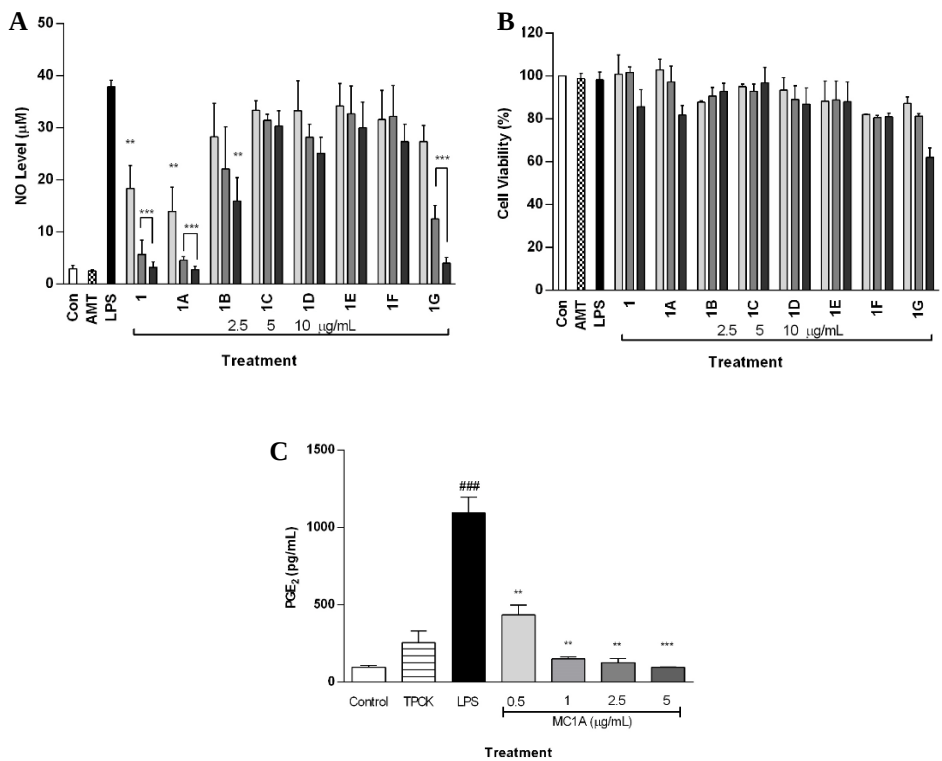

Figure 9. Effect of MC1 silica CC fractions on (A) NO production and (B) Cell Viability. (C) Effect of MC1A fraction on PGE_2 production

Data were derived from three independent experiments and are expressed as mean ± SD. (**) *P<0.01* and (***) *P<0.001* indicate significant difference from the LPS-stimulated group. (###) *P<0.001* indicates significant difference from the unstimulated control group. Control (vehicle), LPS (LPS + vehicle)-treated cells alone, 1 (MC1 fraction), 1A – 1G (MC1A – MC1G fraction). AMT and TPCK 10 μM were used as control positive.

6. Separation of MC1B fraction

The separation of MC1B fraction was initiated with HPLC analysis. HPLC condition was set as following: eluents water + 0.1% FA (A) and methanol + 0.1% FA (B); gradient program: 0-25 min (18% B), 25-35 min (18-100% B), 35-43 min (100 % B), 45-55 min (saturation with 18% B) in 0.3 mL/min. Sample was prepared in methanol with concentration of 100 µg/mL and 5 µL was injected. The column used for analysis was Zorbax SB-C18 column (75 mm x 4.6 mm id, 3.5 µm particle size).

Based on the HPLC chromatogram which showed nine peaks, HPCCC was selected to separate and isolate major peaks. Several solvent system were tested to investigate the optimum partition coefficient (*K*) as shown in Table 1 and HEMW solvent system (2:5:1:4 v/v/v/v) was selected for HPCCC operation. This solvent system was chosen because the peak no 6 and 8 as shown in Figure 10, which are the major peaks in this fraction, could be separated from other peaks.

The HPCCC operation was conducted as described in methods section. However, the target compounds could not be separated from other peaks. It might be caused by the UV detection wavelength selection which detected all compounds at their maximum absorption so all of the peaks were overlapped. The HPCCC chromatogram of MC1B fraction is shown in Figure 11. The yield of the target peak was 40.2 mg.

The peak was further isolated by preparative HPLC as described in methods section. Compound III, mixture of compound IV and V, and compound VI were obtained with yield 1.0 mg, 5.0 mg, and 0.6 mg, respectively. The representative HPLC chromatogram is shown in Figure 12.

Table 1. Solvent system screening for MC1B fraction separation

HEMW	*K* Value								
Ratio	1	2	3	4	5	6	7	8	9
2:5:2:5	1.48	2.94	1.87	5.80	2.66	5.64	5.68	3.37	3.75
2:5:1:4	0.42	2.11	1.49	7.26	2.19	**4.15**	**4.27**	**4.18**	2.08
2:4:2:4	0.89	1.37	1.85	1.95	2.44	2.72	2.79	3.66	4.07
3:4:2:4	0.89	1.61	1.10	2.83	1.53	2.08	2.59	1.62	2.04

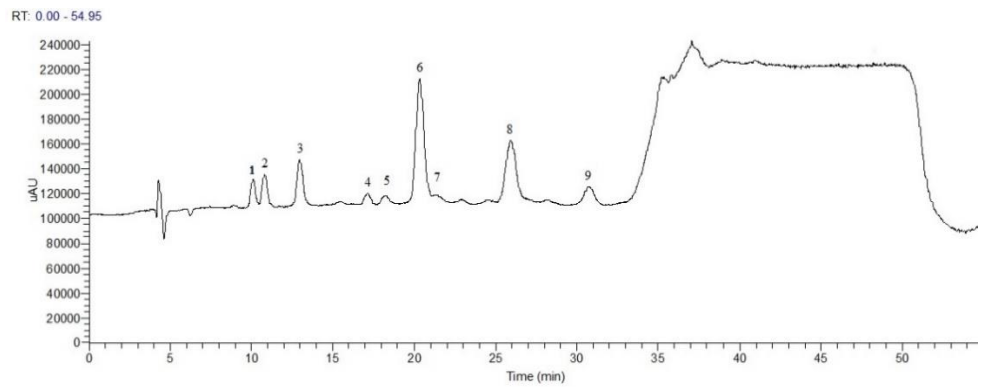

Figure 10. HPLC chromatogram of MC1B fraction

HPLC chromatogram of MC1B fraction analysis. Sample injection 5 µL from 100 µg/mL in methanol solution. Diode array detector was used for peak detection.

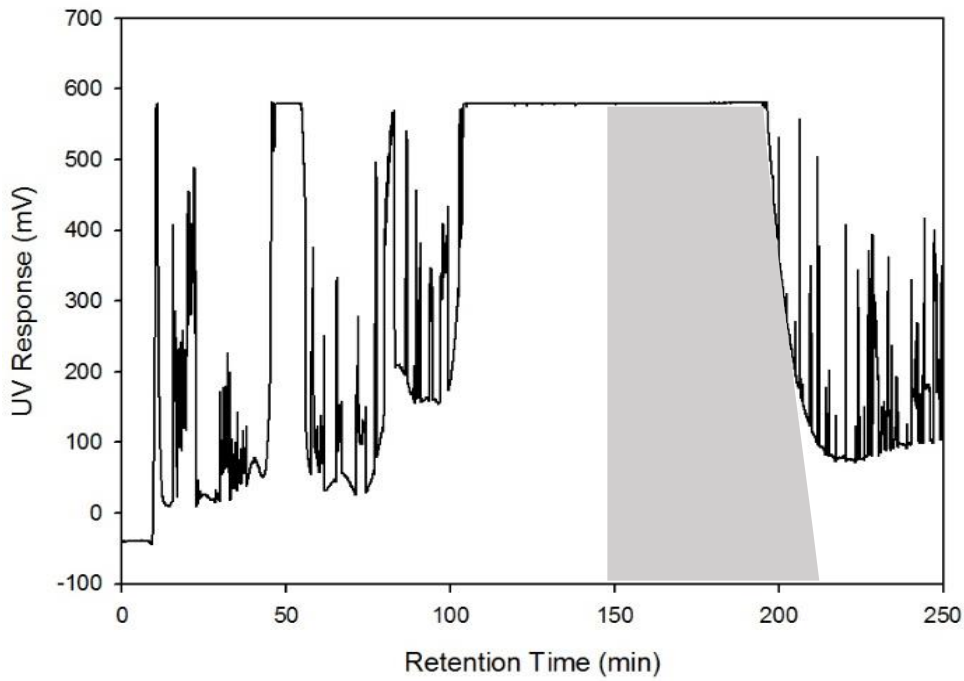

Figure 11. HPCCC chromatogram of MC1B fraction

HPCCC chromatogram of MC1B fraction is shown in above figure. The stationary phase retention was 70.11%. Sample injection was 130.3 mg in 6 mL of solvent system mixture and detected with UV detector at 280 nm for 200 minutes. The gray area marks the target peaks (149 min – 210 min). Peaks were detected with UV detector set at 280 nm.

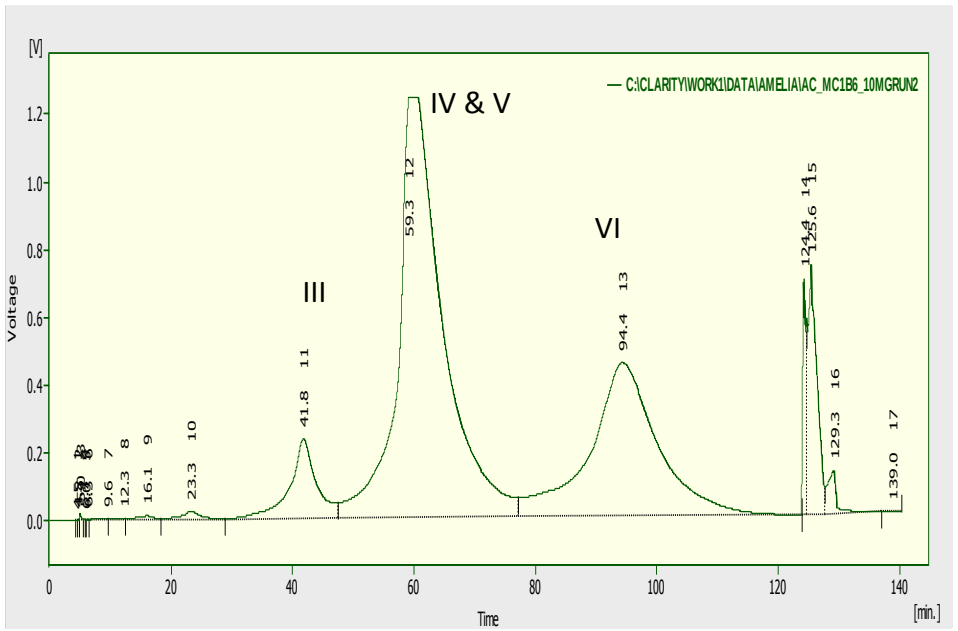

Figure 12. Preparative HPLC chromatogram of MC1B fraction after HPCCC separation

Target peaks separated from other peaks with HPCCC were isolated using preparative HPLC method. Separation was performed in isocratic mode (18% of MeOH with 0.05% FA) with UV detector set at 246 nm.

7. Separation of Ethyl Acetate Fraction

The ethyl acetate fraction was subjected to Diaion® HP-20 resin column chromatography and eluted with aqueous methanol in increasing concentration from 20%, 40%, 60%, and 80% methanol. The 20% MeOH fraction showed NO inhibition activity and was further separated with HPCCC. Several solvent system was tested to estimate the optimum *K* values and HEMW system (2:5:2:5 v/v/v/v) was selected for HPCCC operation.

The operation of HPCCC separation was conducted with UV detection set at 280 nm. The sample was weighed for 200.3 mg and dissolved in 6 mL of upper phase and lower phase mixture. The operation was performed for 200 minutes. Compound VII, VIII, and II were obtained with yield 18.7 mg, 3.3 mg, and 25.4 mg, respectively. The HPCCC chromatogram is shown in Figure 14.

Table 2. Solvent system evaluation for EA-20% MeOH fraction separation

Solvent system	*K* Value				
	1	2	3	4	5
BuOH - DW (5:5)	-	-	-	-	8.70
BuOH - MeOH - DW (5:1:5)	-	3.89	-	11.75	2.35
BuOH - MeOH - DW (5:1:3)	-	3.00	-	6.00	1.90
HEMW (2:5:2:5)	**1.61**	**0.75**	**1.15**	**2.83**	**3.48**
HEMW (2:5:2:10)	1.42	1.34	0.41	5.34	5.80

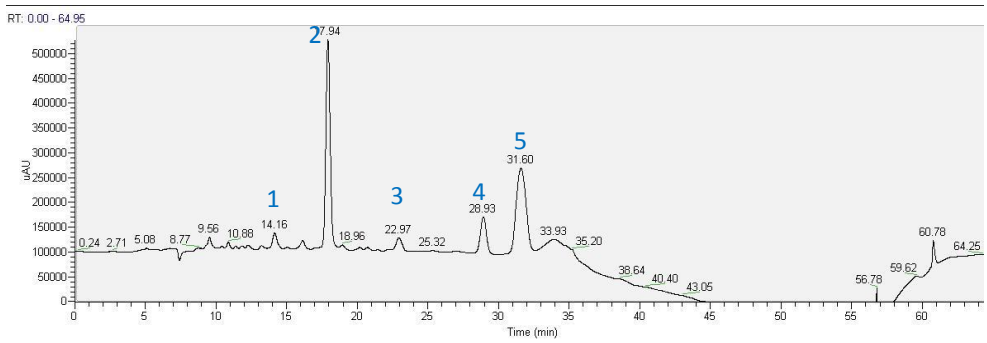

Figure 13. HPLC chromatogram of EA-20% MeOH fraction

The 20% MeOH fraction obtained from Diaion® HP-20 resin open column chromatography was analyzed with HPLC using LUNA C18 column (150 mm x 4.6 mm id, 3µm particle size). The mobile phase used was 0.1% FA in water (A) and acetonitrile (B) The separation was performed in gradient elution as following condition: 0 – 20 min (10% B), 20 – 40 min (10 – 100% B), 40 – 48 min (washing with 100% B), 50 – 60 min (column saturation with 10% B). The sample injection volume was 10 µL from 500 µg/mL concentration. Peaks were detected with diode array detector.

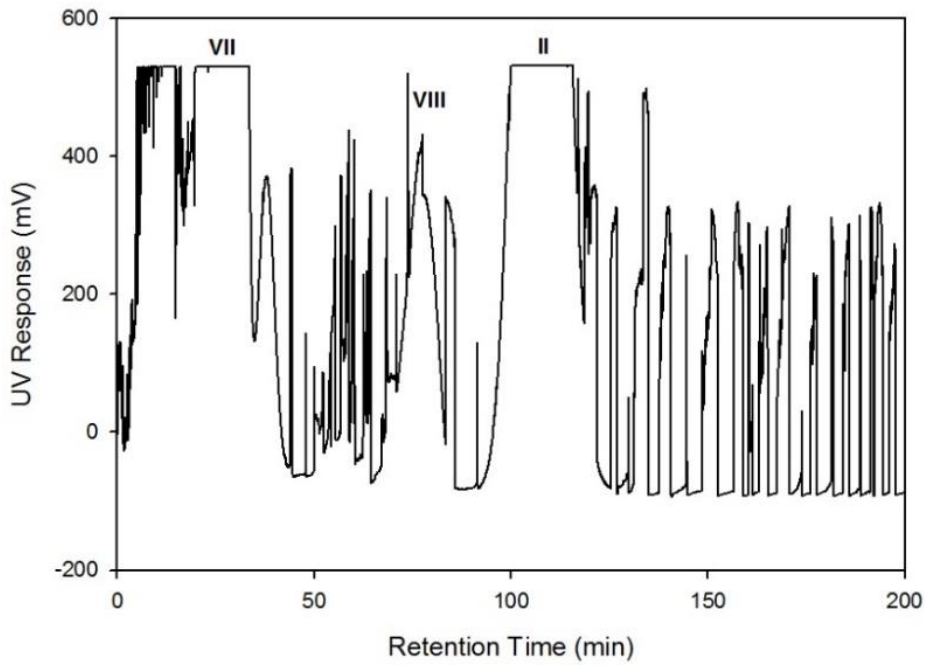

Figure 14. HPCCC chromatogram of EA-20% MeOH fraction

The HPCCC chromatogram of 20% MeOH fraction obtained from Diaion® HP-20 resin open column chromatography. Sample injection volume was 200.3 mg and detected with UV detector at 280 nm. The HPCCC separation was operated for 200 hours at 3 mL/min and 1600 rpm.

8. Suppression of LPS-induced NO production by ethyl acetate fractions obtained from Diaion® HP-20 resin column chromatography separation

Fractions obtained from Diaion® HP-20 resin column chromatography were tested at 5, 10, and 25 µg/mL. 20% MeOH fractions suppressed the LPS-induced NO production to lower level than other fractions. As shown in Figure 15, EA20 fraction showed the highest NO inhibition activity among all tested fractions with IC_{50} value 9.53 µg/mL. The IC_{50} values of other fractions were more than 25 µg/mL. The EA20 fraction might be rich of active compounds in inhibiting NO production, thus this fraction was subjected to further separation.

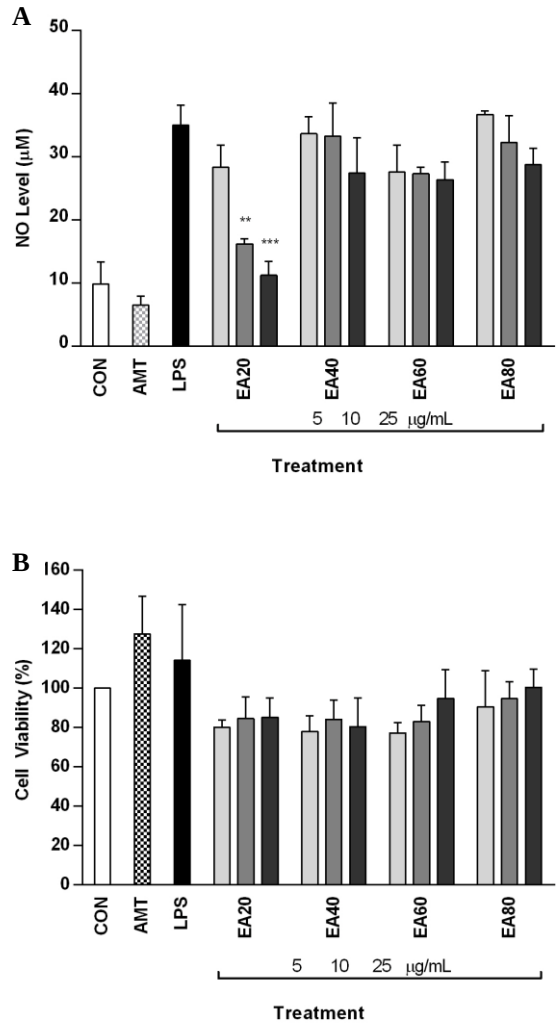

Figure 15. Effect of EA Diaion® HP-20 column fractions on (A) LPS-induced NO production and (B) cell viability

Data were derived from three independent experiments and are expressed as mean ± standard deviation (S.D). (**) *P<0.01* and (***) *P<0.001* indicate significant difference from the LPS-stimulated group. Control (vehicle), LPS (LPS + vehicle)-treated cells alone, EA20, 40, 60, and 80 (% of MeOH eluting the EA fraction). AMT 10 μM was used as positive control.

9. Structure Identification of Isolated Compounds

9.1 Identification of compound I

Compound I (MC1G fraction) was obtained as amorphous powder with slightly yellow color with >95% purity. When analyzed with HPLC-DAD detector, the UV spectrum of this compound showed maximum absorption at 218 and 280 nm. The positive-ion mode of ESI-MS showed molecular ion peak $[M+H]^+$ at m/z 307.1 and its negative-ion ESI-MS showed $[M-H]^-$ at m/z 305.1 (Figure 16).

^{1}H NMR spectrum of compound I showed signals at δ 8.35 (2H, s), 6.81 (4H, s), and 3.83 (12H, s) ppm. The ^{13}C NMR spectrum of compound I showed signal at δ 148.25 (C-2, C-6, C-9 and C-11), 134.92 (C-1 and C-10), 131.43 (C-4 and C-7), 104.37 (C-3, C-5, C-8, and C-12) and 56.25 ppm (methoxy carbons). The ^{13}C NMR spectrum of compound I was compared with ^{13}C NMR spectrum of monomer syringol [18] and almost all peaks are similar except for the peak at 131.43 ppm. Comparing the ESI-MS with another literature [19], it is proposed that this compound is a C-C dimeric syringol which has molecular weight 306 Da. The peak at 131.43 ppm is probably the attachment point of the other ring. The proposed structure is shown in Figure 18.

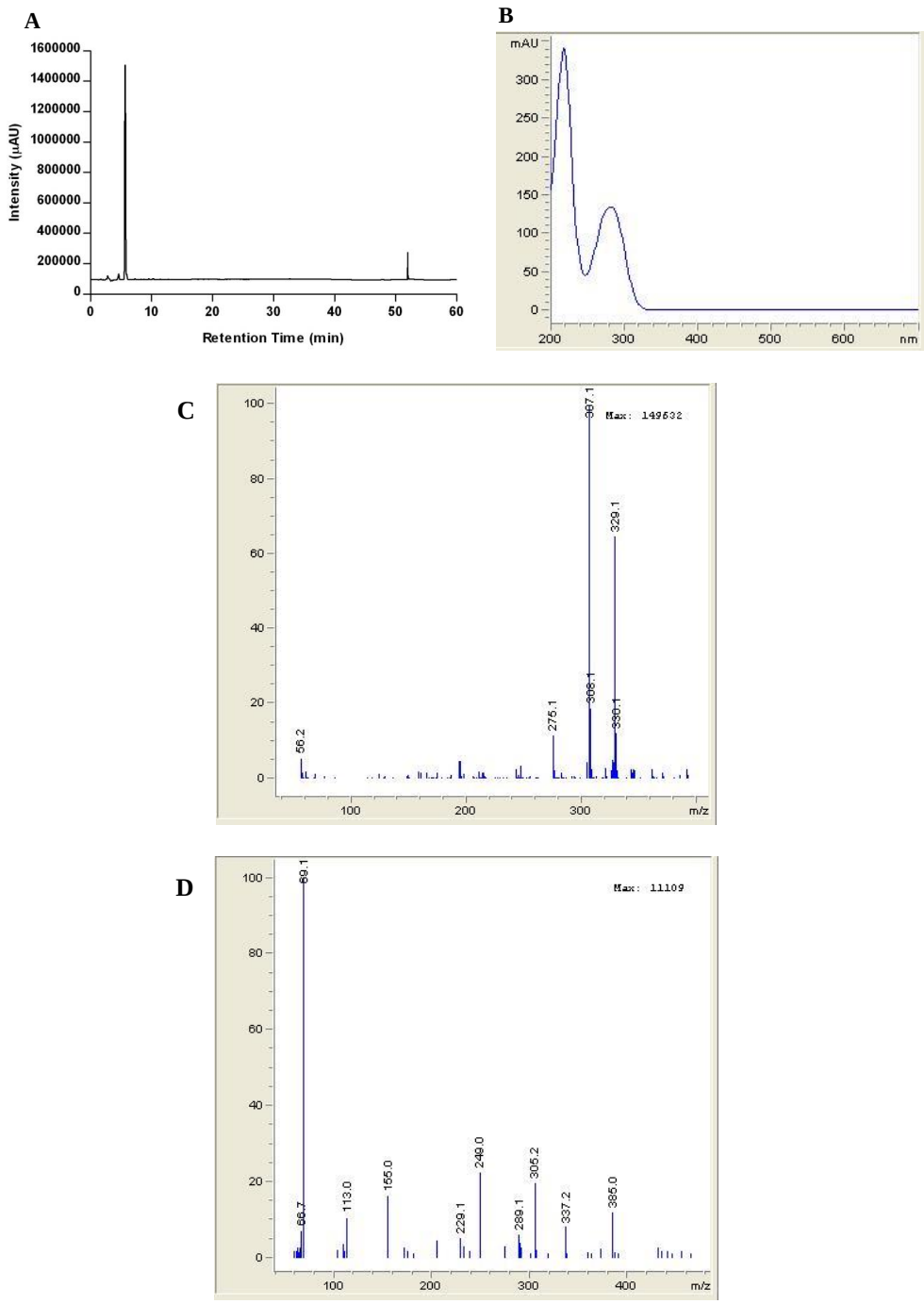

Figure 16. HPLC and ESI-MS analysis of compound I. (A) HPLC chromatogram (B) UV spectrum (C) ESI-MS positive-ion mode (D) ESI-MS negative-ion mode

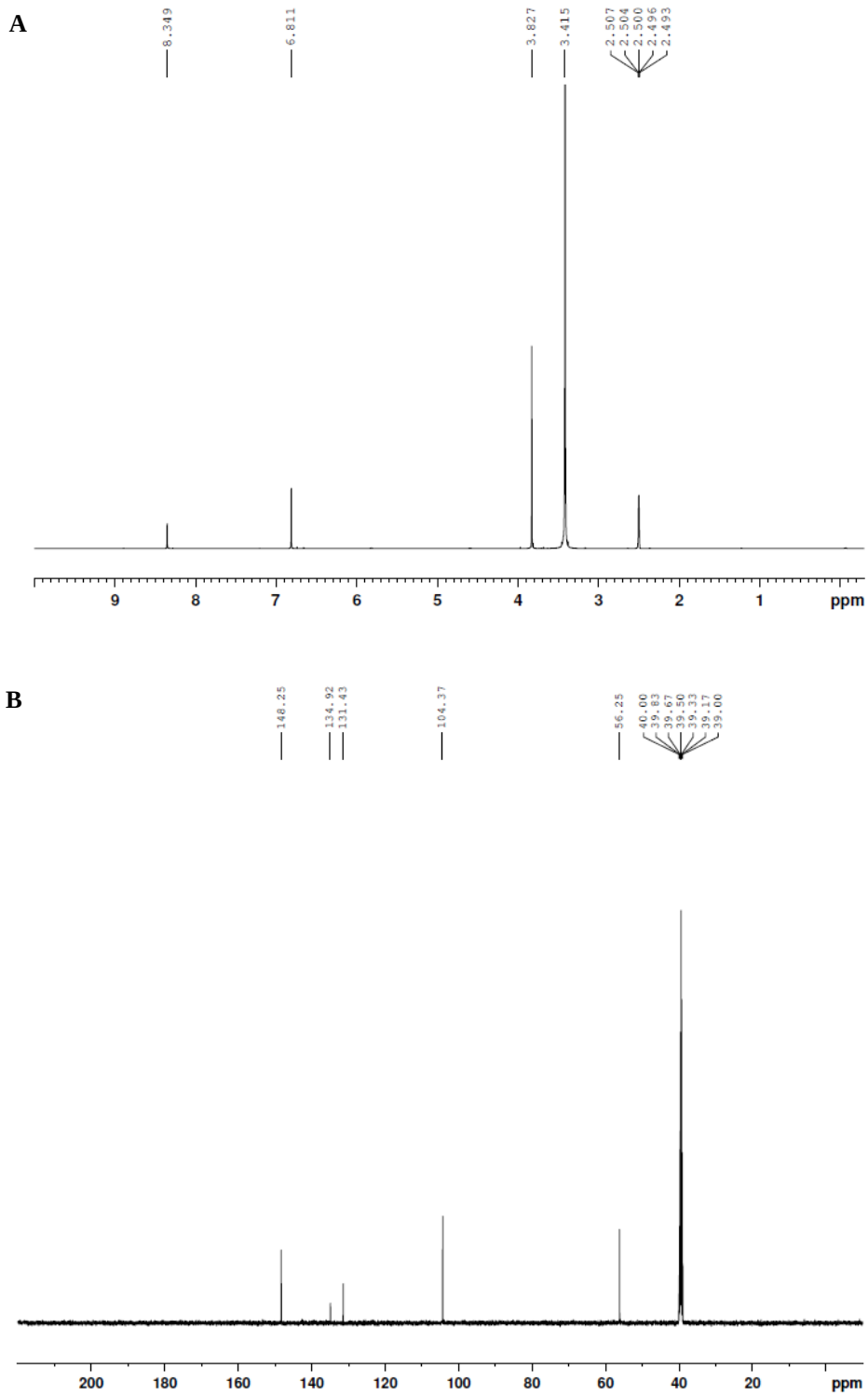

Figure 17. (A) ^{1}H NMR and (B) ^{13}C NMR spectrum of compound I at 500 MHz in DMSO-d_6

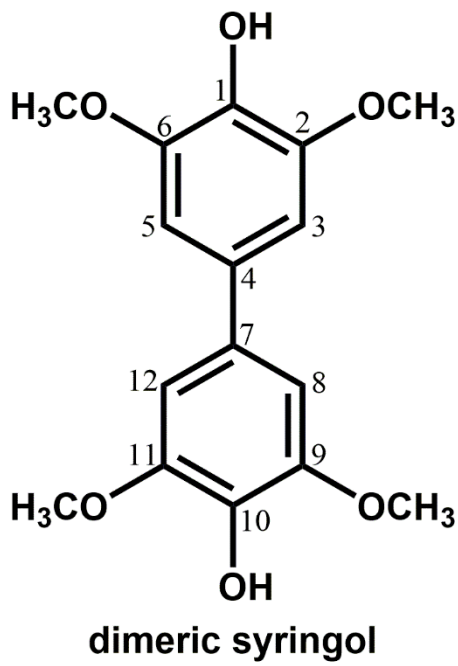

Figure 18. Proposed structure of compound I

9.2 Identification of compound II

Compound II was isolated from MC1A fraction eluted with 20% MeOH and 30% MeOH in Diaion® HP-20 resin open column chromatography. It was obtained as white to slightly gray amorphous powder. Compound II showed maximum absorption at 204, 218 and 276 nm in HPLC-DAD analysis and the negative-ion ESI-MS showed molecular ion peak $[M-H]^-$ at m/z 109.1 (Figure 19).

^{1}H NMR spectrum of compound II showed signals for aromatic ring group at δ 6.74 (2H, m, *J* = 9.5 Hz, 3.5 Hz) and 6.58 (2H, m, *J* = 9.5 Hz, 3.5 Hz) and hydroxyl group at δ 8.82 ppm (1H, br s). The ^{13}C NMR spectrum of compound II showed signal at δ 145.34 (C-1 and C-2), 119.39 (C-4 and C-5) and 115.77 (C-3 and C-6). The NMR spectral data were in alignment with reference data [20] thus compound II was assigned as catechol.

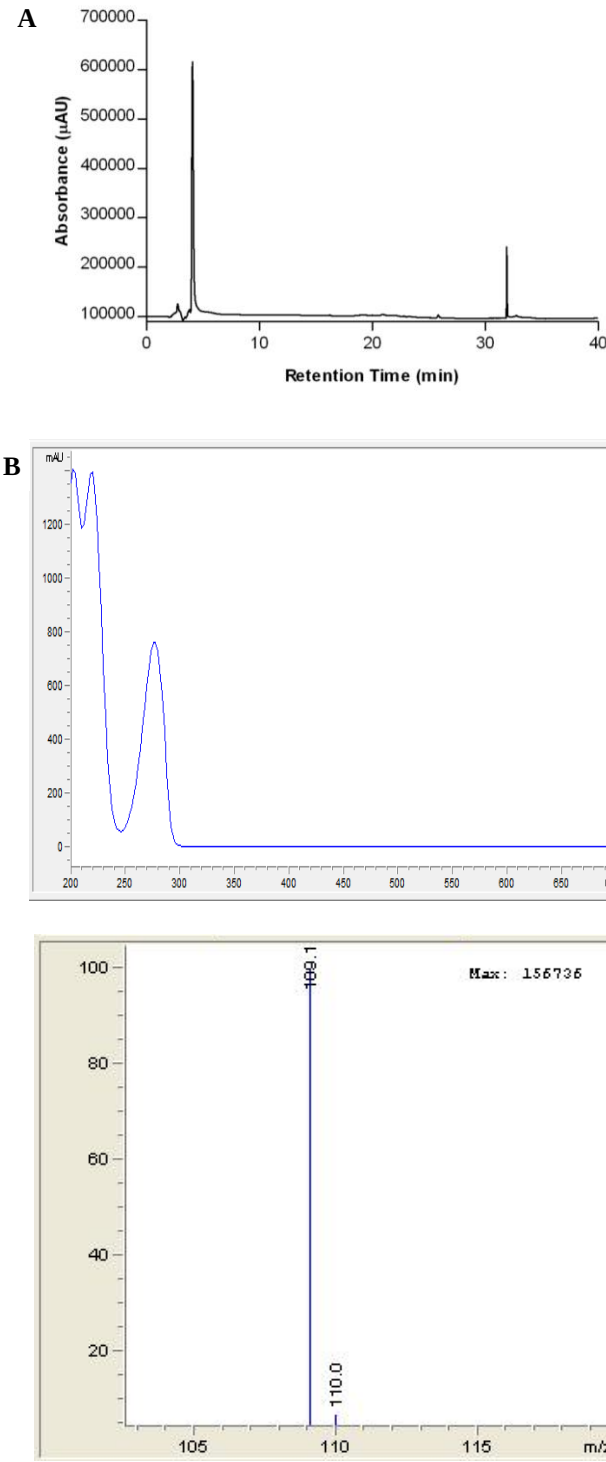

Figure 19. HPLC and ESI-MS analysis of compound II (A) HPLC chromatogram (B) UV spectrum (C) ESI-MS negative-ion mode spectrum

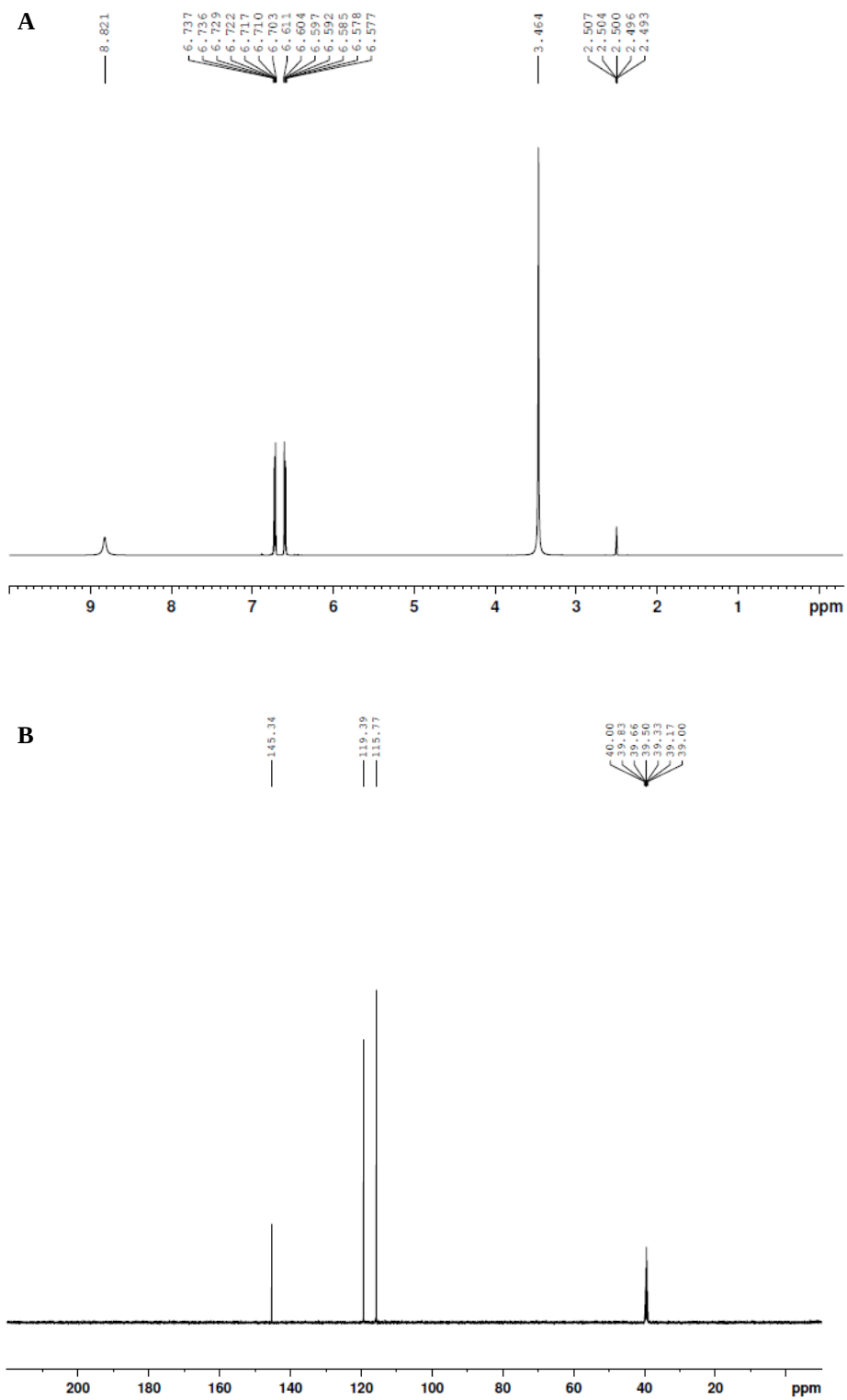

Fig 20. (A) ^{1}H NMR and (B) ^{13}C NMR spectrum of compound II at 500 MHz in DMSO-d6

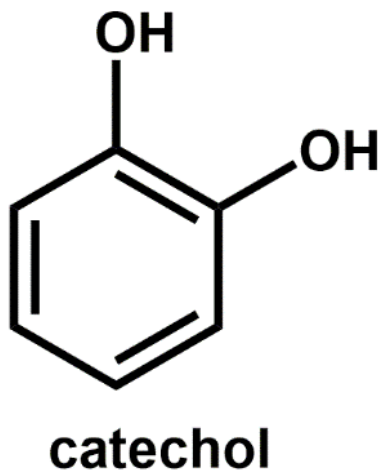

Figure 21. Structure of catechol

9.3 Identification of compound III

Compound III was obtained as white amorphous powder from separation of MC1B fraction. The UV detection of compound III showed maximum absorption at 196, 220, and 284 nm. The ESI-MS negative-ion mode spectra showed base ion peak at m/z 407.0 and an ion peak at m/z 121.1. Observing the NMR spectra, the molecular weight of the compound is most probably 122 Da.

^{1}H NMR spectrum of compound III showed signals for aldehyde proton attached to aromatic ring at δ 9.76 (1H, s), aromatic ring group at δ 7.75 (2H, d, J = 8.5 Hz) and 6.92 ppm (2H, d, J = 8.5 Hz). Due to the low yield of compound III, the ^{13}C NMR spectrum was not available. Instead, 2D NMR (COSY, HSQC, and HMBC) analysis was performed. Based on the HSQC and HMBC NMR spectra, the carbon signals detected at δ 191.11 (C-7), 163.95 (C-4), 132.33 (C-1), 128.28 (C-2 and C-6) and 116.03 ppm (C-3 and C-5) were correlated with the proton NMR and summarized in Table 3. The NMR spectral data of compound III were in alignment with reference [21] thus this compound was assigned as 4-hydroxybenzaldehyde.

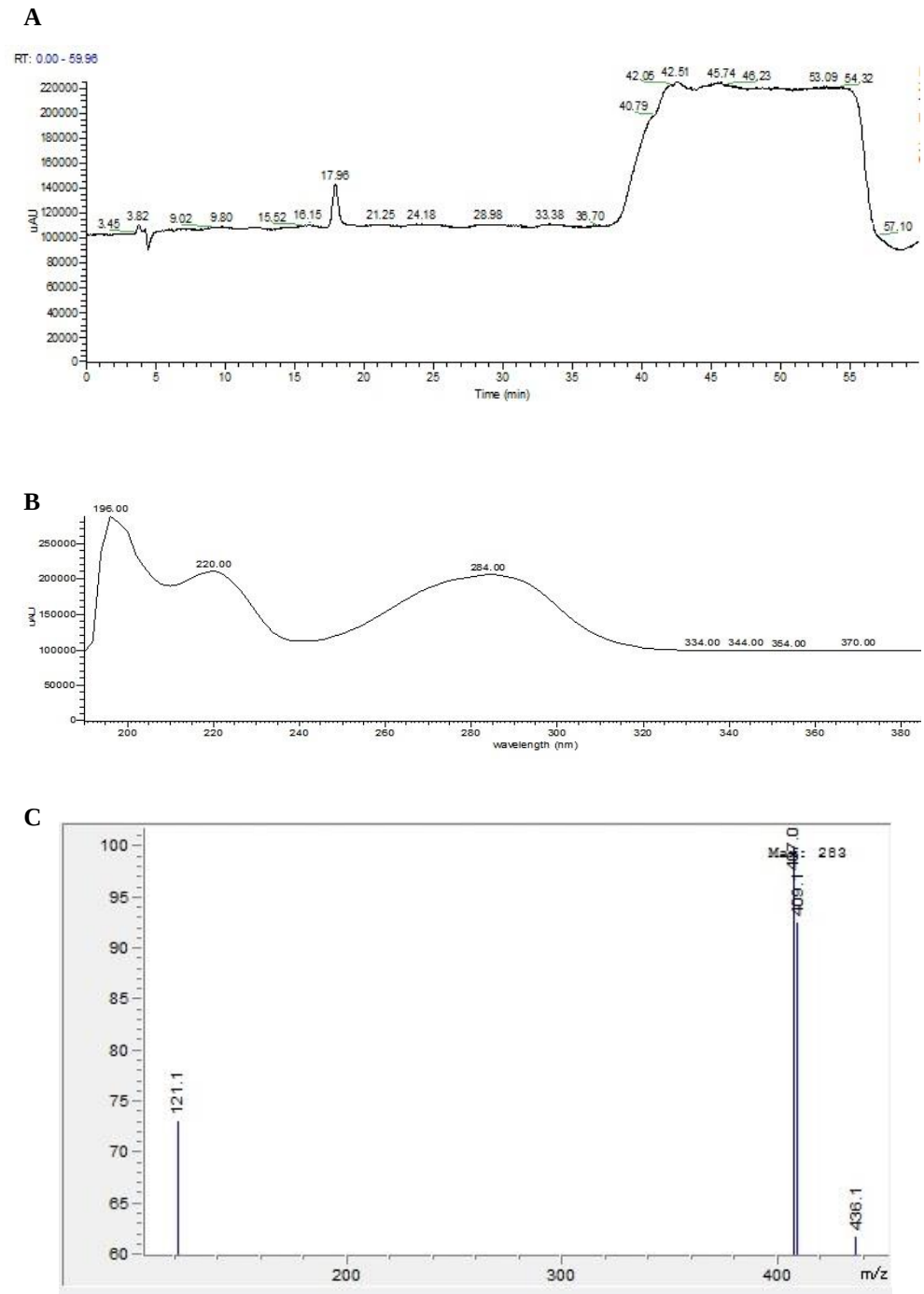

Figure 22. HPLC and ESI-MS analysis of compound III (A) HPLC chromatogram (B) UV spectrum (C) ESI-MS negative-ion mode spectrum

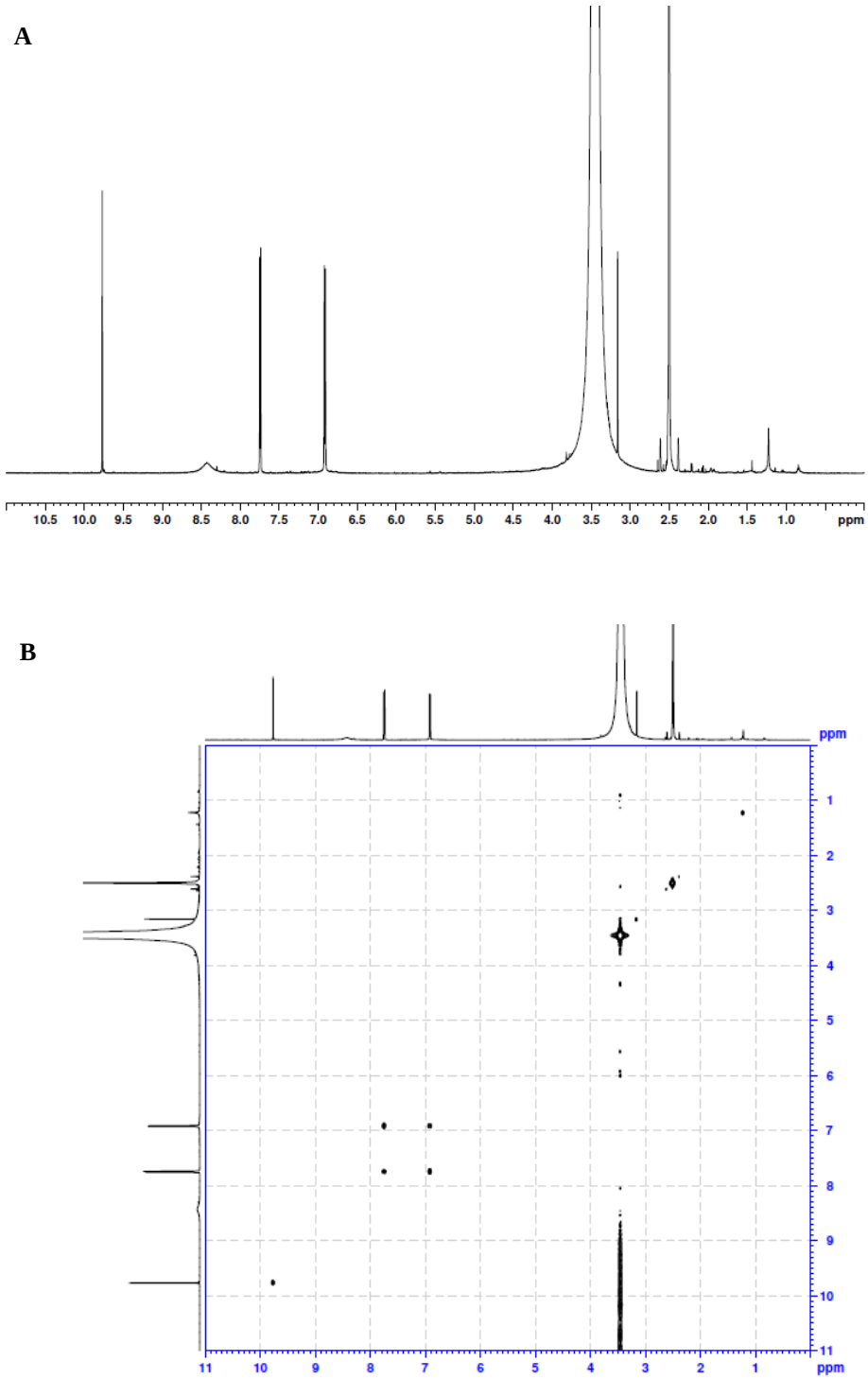

Figure 23. NMR spectra of compound III (A) ^{1}H NMR spectrum (B) ^{1}H-^{1}H COSY spectrum 600 MHz in DMSO-d_6

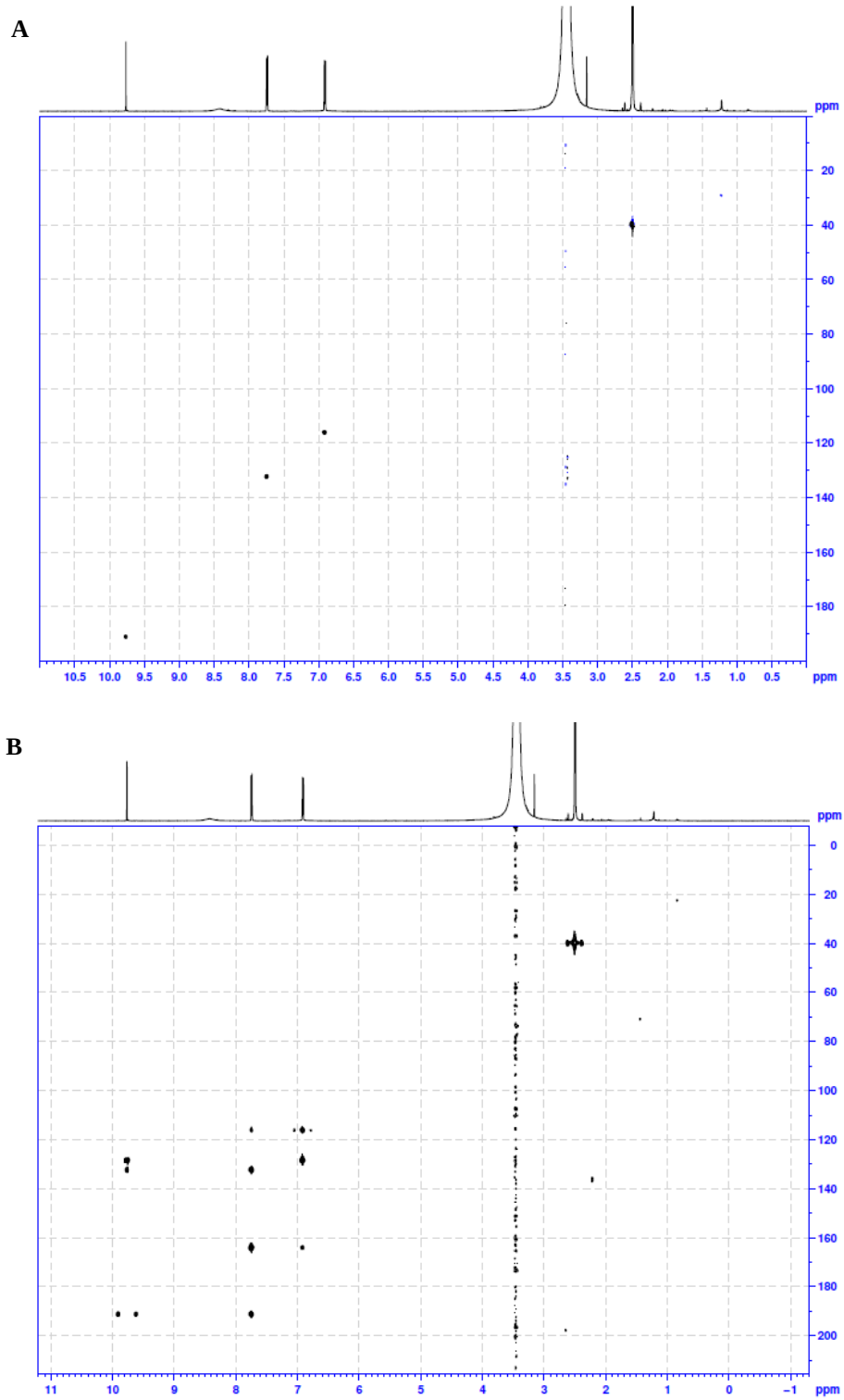

Figure 24. NMR spectra of compound III (A) ^{1}H-^{13}C HSQC NMR spectrum (B) ^{1}H-^{13}C HMBC spectrum 600 MHz in DMSO-d_6

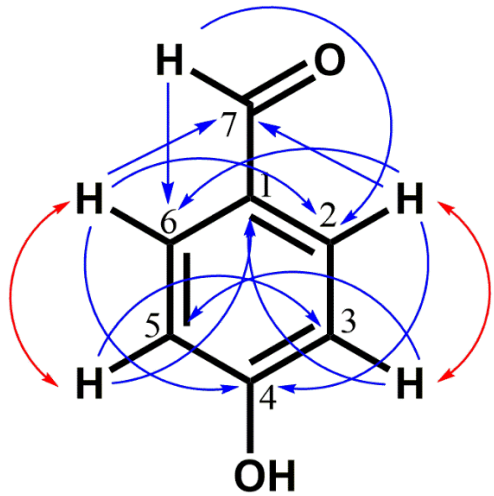

4-hydroxybenzaldehyde

Figure 25. Structure of compound III

9.4 Identification of compound IV and V

Compound IV and V were identified as a mixture. When it was analyzed with LC-ESI/MS, the compounds showed different molecular ion peaks in positive and negative-ion mode. The NMR spectra also showed that there were two different structures in the sample. The UV spectra showed maximum absorption at 198, 222, 276, and 304 nm. The positive-ion mode of ESI-MS showed molecular ion peak at m/z 282.3 while the negative-ion mode at m/z 476.9. Peaks that might relate to each other are peaks at m/z 137.0 and 153.1 in positive-ion mode and m/z 134.8 and 151.0 in negative-ion mode.

^{1}H NMR spectrum of compound IV and V mixture showed signals for aldehyde proton attached to aromatic ring at δ 9.73 (1H, s), aromatic ring group at δ 7.82 (2H, d, *J* = 8.5 Hz), 7.40 (1H, d, *J* = 7.6 Hz), 7.35 (1H, s), 6.92 (1H, d, *J* = 7.6 Hz) and 6.84 ppm (2H, d, *J* = 8.5 Hz). Due to the low yield of obtained compounds, the ^{13}C NMR spectrum was not available. 2D NMR (^{1}H-^{1}H COSY, ^{1}H-^{13}C HSQC, and ^{1}H-^{13}C HMBC) was performed. Observing the HSQC and HMBC NMR spectra, the carbon signals were detected at δ 190.9 (C-7 of compound IV), 154.0 (C-4 of compound IV), 148.5 (C-3 of compound IV), 128.0 (C-1 of compound IV), 126.3 (C-6 of compound IV), 110.32 (C-2 of compound IV), 26.1 ppm (methyl at ketone group); 196. 3 (C-7 of compound V), 162.1 (C-4 of compound V), 130.7 (C-2 and C-6 of compound V), 128.5 (C-1 of compound V), 115.4 (C-5 of compound IV), 115.0 (C-5 of compound V), and 55.3 (methoxy carbon). The NMR spectra data were compared with reference [22, 23] thus compound IV was assigned as vanilic aldehyde and compound V as 4-hydroxyacetophenone. The data are summarized in Table 3.

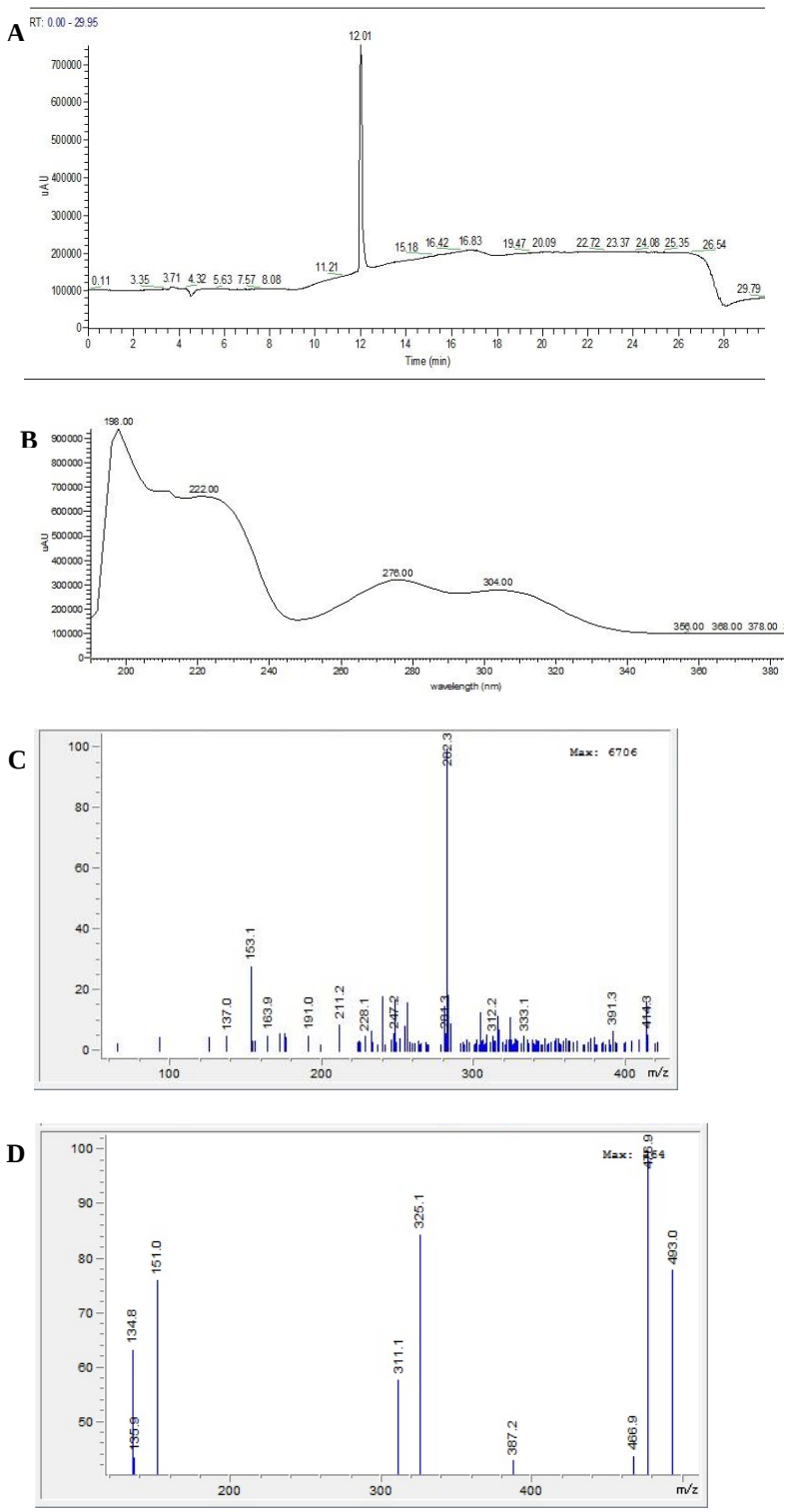

Figure 26. HPLC and ESI/MS analysis of compound IV and V mixture. (A) HPLC chromatogram (B) UV spectrum (C) ESI-MS positive-ion mode (D) ESI-MS negative-ion mode

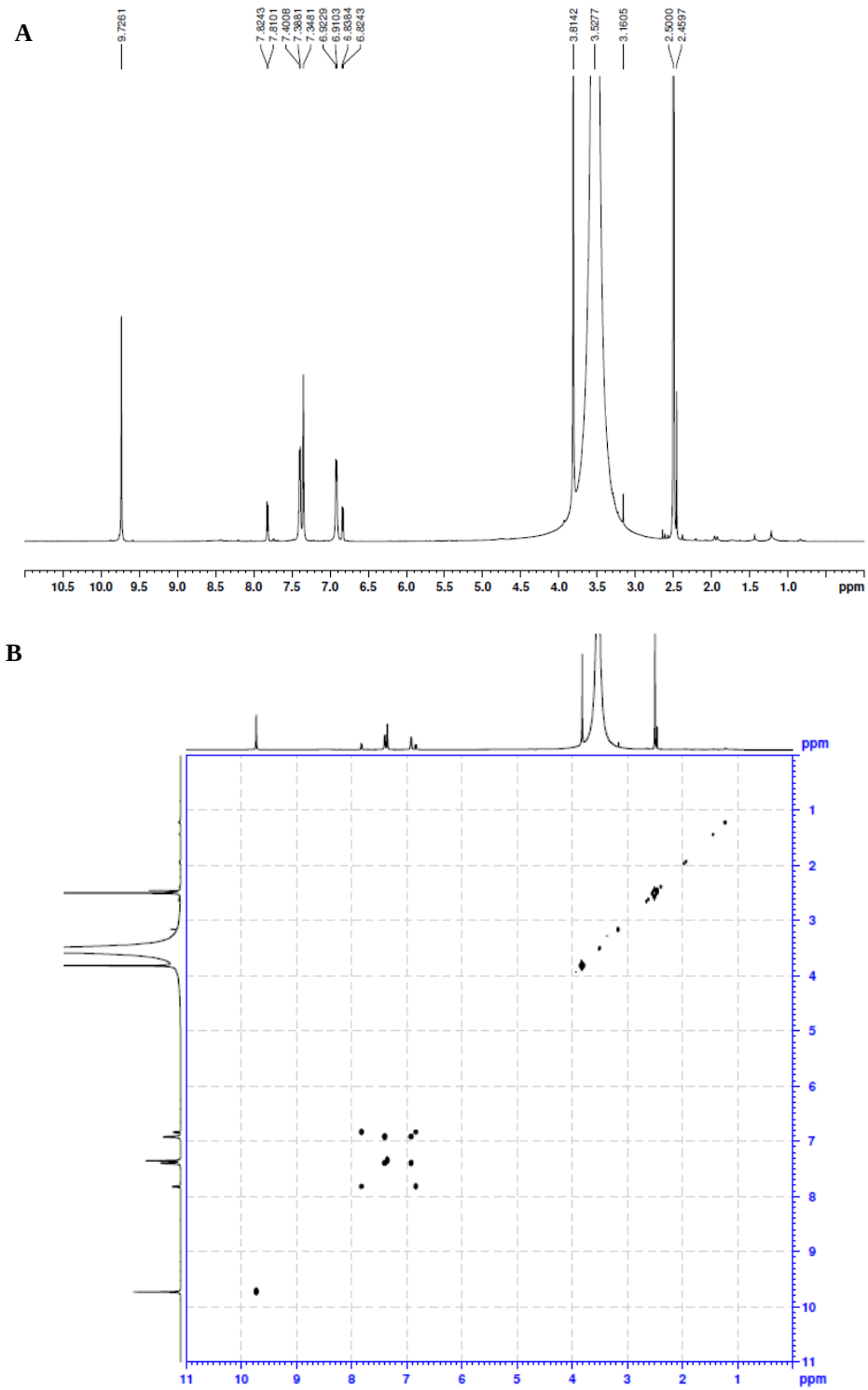

Figure 27. NMR spectra of Compound IV and V mixture at 600 MHz in DMSO-d_6 (A) ^{1}H NMR spectrum (B) ^{1}H-^{1}H COSY spectrum

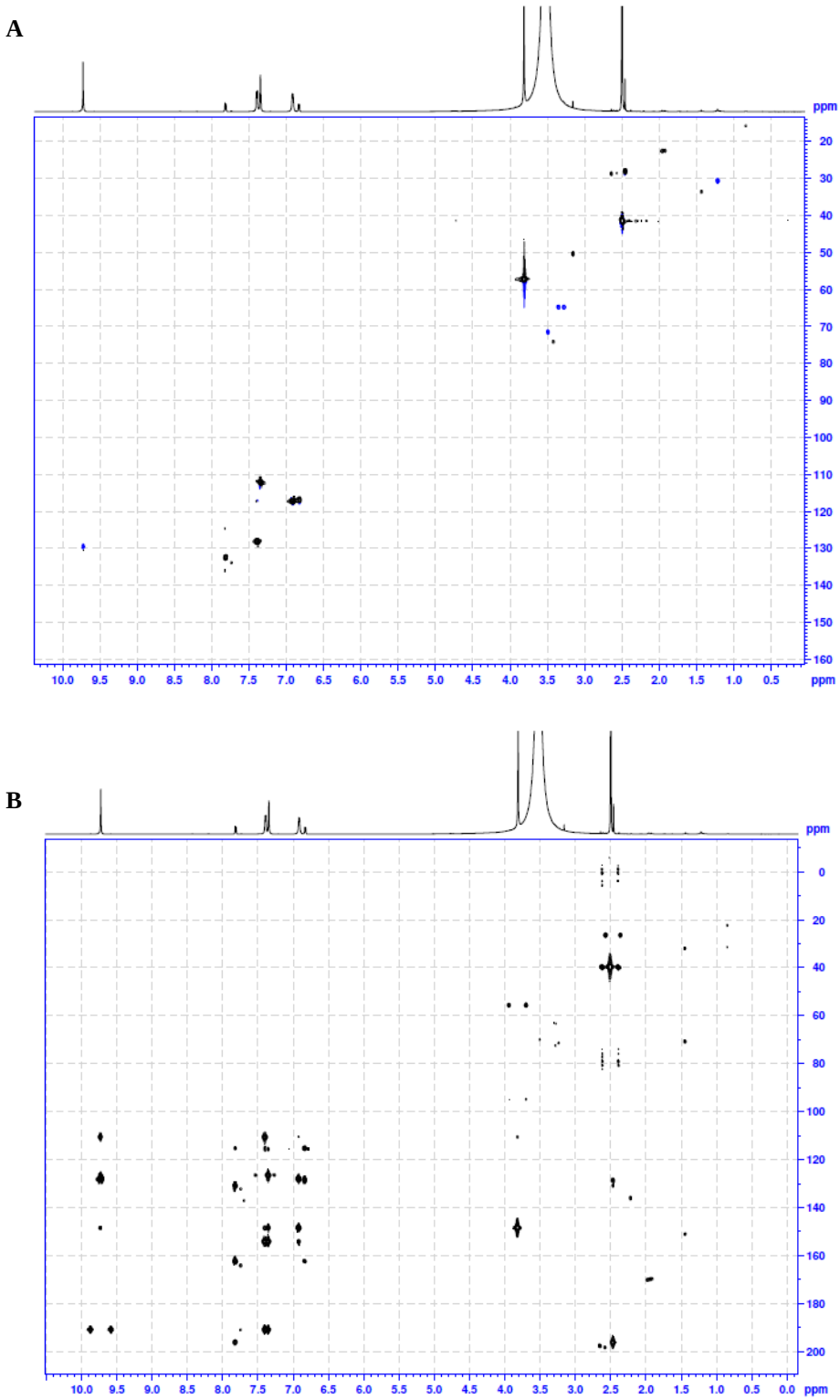

Figure 28. NMR spectra of Compound IV and V mixture at 600 MHz in DMSO-d_6 (A) ^{1}H-^{13}C HSQC spectrum (B) ^{1}H-^{13}C HMBC spectrum

A

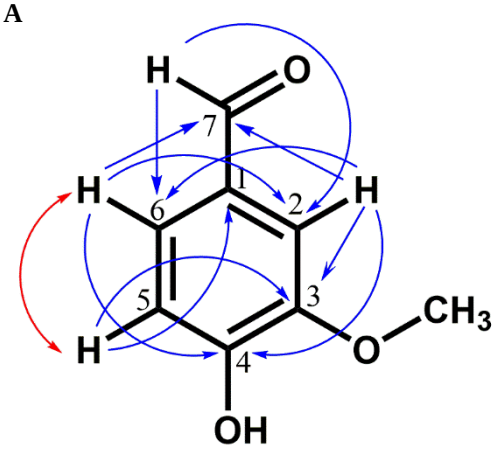

vanillic aldehyde

B

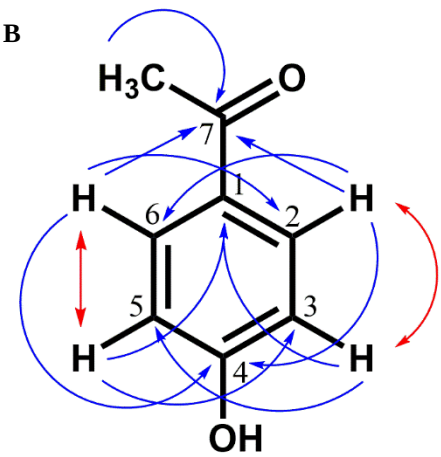

4-hydroxyacetophenone

Figure 29. Structure of (A) compound IV and (B) compound V with HMBC and COSY correlation

9.5 Identification of compound VI

Compound VI was isolated from MC1B fraction and obtained as off white solid. It has maximum absorption at 200, 214, 232, 280, and 310 nm. The ESI-MS positive-ion mode spectrum showed molecular ion peak at m/z 167.1 and the negative-ion mode spectrum showed molecular ion peak at m/z 165.1.

^{1}H NMR spectrum of compound VI showed signals of aromatic ring protons at δ 7.49 (1H, dd, *J* = 8.2 Hz, 1.9 Hz), 7.42 (1H, d, *J* = 1.7 Hz), 6.85 (1H, d, *J* = 8.2 Hz), methoxy proton at 3.81 (3H, s) and ketone proton at 2.48 ppm (3H, s). Due to the low yield of obtained compound, the ^{13}C NMR spectrum was not available so 2D NMR (^{1}H-^{1}H COSY, HSQC, and HMBC) was performed to determine the carbon peaks. Observing the HSQC and HMBC NMR spectra, the carbon signals were detected at δ 196. 3 (C-1), 152.0 (C-4), 147.7 (C-3), 123.4 (C-6), 114.7 (C-5), 110.8 (C-2), 55.3 (methoxy carbon), 26.1 ppm (methyl at ketone group). One impurity peak was found at δ 8.44 ppm attached to δ 165.9 ppm. It is assumed to be trace of formic acid used in preparative HPLC separation solvent system which might not completely evaporated. The summary of the spectral data is shown in Table 3. The NMR spectral data were in alignment with reference data [24]. Thus, compound VI was assigned as apocynin.

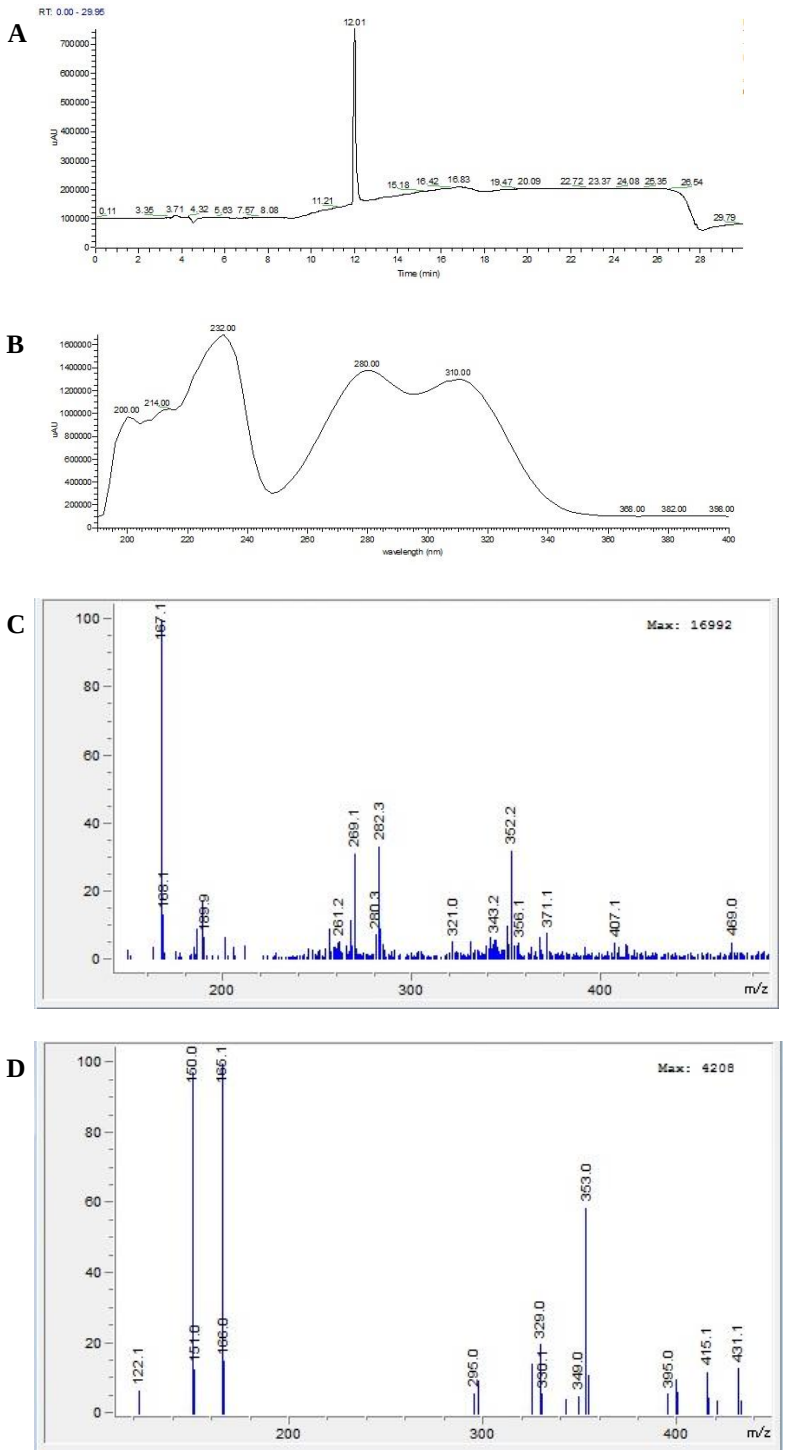

Figure 30. HPLC and ESI/MS analysis of compound VI. (A) HPLC chromatogram (B) UV spectrum (C) ESI-MS positive-ion mode (D) ESI-MS negative-ion mode

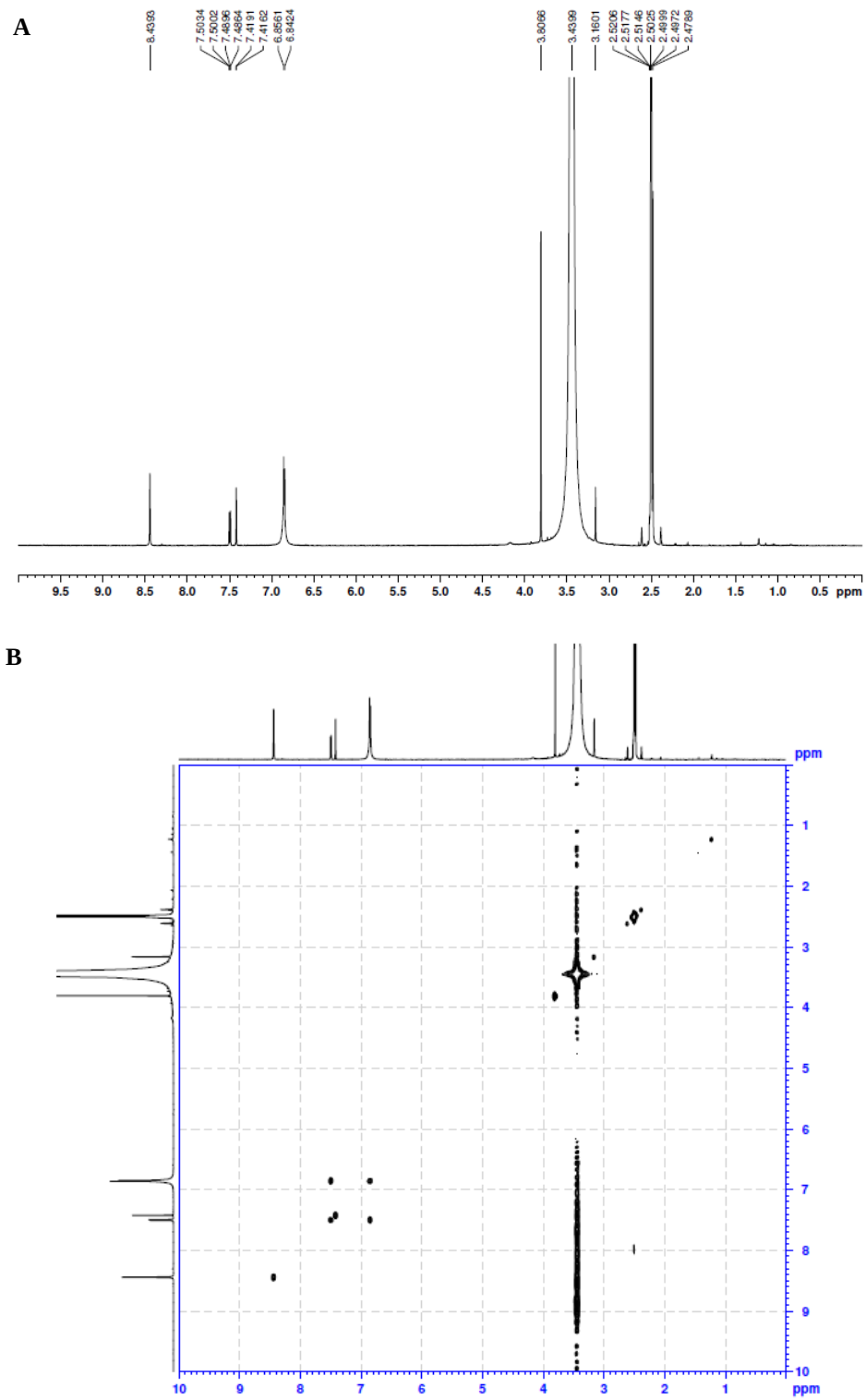

Figure 31. NMR spectra of Compound VI at 600 MHz in DMSO-d_6 (A) ^{1}H NMR spectrum (B) ^{1}H-^{1}H COSY spectrum

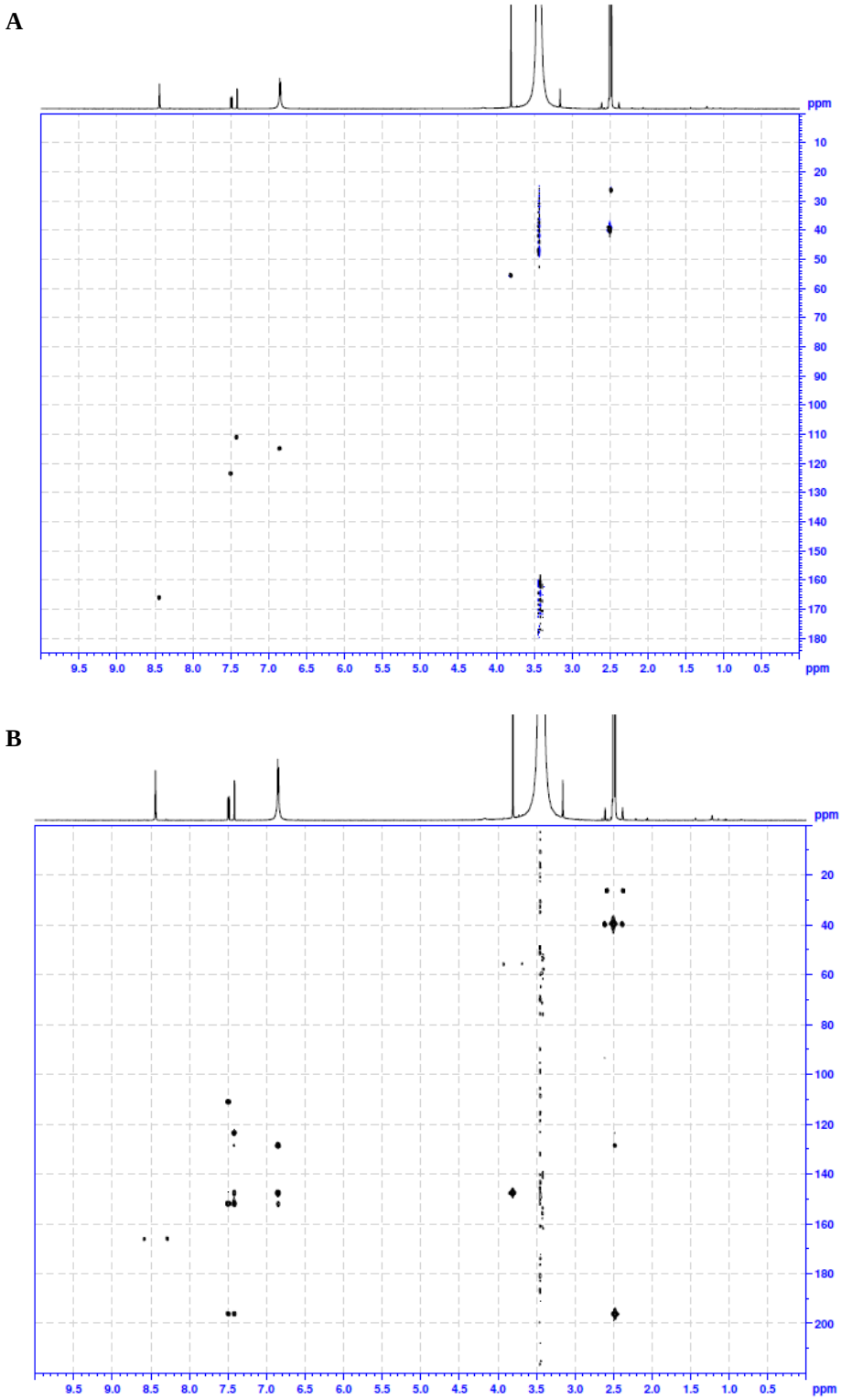

Figure 32. NMR spectra of Compound VI at 600 MHz in DMSO-d_6 (A) ^{1}H-^{13}C HSQC spectrum (B) ^{1}H-^{13}C HMBC spectrum

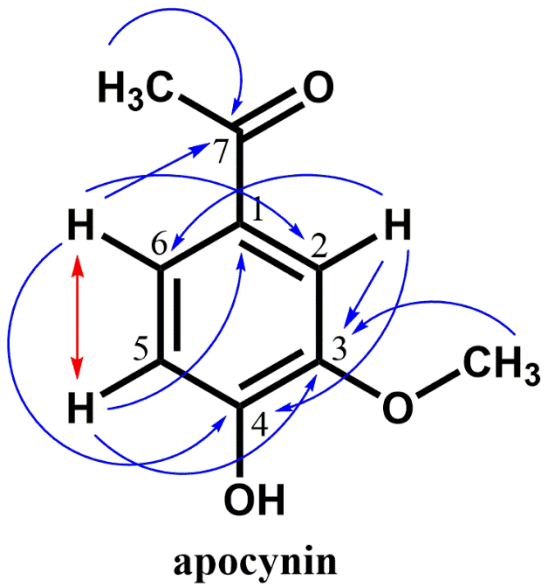

Figure 33. Structure of compound VI

Table 3. ^{1}H and ^{13}C NMR data of compound III, IV, V and VI

No	Compound III		Compound IV		Compound V		Compound VI	
	δH (mult; *J* in Hz)	δC	δH (mult; *J* in Hz)	δC	δH (mult; *J* in Hz)	δC	δH (mult; *J* in Hz)	δC
1		132.3		128.0		128.5		128.5
2	7.75 (2H, d, 8.5)	128.3	7.35 (1H, s)	110.3	7.82 (2H, d, 8.6)	130.7	7.42 (1H, d, 1.7)	110.8
3	6.92 (2H, d, 8.5)	116.0		148.5	6.83 (2H, d, 8.6)	115.0		147.7
4		164.0		154.0		162.1		152.0
5	6.92 (2H, d, 8.5)	116.0	6.92 (1H, d, 7.6)	115.4	6.83 (2H, d, 8.6)	115.0	6.85 (1H, d, 8.2)	114.7
6	7.75 (2H, d, 8.5)	128.3	7.39 (1H, d, 7.6)	126.3	7.82 (2H, d, 8.6)	130.7	7.49 (1H, dd, 8.2, 1.9)	123.4
7	9.76 (1H, s)	191.1	9.73 (1H, s)	190.9		196.3		196.3
	OCH3		3.79 (3H, s)	55.3			3.81 (3H, s)	55.3
	CH3				2.46 (3H, s)	26.1	2.48 (3H, s)	26.1

9.6 Identification of compound VII

Compound VII was obtained as white with slightly brown colored solid. It has maximum absorption at 205, 220, 260 and 296 nm. The ESI-MS positive-ion mode spectrum showed base ion peak at m/z 137.1. However, another peak at m/z 155.1 corresponds well with the negative-ion mode spectrum which showed base ion peak at m/z 153.1. Thus, the molecular weight of the compound was assumed to be 154.1 Da.

^{1}H NMR spectrum of compound VII showed signals of two hydroxyl groups attached to aromatic ring at δ 9.66 (1H, br s), 9.34 (1H, br s) and aromatic ring protons at 7.32 (1H, d, *J* = 2 Hz), 7.28 (1H, dd, *J* = 8 Hz, 2 Hz) and 6.78 ppm (1H, d, *J* = 8 Hz). The ^{13}C NMR spectra showed signals at δ 167.40 (C-7), 150.06 (C-4), 144.93 (C-3), 121.95 (C-2 and C-6), 121.71 (C-1), 116.59 (C-H aromatic ring), and 115.20 ppm (C-H aromatic ring. The NMR spectral data were in alignment with reference data [25] thus compound VII was assigned as protocatechuic acid.

Several other peaks were also detected in ^{1}H and ^{13}C NMR spectra. The ^{1}H NMR spectra showed peaks at δ 3.58 ppm whereas the ^{13}C NMR spectra showed peaks at δ 173.50, 51.46, 28.74 and 28.58 ppm. However, these peaks were not correlated to the peaks of compound VII based on the HSQC and HMBC NMR spectra. Thus, these peaks were concluded to be impurities.

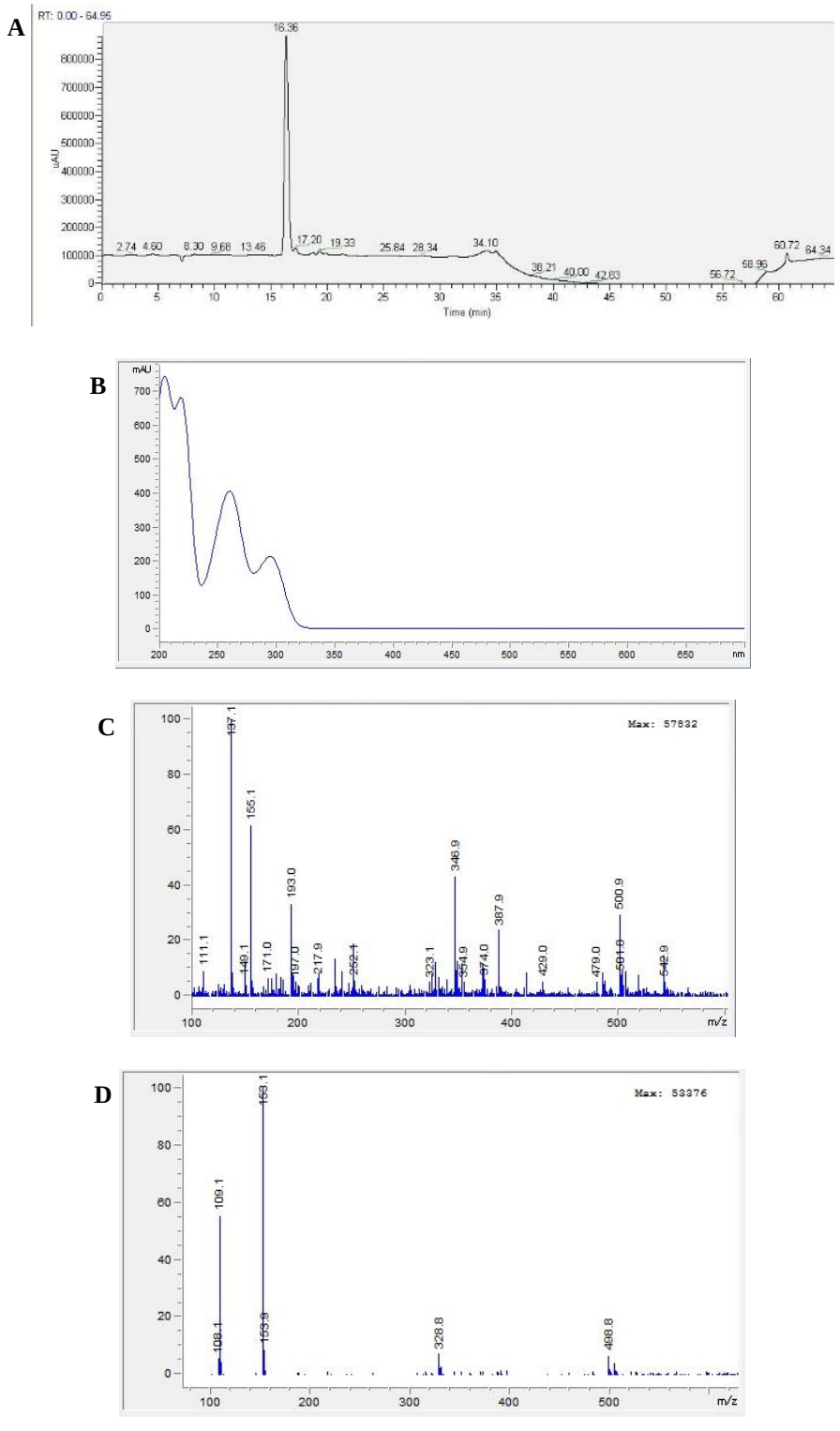

Figure 34. HPLC and ESI-MS spectrum of compound VII. (A) HPLC chromatogram (B) UV spectrum (C) ESI-MS positive-ion mode (D) ESI-MS negative-ion mode

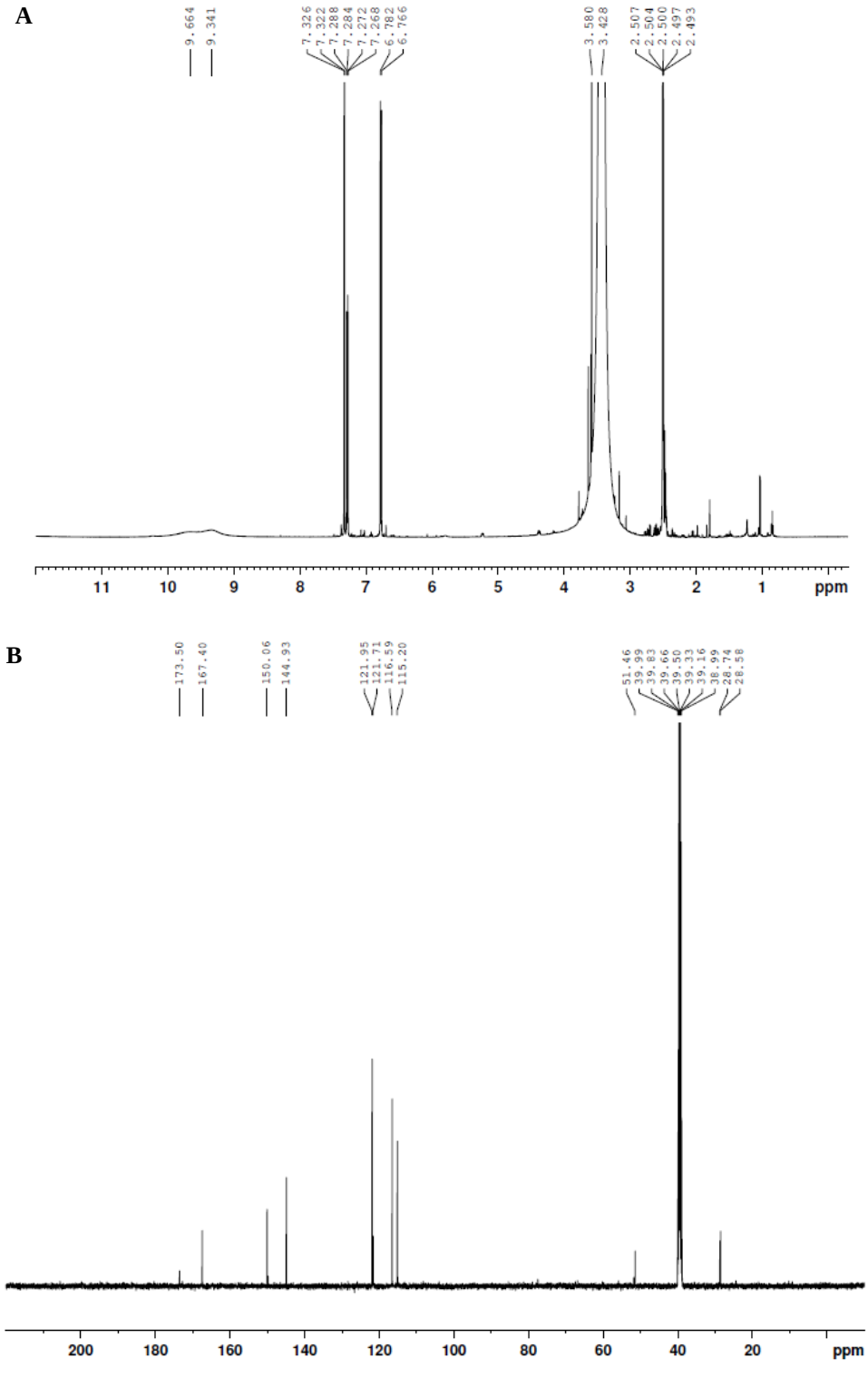

Figure 35. One dimension NMR spectra of compound VII at 500 MHz in DMSO-d_6. (A) ^{1}H NMR (B) ^{13}C NMR

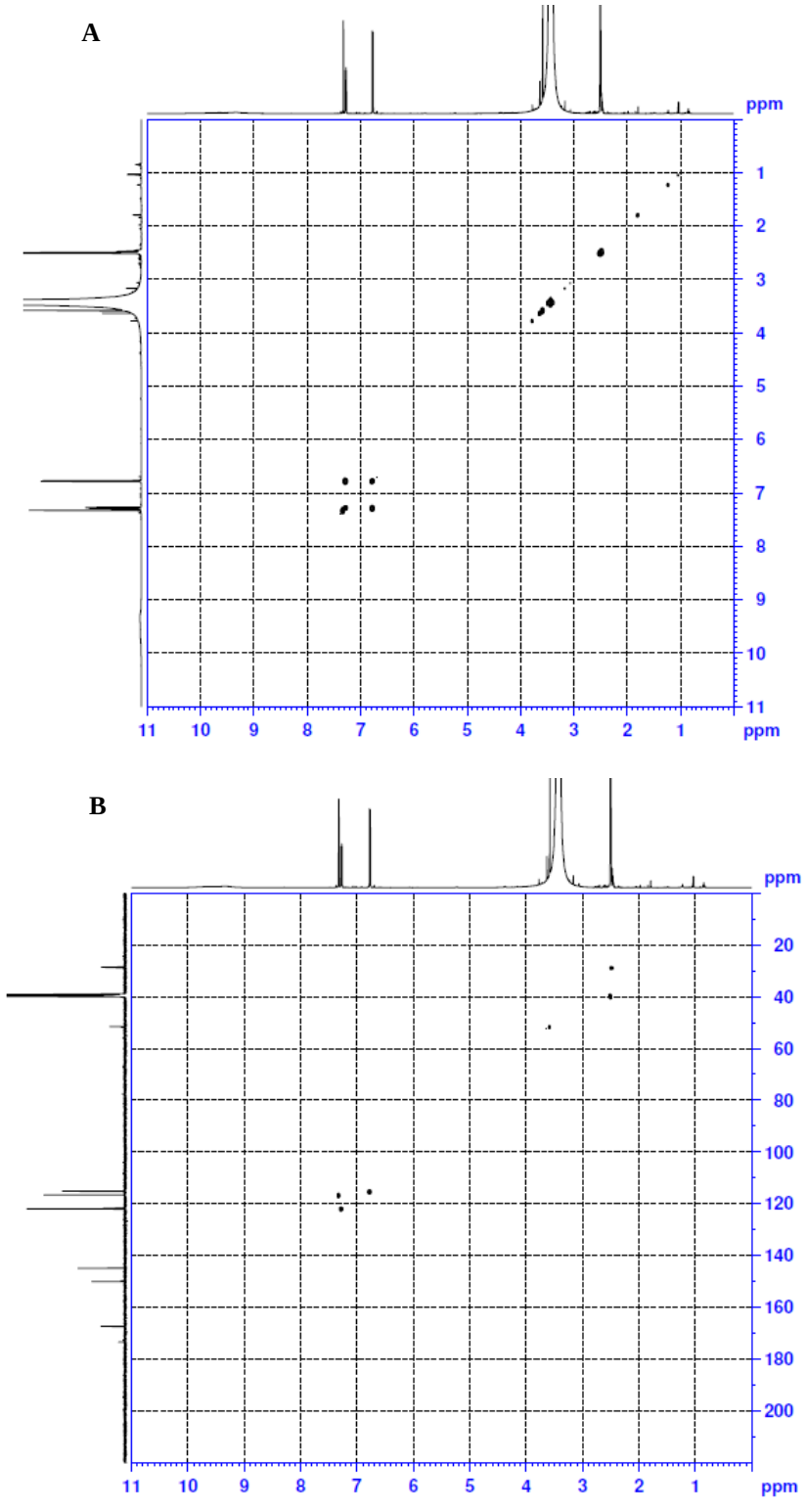

Figure 36. NMR spectra of compound VII at 500 MHz in DMSO-d_6. (A) ^{1}H-^{1}H COSY spectrum and (B) ^{1}H-^{13}C HSQC spectrum

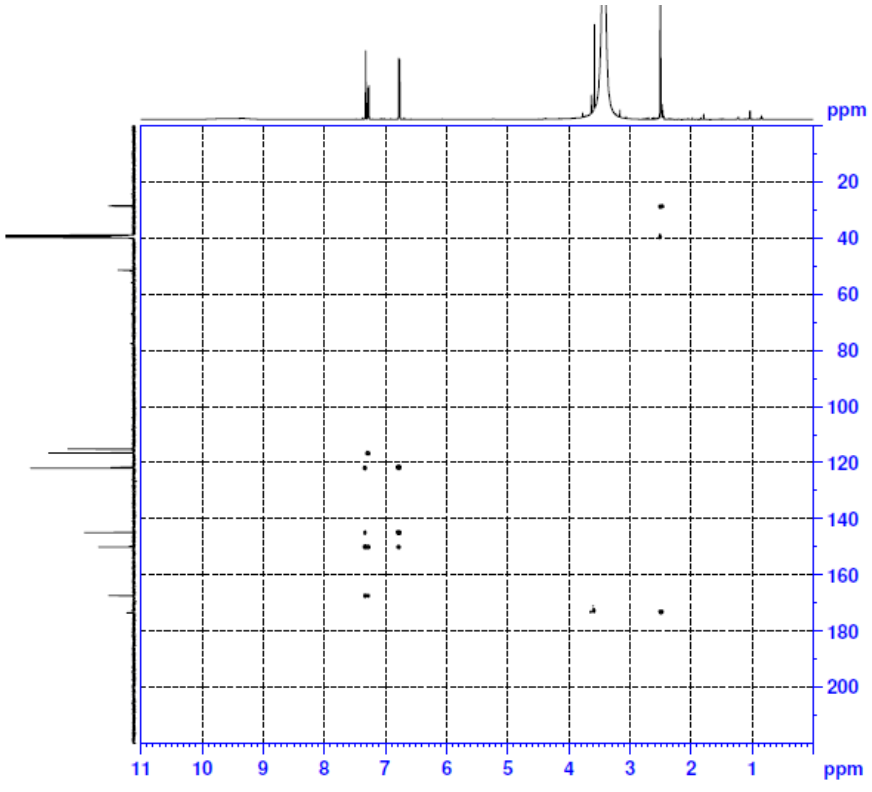

Figure 37. ^{1}H-^{13}C HMBC spectrum of compound VII at 500 MHz in DMSO-d_6

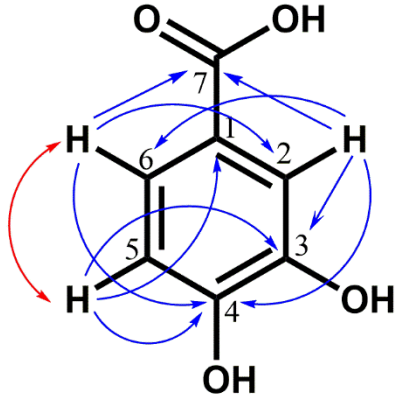

protocatechuic acid

Figure 38. Structure of compound VII

9.7 Identification of compound VIII

Compound VIII was obtained as white solid. It has maximum absorption at 252 nm. The ESI-MS positive-ion mode spectrum showed base ion peak at m/z 139.1 and the negative-ion mode spectrum which showed base ion peak at m/z 137.0.

^{1}H NMR spectrum of compound VIII showed peaks of hydroxyl group attached to aromatic ring at δ 10.26 (1H, br s) and aromatic ring protons at 7.79 (2H, dt, *J* = 10 Hz, 5 Hz, 3Hz) and 6.82 ppm (2H, dt, *J* = 10 Hz, 5 Hz, 3 Hz). The ^{13}C NMR spectra showed peaks at δ 167.31 (C-7), 161.69 (C-4), 131.65 (C-2 and C-6), 121.44 (C-1), and 115.23 ppm (C-3 and C-5). The NMR spectral data were in alignment with reference [26] and it is concluded that compound VIII is 4-hydroxybenzoic acid. This compound was also found in the 40% MeOH elution of EA fraction in Diaion HP-20 column chromatography.

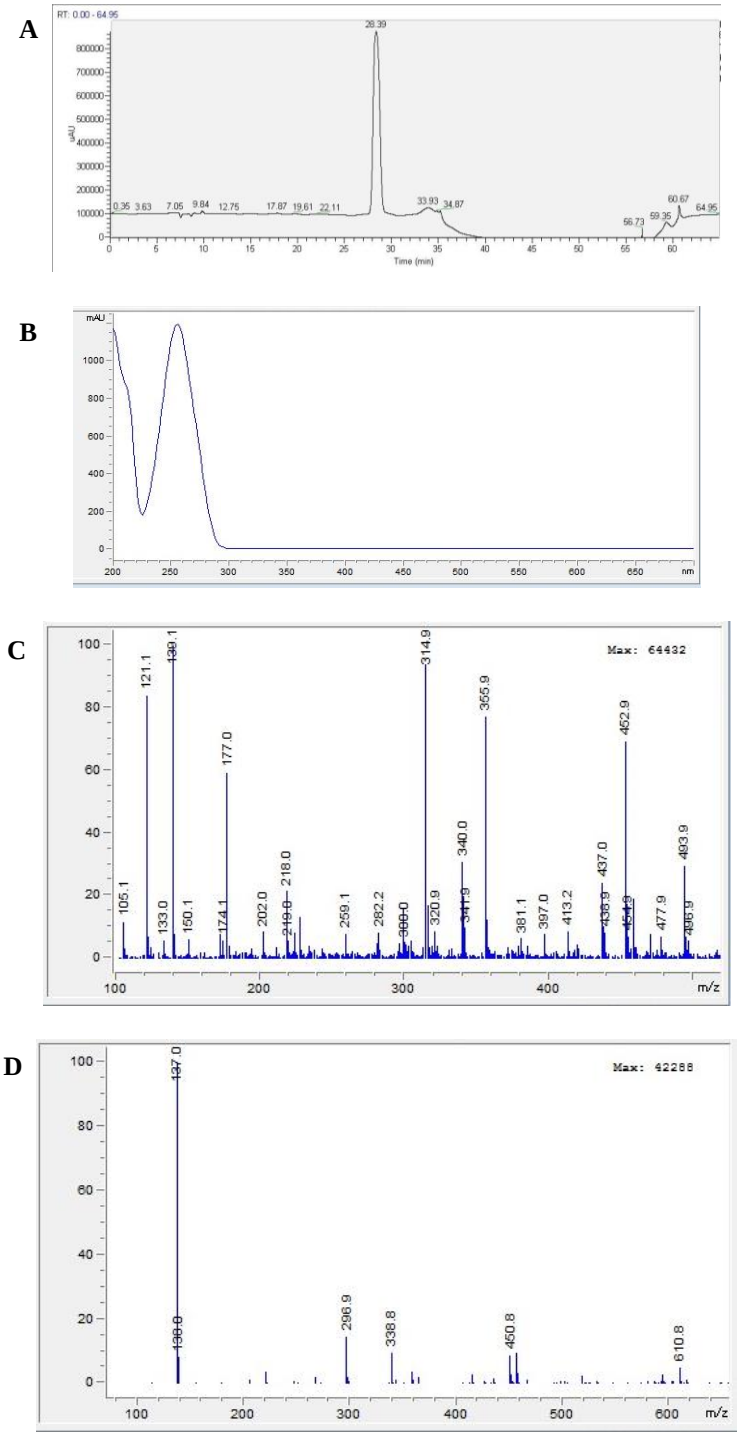

Figure 39. HPLC and ESI-MS spectrum of compound VIII. (A) HPLC chromatogram (B) UV spectrum (C) ESI-MS positive-ion mode (D) ESI-MS negative-ion mode

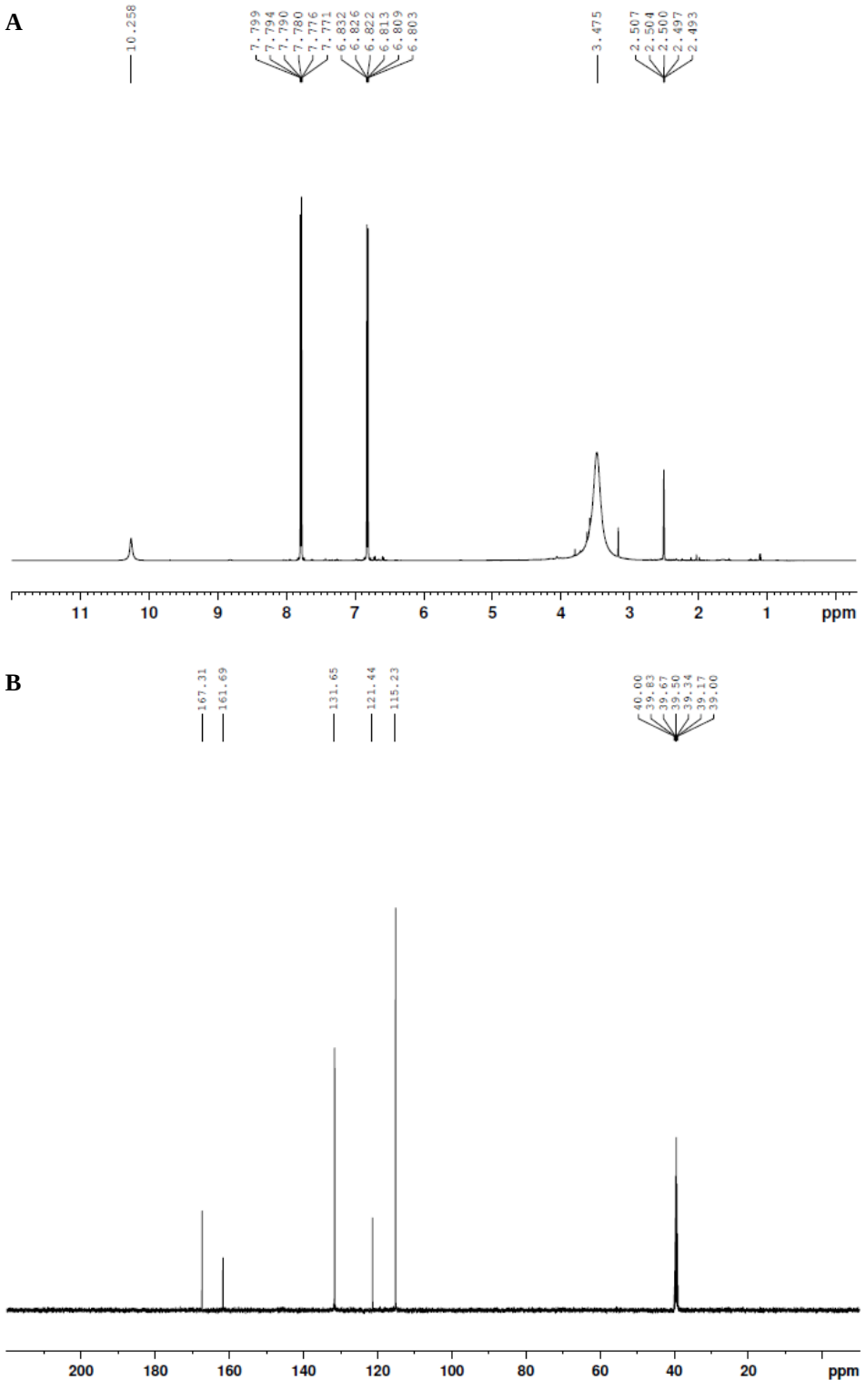

Figure 40. NMR spectra of compound VIII at 500 MHz in DMSO-d_6. (A) ^{1}H NMR (B) ^{13}C NMR

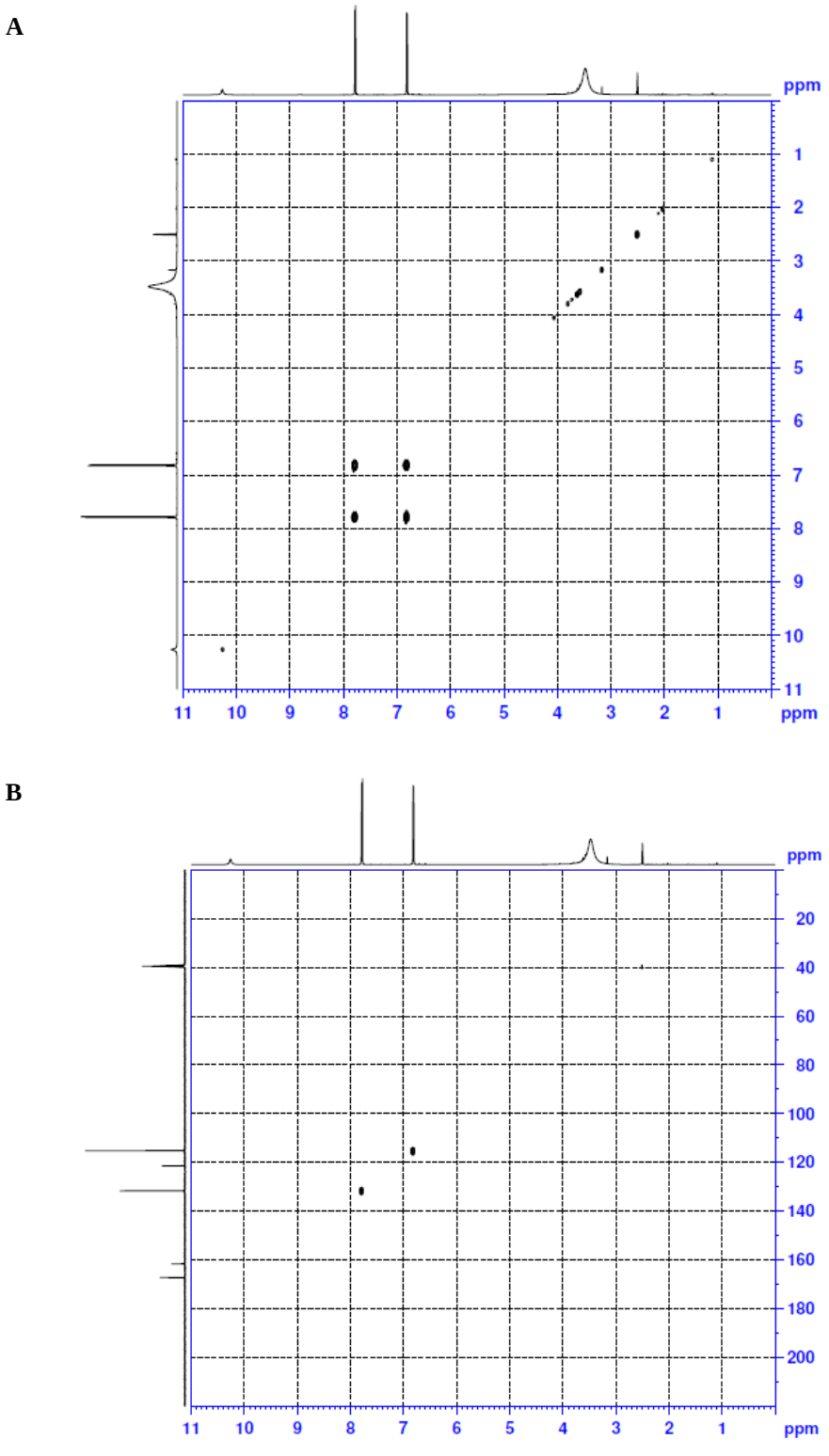

Figure 41. NMR spectra of compound VIII at 500 MHz in DMSO-d_6. (A) ^{1}H-^{13}C HSQC spectrum (B) ^{1}H-^{13}C HMBC spectrum

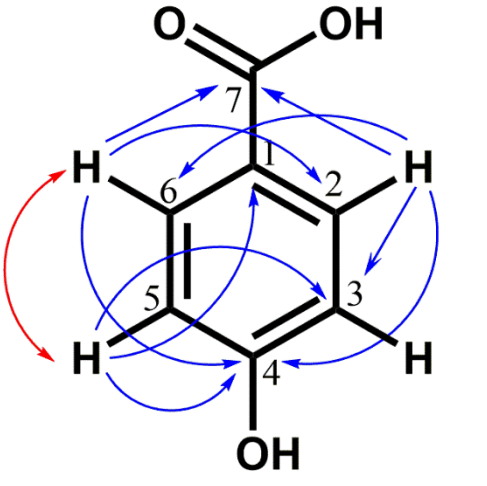

Figure 42. Structure of compound VIII

Table 4. ^{1}H and ^{13}C NMR data of compound VII and VIII

No	Compound VII		Compound VIII	
	δH (mult; *J* in Hz)	δC	δH (mult; *J* in Hz)	δC
1		121.7		121.4
2	7.32 (1H, d, 2.1)	116.6	7.79 (2H, d, 10, 5, 3)	131.6
3		144.9		115.2
4		150.1	10.26 (1H, s)	161.7
5	6.77 (1H, d, 8)	115.2	6.77 (2H, d, 10, 5, 3)	115.2
6	7.27 (1H, d, 2.1)	122.0	7.79 (2H, d, 10, 5, 3)	131.6
7		167.4		167.4

10. Suppression of LPS-induced NO activity of isolated compounds

The ability of the isolated compounds to inhibit LPS-induced NO production were examined. The compounds were tested at 5, 10, 20 and 40 µM for syringol and catechol because above 40 µM both compounds showed cytotoxicity. The remaining compounds were tested at 10, 50 and 100 µM. Among all tested compounds, only syringol and catechol showed dose-dependent NO inhibition activity with catechol showing the most potent inhibition activity.

Further on, NF-κB SEAP assay was performed for catechol and syringol to examine their ability to inhibit NF-κB expression. The result showed that catechol was able to decrease NF-κB expression significantly with IC_{50} value 13.56 µM while the IC_{50} value of syringol was more than 40 µM.

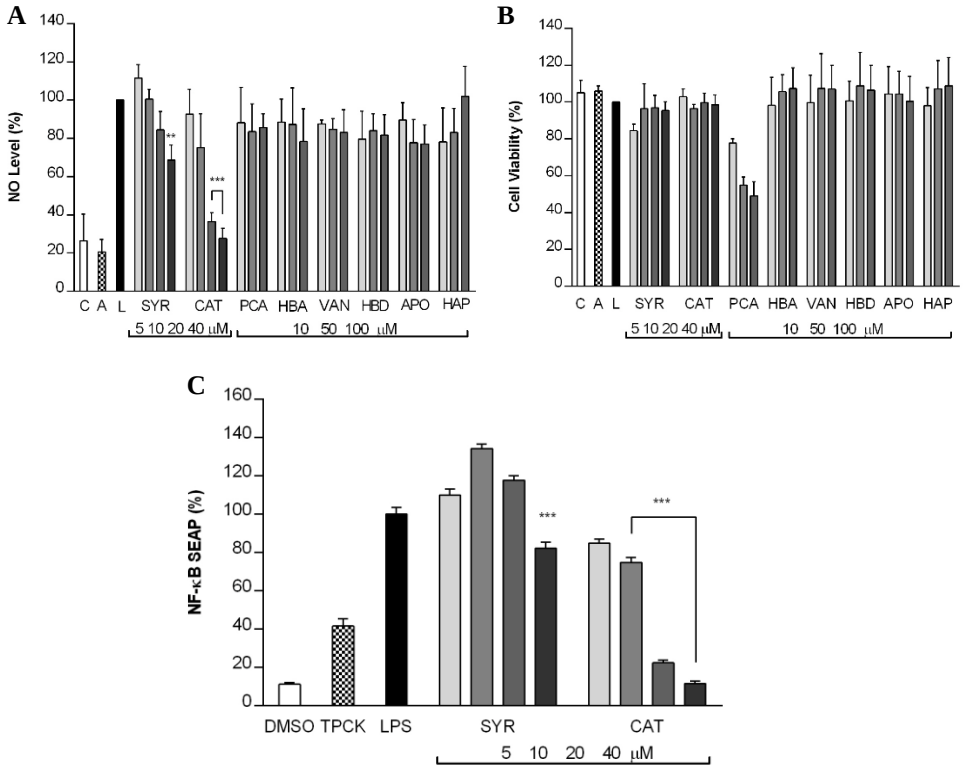

Figure 43. Effect of isolated compounds on (A) NO production and (B) cell viability and (C) NF-κB inhibition activity of syringol and catechol

Data were derived from three independent experiments and are expressed as mean ± SD. (***) *P<0.001* indicates significant difference from the LPS-stimulated group. C is control (vehicle), L is (LPS + vehicle)-treated cells alone, A is AMT 10 µM used as positive control. TPCK (20 µM) was used as positive control for NF-κB SEAP assay. SYR: syringol, CAT: catechol, PCA: protocatechuic acid, HBA: 4-hydroxybenzoic acid, VAN: vanillic aldehyde, HBD: 4-hydroxybenzaldehyde, APO: apocynin, and HAP: 4-hydroxyacetophenone.

IV. DISCUSSION

The search of new drugs from natural products have been continuously conducted to treat human diseases. Basically, the ethnopharmacology use of a natural product is employed as the basis of its drug discovery research where the separation process is performed in order to "find and follow" the supposed pharmacological activity with the final aim to isolate and identify the bioactive compounds, especially if information on the secondary metabolite is limited [27]. In the current study, Arecae Pericarpium, which has been used in TCM to treat edematous diseases, was examined to elucidate its potential anti-inflammatory effect and to discover the active compound contributing to this activity.

The potential anti-inflammatory activity of Arecae Pericarpium is screened by examining the ability of tested fractions to suppress LPS-induced NO production in murine macrophage cells. Macrophage play a central role in a host's defense against bacterial infection through phagocytosis, cytotoxicity, and intracellular killing [28, 29]. Stimulation of murine macrophages by LPS results in the expression of iNOS and increased NO production which plays a critical role in macrophage activation and is associated with acute and chronic inflammations [29]. The increased NO production is examined with Griess reaction by quantifying the nitrite level in the conditioned medium of RAW264.7 cells treated with LPS. This cell-based assay system has been used for drug screening and the evaluation of potential inhibitors of the pathways leading to the induction of iNOS and NO production. Due to its reliability and simplicity, this method is commonly employed in bioassay-guided isolation of anti-inflammatory agent scheme [30].

The result of preliminary study in this research indicated that Arecae Pericarpium was able to suppress LPS-induced NO production in murine macrophages with methylene chloride and ethyl acetate fractions showing the strongest inhibition compared to other fractions. Thus, it is confirmed that Arecae Pericarpium has the potential anti-inflammatory activity and the active compounds are present in these fractions.

The potential anti-inflammatory activity of the methylene chloride fraction was further supported with the PGE_2 assay result of MC1A fraction which was able to reduce the PGE_2 level with IC_{50} less than 0.5 μg/mL. This result suggested that the methylene chloride fraction of Arecae Pericarpium might exert potential anti-inflammatory activity also through the inhibition of COX-2 enzyme.

The methylene chloride fraction was separated with combination of column chromatography, HPCCC, and preparative HPLC. Through column chromatography separation process, dimeric syringol (9.2 mg) and catechol (196.3 mg) were isolated. After column chromatography separation, combination of HPCCC and preparative HPLC was needed to isolate 4-hydroxybenzaldehyde (1.0 mg), mixture of vanillic aldehyde and 4-hydroxyacetophenone (5.0 mg), and apocynin (0.6 mg). The length of the separation process might contribute to the low yield of these compounds.

Ethyl acetate fraction was subjected to Diaion HP-20 resin column chromatography. From 3.2 g of active fraction obtained, 200 mg was separated by HPCCC and protocatechuic acid (18.7 mg), 4-hydroxybenzoic acid (3.3 mg) and catechol (25.4 mg) were isolated.

All of the isolated compounds were tested to compare their activity. Among all of the isolated compounds, catechol exhibited highest inhibition activity of LPS-stimulated NO production, followed by syringol. Other compounds did not or only slightly inhibited the NO production.

NF-κB transcription factor has been shown to play a significant role in LPS-induced expression of pro-inflammatory mediators, including iNOS and COX-2. To investigate the molecular mechanism of inhibition of iNOS and COX-2 transcription mediated by catechol and syringol, NF-κB transcriptional activity was investigated using a reporter gene assay system. The result showed that only catechol was able to inhibit NF-κB transcription with IC_{50} value 13.56 μM while the IC_{50} value of syringol was more than 40 μM. Therefore, it is suggested that catechol suppressed the LPS-induced NO production by inhibiting NF-κB transcription.

Based on the yield and the bioassay results, it is suggested that catechol might be the primary contributing compound to the potential anti-inflammatory activity of Arecae Pericarpium. Catechol is a major phenolic compound in areca nut as well. This compound has been reported to have antioxidant activity [31] and anti-inflammatory in BV2 microglial cells and RAW 264.7 cells [32, 33]. It was reported that catechol was able to exhibit anti-inflammatory effect on LPS-stimulated BV2 microglial cells through inhibiting NF-κB and p38 MAPK signaling pathway [33]. The data in the present study support the pharmacological basis of the use of Arecae Pericarpium as a traditional herbal medicine to treat inflammatory diseases.

V. CONCLUSION

This result of this study have showed that Arecae Pericarpium suppressed NO production induced by LPS in RAW 264.6 cells and eight phenolic compounds were isolated from the methylene chloride and ethyl acetate fractions by applying bioassay-guided isolation scheme. The phenolic compounds are dimeric syringol, catechol, 4-hydroxybenzyl aldehyde, vanilic aldehyde, 4-hydoxyacetophenone, apocynin, protocatechuic acid and 4-hydroxybenzoic acid. Catechol was found to be the major compound and might be the primary contributing compound to the inhibition activity of Arecae Pericarpium on LPS-stimulated NO production in RAW 264.7 macrophage cells. The result of this study can enrich the existing study on Arecae Pericarpium and support the further study on the use of Arecae Pericarpium in treating inflammatory diseases.

REFERENCES

1. Rimando, A.M., et al., *Searching for rice allelochemicals: An example of bioassay-guided isolation.* Agronomy Journal, 2001. 93(1): 16-20.
2. Koehn, F.E., and Carter, G.T., *The evolving role of natural products in drug discovery.* Nat Rev Drug Discov, 2005. 4(3): 206-221.
3. Killeen, Matthew J., Linder, Mark, Pontoniere, Paolo, Crea, Roberto, *NF-kb signaling and chronic inflammatory diseases: exploring the potential of natural products to drive new therapeutic opportunities.* Drug Discovery Today, 2014. 19 (4): 373-378.
4. Zamora, Ruben, Vodovotz, Yoram, Billiar, Timothy R., *Inducible nitric oxide synthase and inflammatory diseases.* Molecular Medicine, 2000. 6(5):347-373.
5. Korhonen, Riku, Lahti, Aleksi, Kankaanranta, Hannu, Moilanen, Eeva, *Nitric oxide production and signaling in inflammation*. Current Drug Targets – Inflammation & Allergy, 2005. 4: 471-479.
6. Sun, Jie, Zhang, Xhueji, Broderick, Mark, Fein, Harry. *Measurement of nitric oxide production in biological systems by using Griess reaction assay.* Sensors, 2003. 3: 276-284.
7. Ito, Yoichiro. *Golden rules and pitfalls in selecting optimum conditions for high-speed counter-current chromatography*. J Chromatography A, 2005. 1065: 145-168.
8. Guzlek, H, Wood, P.L, Janaway, Lee. *Performance comparison using the GUESS mixture to evaluate counter-current chromatography instruments*. J Chromatography A, 2009. 1216: 1481-1486.
9. Shehzad, Omer, et al., *Application of stepwise gradients in counter-current chromatography: A rapid and economical strategy for the one-step separation of eight coumarins from Seseli resinosum*. J Chromatography A, 2013. 1310: 66-73.

10. Friesen, J. B., Pauli, G. F., *G.U.E.S.S.- A generally useful estimate of solvent systems for CCC*. Journal of Liquid Chromatography and Related Technologies, 2005. 28 (17): 2777-2806.
11. Peng, Wei, et al., *Areca catechu L. (Arecaceae): A review of its traditional uses, botany, phytochemistry, pharmacology and toxicology*. J Ethnopharmacology, 2015. 164: 340-356.
12. Bhandare, A.M., Kshirsagar, A.D., Vyawahare, N.S., Hadambar, A.A., Thorve, V.S., *Potential analgesic, anti-inflammatory and antioxidant activities of hydroalcoholic extract of Areca catechu L. nut*. Food and Chemical Toxicology, 2010. 48: 3412–3417.
13. Huang, P.L., Chi, C.W., Liu, T.Y., *Effects of Areca catechu L. containing procyanidins on cyclooxygenase-2expression in vitro and in vivo*. Food and Chemical Toxicology, 2010. 48: 306–313.
14. Lee, Kang Pa, et al., *The anti-inflammatory effect of Indonesian Areca catechu leaf extract in vitro and in vivo.* Nutrition Research and Practice, 2014. 8(3): 267-271.
15. Moon, Sang-Kwan et al., *Inhibition of human endothelial cell proliferation by Gami–Jeonggi–San (Jiawei–Zhenqi–San) is accompanied by transcriptional up-regulation of p53 and Waf1 tumor suppressor genes.* J Ethnopharmacology, 2005. 100: 187-192.
16. Yenjit, P., Issarakraisila, M., Intana, W., Chantrapromma, Kan., *Fungicidal activity of compounds extracted from the pericarp of Areca catechu against Colletotrichum gloeosporioides in vitro and in mango fruit.* Postharvest Biology and Technology, 2010. 55: 129-132.
17. Phaechamud, T., Toprasri P., Chinpaisal, C., *Antioxidant activity of Areca catechu extracts in human hepatocarcinoma HepG$_2$ cell lines*. Pharmaceutical Biology, 2009. 47(3): 242–247.
18. Atadana, Frederick W., *Catalytic pyrolysis of cellulose, hemicellulose and lignin model compounds.* Master thesis, 2010.

19. Sun, Y.L., Zhang, Q., Anastasio C., and Sun, J., *Insights into secondary organic aerosol formed via aqueous-phase reactions of phenolic compounds based on high resolution mass spectrometry*. Atmos. Chem. Phys., 2010. 10: 4809–4822.
20. WSS: Spectral data were obtained from Wiley Subscription Services, Inc. (US).
21. Gui, Ren-Yi et al., *Chaetominine, (+)-alantrypinone, questin, isorhodoptilometrin, and 4-hydroxybenzaldehyde produced by the endophytic fungus Aspergillus sp. YL-6 inhibit wheat (Triticum aestivum) and radish (Raphanus sativus) germination*. Journal of Plant Interactions, 2015. 10 (1): 87-92.
22. Stella Christophoridou, Photis Dais. *Detection and quantification of phenolic compounds in olive oil by high resolution 1H nuclear magnetic resonance spectroscopy.* Analytica Chimica Acta, 2009. 633: 283-292.
23. Liu, Qian, et al. *Chemical constituents from Qianliang tea*. Journal of Chinese Pharmaceutical Sciences, 2013. 22 (5): 427–430.
24. ACD: Spectral data were obtained from Advanced Chemistry Development, Inc.
25. Hur, Jong Moon, Park, Jong Cheol, Hwang, Young Hee. *Aromatic Acid and Flavonoids from the Leaves of Zanthoxylum piperitum.* Natural Product Sciences, 2001. 7(1): 23-26.
26. Liang, Yong-hong, et al. *Two new phenolic acids from Drynariae Rhizoma*. Acta Pharm Sin, 2010. 45: 874-878
27. Brusotti, G., et al. *Isolation and characterization of bioactive compounds from plant resources: The role of analysis in the ethnopharmacological approach.* Journal of Pharmaceutical and Biomedical Analysis, 2014. 87: 218-228.
28. Adams, D.O., Hamilton, T.A.. *The cell biology of macrophage activation.* Annual Review of Immunology, 1984. 2: 283-318.
29. Zhou, H.Y., et al. *Anti-inflammatory activity of 4-methoxyhonokiol is a function of the inhibition of iNOS and COX-2 expression in RAW 264.7*

macrophages via NF-κB, JNK and p38 MAPK inactivation. European Journal of Pharmacology, 2008. 586: 340-349.

30. Sae-Wong, Chutha, et al. *Suppresive effects of methoxyflavonoids isolated from Kaempferia parviflora on inducible nitric oxide synthase (iNOS) expression in RAW 264.7 cells.* Journal of Ethnopharmacology, 2011. 136: 488-495.
31. Loo, A. Y., Jain, K., Darah, I. *Antioxidant activity of compounds isolated from the pyroligneous acid, Rhizophora apiculata*. Food Chemistry, 2008. 107: 1151–1160.
32. Zheng, Long Tai, et al. *Anti-inflammatory effects of catechols in lipopolysaccharide-stimulated microglia cells: Inhibition of microglial neurotoxicity*. European Journal of Pharmacology, 2008. 588: 106–113.
33. Kazłowskaa, Katarzyna et al. *Anti-inflammatory properties of phenolic compounds and crude extract from Porphyra dentata*. Journal of Ethnopharmacology, 2010. 128: 123–130.

국문초록

RAW 264.7 세포내 지질다당류로 유도된 산화질소의 생성 억제에 따른 대복피 유래 페놀성 화합물의 분리

Amelia Indriana

서울대학교 대학원

약학과 천연물과학 전공

Arecae Pericarpium는 *Areca catechu* L. (Arecaceae)의 과피이다. 중의학에서는 복부 팽만, 구토증세, 설사를 완화하는 곽향정기산에, 한의학에서는 혈관질환의 치료를 위한 가미정기산에 처방된다. Arecae Pericarpium의 항산화 및 항진균 효과와 그것의 지표물질 추출이 보고된 바 있다. 그러나 Arecae Pericarpium의 항염증 효과는 현재까지 보고된 바가 없어 본 연구에서는 RAW 264.7 대식세포에서 산화질소 생성을 억제하는 Arecae Pericarpium의 항염성분 분리를 목표로 하였다. Arecae Pericarpium 유래 물질의 분리는 RAW 264.7 대식세포에서 LPS 처리에 의해 유도되는 산화질소 생성의 억제 정도에 따라 수행되었다. 건조된 Arecae Pericarpium을 메탄올로 침출하여 농축하고 헥산, 메틸렌클로라이드, 에틸아세테이트, 부탄올을 이용하여 순차적 용매 분획을 시행하였다.

산화질소 생성 억제 활성이 뛰어난 메틸렌클로라이드와 에틸아세테이트 층을 선택하여 물질 분리를 진행하였다. 메틸렌클로라이드 층은 실리카겔 컬럼 크로마토그래피를 통하여 7개의 분획(MC1A~MC1G)으로 나누었다. 그 중 MC1A, MC1B, MC1G 분획이 산화질소 생성 억제 효과를 보였으며 MC1G은 syringol dimer (compound **I**)를 단일 물질로 포함하고 있음을 밝혔다. Diaion® HP-20 수지를 이용한 컬럼크로마토그래피를 통한 MC1A 유래의 20 %, 30 % 메탄올 용출액에서 catechol (compound **II**)을 정제하였다. MC1B에서 유래한 4-hydroxybenzaldehyde (compound **III)**, vanillin (compound **IV**), 4-hydroxyacetophenone (compound **V**), apocynin (compound **VI**) 등 네 개의 물질은 헥산-에틸아세테이트-메탄올-물(2:5:1:4, v/v/v/v)로 구성된 용매계를 이용한 HPCCC(고성능향류크로마토그래피)와 preparative HPLC를 통하여 분리되었다. Ethyl acetate 층은 Diaion® HP-20 수지를 이용한 컬럼크로마토그래피를 통하여 분획하고 그 중 20% 메탄올 용출액을 선택하여 HPCCC를 수행하였다. 헥산-에틸아세테이트-메탄올-물 2:5:2:5(v/v/v/v)의 비율로 조성된 용매계를 통하여 protocatechuic acid (compound **VII)**와 4-hydroxybenzoic acid (compound **VIII**)를 분리하였다. 본 연구에서 분리된 Arecae Pericarpium 유래 화합물들이 중에서 catechol이 LPS에 의해 유도되는 산화질소 생성 억제의 주된 활성에 기여함을 밝혔다.

주요어: 대복피, *Areca catechu* (L.), HPCCC, 페놀성 화합물, 생물학적 검정법, 산화질소 생성의 억제

학번: 2013-23937